國 立 交 通 大 學

電信工程學系

博 士 論 文

行動通訊網路之類神經乏晰無線資源配置技術

Radio Resource Allocation Schemes for Mobile Communication Networks Using Neural/Fuzzy Techniques

研究生：陳義昇

指導教授：張仲儒 博士

中 華 民 國 九十三 年 七 月

博碩士論文授權書

(國科會科學技術資料中心版本，93.2.6)

本授權書所授權之論文爲本人在交通大學大學(學院)電信工程系所甲組九十二學年度第二學期取得博士學位之論文。

論文名稱：(中) 行動通訊網路之類神經乏晰無線資源配置技術
(英) Radio Resource Allocation Schemes for Mobile Communication Networks Using Neural/Fuzzy Techniques

■同意　□不同意

本人具有著作財產權之論文全文資料，授予行政院國家科學委員會科學技術資料中心(或其改制後之機構)、國家圖書館及本人畢業學校圖書館，得不限地域、時間與次數以微縮、光碟或數位化等各種方式重製後散布發行或上載網路。
本論文爲本人向經濟部智慧財產局申請專利（未申請者本條款請不予理會）的附件之一，申請文號爲：_____，註明文號者請將全文資料延後半年後再公開。

■同意　□不同意

本人具有著作財產權之論文全文資料，授予教育部指定送繳之圖書館及本人畢業學校圖書館，爲學術研究之目的以各種方法重製，或爲上述目的再授權他人以各種方法重製，不限地域與時間，惟每人以一份爲限。

上述授權內容均無須訂立讓與及授權契約書。依本授權之發行權爲非專屬性發行權利。依本授權所爲之收錄、重製、發行及學術研發利用均爲無償。上述同意與不同意之欄位若未鉤選，本人同意視同授權。

指導教授姓名：張仲儒

研究生簽名：　　學號：8813811
（親筆正楷）　　（務必填寫）

日期：民國　93　年　6　月　26　日

---

1. 本授權書 (得自 http://sticnet.stic.gov.tw/sticweb/html/theses/authorize.html 下載或至 http://www.stic.gov.tw首頁右下方下載) 請以黑筆撰寫並影印裝訂於書名頁之次頁。
2. 授權第一項者，請確認學校是否代收，若無者，請個別再寄論文一本至台北市(106)和平東路二段106號1702室　國科會科學技術資料中心　黃善平小姐。(電話:02-27377606　傳真：02-27377689)

行動通訊網路之類神經乏晰無線資源配置機制

Radio Resource Allocation Schemes for Mobile Communication Networks Using Neural/Fuzzy Techniques

研究生：陳義昇　　Student: Yih-Shen Chen

指導教授：張仲儒　博士　　Advisor: Dr. Chung-Ju Chang

國立交通大學

電信工程學系

博士論文

A Dissertation
Submitted to Institute of Communication Engineering
College of Electrical Engineering and Computer Science
National Chiao Tung University
in Partial Fulfillment of the Requirements
for the Degree of Doctor of Philosophy
in
Communication Engineering
Hsinchu, Taiwan

2004 年 7 月

行動通訊網路之類神經乏晰無線資源配置機制

研究生：陳義昇　　指導教授：張仲儒

國立交通大學電信工程學系

摘要

爲了支援多媒體服務之叢集性傳輸和異質性服務品質之要求，精確設計無線資源配置機制是必備的，藉以有效提升系統資源使用效率。現有文獻已指出，多媒體服務之特性爲動態傳輸和多樣化傳輸需求，因此有必要應用智慧型技術來解決傳統無線資源配置問題。在本論文中，我們探討行動通訊網路中，應用類神經乏晰技術之無線資源配置機制。

我們首先探討分時多工行動通訊網路之無線資源配置機制。我們採用適應性網路式乏晰推論系統技術，提出一『乏晰資源配置控制器』。該乏晰控制器爲雙層式架構，並挑選新連線需求之頻寬需求、未來換手連線之頻寬保留，以及空中介面效能爲輸入語意變數，所以，此控制器可最大化行動多媒體網路之統計多工特點所衍生之頻寬增益。模擬結果顯示，乏晰資源配置控制器可有效降低換手失敗機率，但不會大幅增加塞機率。同時，與傳統機制相比，此乏晰資源配置控制器可確保服務品質，並且提升系統效能。

接著我們探討 WCDMA 系統之多速率傳輸控制機制。該多速率傳輸控制問題可模型化爲一馬可夫決策鍊過程，而爲了滿足服務品質並提升資源使用率之目的，傳輸成本採用服務品質爲參數。我們應用『Q-learning』學習演算法來精確估算傳輸成本，因此設計了一『Q-learning 式多速率傳輸控制』機制。此外，我們也採用特徵擷取法和 RBFN 類神經網路來解決 Q 函數近似問題，可以降低此機制之狀態空間和記體體需求，並且增進 Q-learning 之收斂特性。模擬結果顯示，Q-learning 式多速率傳輸控制機制可提升 WCDMA 系統之系統容量、用戶滿意度，同時保證服務品質。

最後我們探討多細胞 WCDMA 通訊系統之封包接取控制機制，並且提出一『乏晰 Q-learning 式封包接取控制器』。該控制器包含一『乏晰 Q-learning 式剩餘資源預估器』，和一『封包速率排程器』。該剩餘資源預估器可依據負載狀態，精確預估系統剩餘資源；它選用自身細胞和相鄰細胞之接收干擾量爲輸入語意變數，並採用感知式協調機制來將多細胞環境簡化爲單細胞環境。該排程器則採用改良式指數型排程原則，有效地爲非及時性用戶配置系統資源。模擬結果顯示，在同質性和非同質性多細胞 WCDMA 環境中，該乏晰 Q-learning 式封包接取控制器可有效降低封包錯誤率，並提升非及時性訊務之傳輸速率。

Radio Resource Allocation Schemes for Mobile Communication Networks Using Neural/Fuzzy Techniques

Student: Yih-Shen Chen Advisor: Chung-Ju Chang

Institute of Communication Engineering
National Chiao Tung University

Abstract

To support bursty-transmission and heterogeneous quality of services (QoS) requirements for multimedia services, a well-designed sophisticated radio resource allocation scheme is required to effectively enhance the system utilization. Research has shown that the non-stationarity of work-loads, together with heterogeneous traffic characteristics and QoS constraints of multimedia services, constitute the necessity for applying intelligent techniques in future mobile multimedia networks. In this dissertation, the radio resource allocation schemes by using neural/fuzzy techniques for mobile communication networks are studied.

Firstly, the radio resource allocation scheme for TDMA-based mobile communication networks is investigated. The adaptive-network-based fuzzy inference system (ANFIS) is applied to propose a fuzzy resource allocation controller (FRAC). The FRAC is designed in a two-layer architecture and properly selects the capacity requirement of new call request, the capacity reservation for future handoffs, and the air interface performance as input linguistic variables. Therefore, the statistical multiplexing gain of mobile multimedia networks can be maximized in FRAC. Simulation results indicate that FRAC can keep the handoff call blocking rate low without jeopardizing the new call blocking rate. Also, compared to the conventional schemes, FRAC can indeed guarantee QoS contracts and achieve higher system

performance.

And then, the multi-rate transmission control scheme for WCDMA communication systems is studied. The multi-rate transmission control problem is modelled as a Markov decision process (MDP), where the transmission cost is defined in terms of the QoS parameters for enhancing spectrum utilization subject to QoS constraints. The Q-learning reinforcement algorithm is adopted to accurately estimate the transmission cost and propose a Q-learning-based multi-rate transmission control (Q-MRTC) scheme. In the meanwhile, The feature extraction method and RBFN network are successfully employed for the Q-function approximation. The state space and memory storage requirement are then reduced, and the convergence property of Q-learning algorithm is improved. Simulation results show that, for a multimedia WCDMA system, the Q-MRTC can achieve higher system throughput and better users' satisfaction while the QoS requirements are guaranteed.

Finally, the data access control scheme for multi-cell WCDMA systems is investigated. By using fuzzy Q-learning technique, a novel situation-aware data access manager (FQ-SDAM) is proposed. The FQ-SDAM contains a fuzzy Q-learning-based residual capacity estimator (FQ-RCE) and a data rate scheduler (DRS). The FQ-RCE can accurately estimate the situation-dependent residual system capacity; it appropriately chooses the received interferences from home-cell and adjacent-cell as input linguistic variables and simplifies the multi-cell environment into a single-cell one by applying a perceptual coordination mechanism. Also, the DRS can effectively allocate the resource for non-real-time terminals by adopting a modified exponential rule which takes the interference influence on adjacent cells into consideration. Simulation results show that the FQ-SDAM can effectively reduce the packet error probability and improve aggregate throughput of the non-real-time services in both the homogeneous and non-homogeneous multi-cell WCDMA environment.

Acknowledgements

First of all, I would like to express my sincere gratitude to my advisor, Dr. Chung-Ju Chang, for his patient guidance and profound influence down the road to graduation.

Special thanks go my colleagues in the Broadband Network Lab. and all of my friends, for their genuine encouragement, kind help, and sweet memories.

Finally, I am deeply indebted to my family for their love and understanding. This dissertation is dedicated to my parents. Without their wholehearted care and full support, it is impossible for me to exploit the life in an unburdened way.

Contents

List of Figures

List of Tables

Chapter 1

Introduction

1.1 Motivation

Over the past decades, the development of wireless communication has been astonishing. So is the evolution of the service provisioning in the field of wireless communication. We are now witnessing the transition from the era of mobile telephone to the era of mobile multimedia. With the breakthrough of advanced digital signal processing and antenna technologies, many transmission problems associated with the error-prone and time-varying propagation conditions in wireless communication have been solved. High-bursty and high-volume services over mobile communication networks are no longer scientifically fictional, but real.

In the early '80s, the first generation mobile communication system such as AMPS and NMT using analog transmission techniques were introduced, where FDMA (frequency division multiple access) technique was applied to support multiple access for common radio bandwidth. For FDMA, all the available radio bandwidths are partitioned into a set of channels, and a channel pair is assigned to a communication pair for carrying the voice-only services. With the emergence of digital transmission, the second generation mobile communication systems were introduced in the late 1980s, such as: Global System for Mobile Communications (GSM), Personal Digital Cellular (PDC), IS-95, and IS-136. These sys-

tems adopted digital multiple access techniques, TDMA (time division multiple access) and CDMA (code division multiple access), to increase the spectrum efficiency and the system capacity is largely enhanced. The TDMA technique divides a frame into several slots, where each specific time slot in a frame performs a channel similar to a FDMA channel; on the other hand, the CDMA technology constructs all channels in a common frequency spectrum where each channel has its own unique binary spreading code to identify itself instead of the specific frequency and the time slot.

Circuit-switching and fixed-rate services are the mainstream of mobile services in the first and second generation systems. It is believed that the vision of future telecommunication is "information at any time, at any place, in any form". The traffic characteristics of future mobile services will be much different from those of the traditional mobile services, among which are high-burstiness, variable-rate transmission, and high mobility. Therefore, in the coming new era, advanced radio access techniques and sophisticated radio resource management (RRM) strategies are necessary for future wireless communication systems to support multimedia services.

Advanced TDMA systems, such as: GPRS, adopt packet-switching and multi-slot capability to support dynamic allocation of radio resources for wireless data services. Meanwhile, the third generation WCDMA system introduces variable-length spreading code and other digital processing techniques to provides four types of UMTS service classes [32]: service class A (low-delay data), class B (low-delay data), class C (long-constrained-delay data), and class D (unconstrained-delay data). These service classes have taken the characteristics of multimedia services, such as delay requirement, error rate requirement, variable transmission rate, asymmetry data rate, and so on, into consideration. New radio access techniques, in either the GPRS or the WCDMA system, indeed free up some limitation of service provisioning. However, to support bursty-transmission and heterogeneous QoS (Quality-of-

Service) requirements for multimedia services, a well-designed sophisticated RRM technique is required to effectively enhance the system utilization.

Among many RRM techniques, the dissertation concentrates on the studies of radio resource allocation (RRA) schemes for TDMA and CDMA-based systems. Generally speaking, the main goal of a radio resource allocation scheme is to adequately allocate system resource to mobile terminals according to their service profiles and QoS requirements. For a TDMA system, a RRA scheme performs the functionality of admission control to decide the acceptance or rejection of new/handoff calls. For a CDMA system, considering the time-scale of traffic management and the characteristics of packet-switching mobile multimedia services, the RRA schemes may be further categorized into two kinds: multi-rate transmission control (MRTC) scheme and data access control (DAC) scheme. The MRTC scheme for CDMA systems is performed on longer time scale (*ex*: second or minute), which allocates *power* and *transmission rate* to call/burst connection requests and ensures that the system will not be overloaded, based on the long-term availability of radio resources. On the other hand, the DAC scheme is performed on the shorter time scale (*e.g.*: frame time), which provides bursty transmission permission for non-real-time services, based on the short-term availability of radio resources.

The RRA problems can be mathematically modelled as credit assignment problems (CAP). That is, maximizing system utilization (revenue) while meeting QoS constraints suggests a constrained Markov decision process (MDP) or semi-Markov decision process (SMDP). These methodologies have been successfully applied to solve many network control problems; however, a large state space is required for the modelling. Consequently, the numerical computation is intractable due to the curse of dimensionality. For the TDMA system, the overall system capacity is bounded by the maximum number of available channels (time slots); on the other hand, for the CDMA system, the overall system capacity is

interference-limited and there is no absolute number of available channels. A continuous state space is necessary for the MDP or SMDP methodologies. Another obstacle to apply the mathematical methodologies is *a priori* knowledge of state transition probabilities, which is hard to obtain in advance. Alternatively, some researchers turn to apply intelligent techniques to deal with the RRA problems.

Intelligent techniques, such as neural networks and fuzzy logic systems, have been applied to deal with some resource allocation related problems. Recent research results have proven that these intelligent computations are capable of producing better results than parametric models or other conventional algorithmic approaches when applied to dynamic, non-linear complex systems. Researches have also shown that the non-stationarity of work-loads, together with heterogeneous traffic characteristics and QoS constraints of multimedia services, constitute the necessity for applying intelligent techniques in future mobile multimedia networks. Henceforth, in this dissertation, it is motivated to exploit the merits of intelligent techniques applying to radio resource allocation schemes for mobile communication networks.

1.2 Paper Survey

A mobile communication network, for the purpose of frequency reuse, is typically organized in geographic regions, called cells. When a user moves from one cell to another, the base station in the target cell must take the responsibility for communicating with the user. The call will be forced to be terminated if no channel is available, which is called handoff blocking. Usually, the handoff blocking rate should be kept at an acceptable level in the mobile networks. Therefore, the RRA schemes in the TDMA systems must be sophisticated enough to take the QoS (Quality of Service) requirements of service, such as handoff blocking rate, into consideration, while keeping the new call blocking rate low.

Generally speaking, the RRA schemes performing the functionality of admission control

for TDMA systems can be categorized into two kinds: fixed guard channel scheme [1]-[3] and dynamic resource allocation scheme [4]-[7]. In the fixed guard channel schemes, some channels are reserved for handoff call requests, while remaining channels are shared by the new and handoff calls. Whenever the channel occupancy exceeds the guard channel threshold, new call requests will be rejected. With an appropriate setting of the threshold, the fixed-threshold guard channel schemes can indeed reduce the handoff blocking probability without jeopardizing the new call blocking probability. However, these schemes are not able to adapt to nonstationary loading condition which is a more realistic environment for future mobile services. Alternatively, dynamic resource allocation methods were proposed to reserve an adequate number of channels for handoff call requests. Naghshineh and Schwartz [4] developed a call admission control scheme that took into account the projected future handoff call blocking probabilities in the originating and neighboring cells. The handoff call blocking probabilities were kept at a target objective by blocking the new call requests even if the capacity was currently available to serve these new call requests. For a more realistic network model, Yu and Leung [5] developed another call admission control scheme by estimating the instantaneous handoff call arrival rate and made the guard channel number adaptation for handoff call requests. Unfortunately, only single traffic type is considered in the above-mentioned dynamic schemes.

To deal with heterogeneous traffic types with diverse resource requirements, Ramanathan *et al.* [7] proposed a novel dynamic scheme called *ExpectedMax* strategy . In this scheme, when a new call request occurs, the expected cell residence time of the new call and the expected maximum additional resources reserved for all possible handoff calls during the time interval are estimated firstly. If the estimated maximum additional resources plus the new call requested resource are less than the available resources, the new call will be accepted. The simulation result showed that *ExpectedMax* strategy can achieve lower handoff

blocking probability than the fixed guard channel scheme and the scheme proposed in [5]. To calculate the resource requirement of a call request, the *ExpectedMax* strategy employed the "effective bandwidth" method which had been widely applied to the resource allocation and call admission control in the ATM network [9], [10]. However, under dynamic non-stationary loading conditions, the effective bandwidth is difficult to exactly capture the complete statistics of the multimedia traffic [10], [14]. The spectrum efficiency would be low consequently. Therefore, in Chapter 2, a radio resource allocation scheme is proposed by using adaptive-network-based fuzzy control technique (ANFIS) for the dynamic radio resource allocation in mobile multimedia network.

As above-mentioned, the RRA schemes for the WCDMA systems supporting multimedia services are more complicated and can be categorized into MRTC schemes for long time scale and DAC schemes for short time scale. Choi and Shin [26] proposed an uplink CDMA system architecture to provide diverse QoS guarantees for heterogeneous traffic. They theoretically derived the admission region of real-time connections, transmission power allocation, and the optimum target signal-to-interference ratio of non-real-time traffic so as to maximize the system throughput and satisfy the predefined QoS of heterogeneous traffic.

The main difficulty for RRA schemes in WCDMA system is due to the nature of the interference-limited capacity. Multiple access interference (MAI) largely affects the system capacity, which is a function of the number of active users, users' location, channel impairments, and heterogeneous QoS requirements. Many researches for CDMA capacity estimation are based on MAI and other considerations [27]-[30]. Hämäläinen and Valkealahti [29] proposed an MAI estimation method to facilitate load control, admission control, and packet scheduling. Based on the MAI estimation methods, Many interference-based access control schemes for the WCDMA systems were proposed to exploit the merit of soft capacity [31]-[33]. Instead of a fixed system capacity, this interference-based scheme can adaptively

assign a channel according to the actual system capacity dependent of interference such that the system utilization and the grade of service can be improved. Shin, Cho, and Sung [31] proposed an interference-based channel assignment scheme for DS-CDMA cellular systems. A channel is assigned if the interference is less than an allowed level which is determined by the network, subject to the QoS constraints. In [32], Dimitriou and Tafazolli developed a mathematical model to determine the outage limits of a multiple-service CDMA system and to achieve the maximum aggregated capacity for different system parameters. Phan-Van and Luong [33] proposed a soft-decision call admission control scheme (SCAC), where the upper bound and the lower bound of the interference-limited WCDMA system capacity are derived. In the SCAC, the new call request obtains an admission grant according to a predefined probability function when the system operates between the upper bound and the lower bound of the system capacity.

As noted, the RRA schemes considering QoS constraints can be modelled as constrained Markov decision processes (MDP) [38] or semi-Markov decision processes (SMDP) [34], [35]. However, the computation complexity and the curse of dimensionality are key bottlenecks for applying this methodologies to more realistic network environments. Alternatively, many researchers turned to apply the reinforcement learning (RL) algorithms to solve the problems [36]-[39]. The most obvious advantage of RL algorithm is that, without *a priori* knowledge of state transition probabilities, it could approach an optimal solution from the on-line operation if the RL algorithm is converged. Therefore, in Chapter 4, the system interference profile is chosen as the system state, the service profile of a new call as event, and the multi-rate assignment as the action, to describe the MDP problem for the multi-rate control in the WCDMA system. A RL technique, called *Q-learning*, is applied to propose a Q-learning-based multi-rate transmission control (Q-MRTC) scheme. Also, the feature extraction method and RBFN (radial basis function network) neural network are employed to

reduce the system state space and to improve the property of convergence.

Based on the research results in Chapter 4, a DAC scheme is further proposed to exploit the nature of intermittent transmission of data services in the WCDMA systems. Mostly, a DAC scheme is considered to operate in the multi-cell WCDMA environment. The main purpose of the DAC scheme in WCDMA systems supporting integrated services is to maximize the throughput of non-real-time services while maintaining the transmission quality of real-time services [48]-[51]. To achieve this goal, dynamic access probability schemes [48]-[50] and a base station-controlled scheduling scheme [51] were proposed, where the residual system capacity for non-real-time services was firstly estimated and then shared to non-real-time terminals. A single-cell environment was considered in [48]-[50], while a multi-cell environment was studied in [51]. In the multi-cell scheme [51], the interference generated from other-cell terminals was treated as if from several home-cell ones, and consequently the multi-cell environment was regarded as a single-cell one. However, the mutual-affected behavior of radio resource allocation in the multi-cell environment was still not considered. Without taking the interference influence from adjacent cells into account, the operation of the WCDMA system then would trap into an overloading condition.

The over-loading phenomenon could be alleviated by an appropriate centralized coordination scheme among cells [52]. However, the data access control scheme operates in the short-term time scale, *e.g.* frame time, which makes a distributed one preferable. Kumar and Nanda [53] proposed a distributed scheme called load and interference-based demand assignment (LIDA). The LIDA is a kind of resource reservation-based scheme in which some portions of resource in each cell are reserved against the interference variation. Also, it employs the concept of burst admission threshold for high-rate transmission in a cell to avoid excess interference to adjacent cells .

Additionally, a rate scheduling scheme is also embedded in the data access control scheme

to allocate the residual capacities for non-real-time terminals according to a service principle [54] [55] [56]. To avoid the starvation phenomenon occurred in [54], Jalali, Padovani, and Pankai proposed a *proportional fairness* criterion [55] for a down link scheduling scheme in a CDMA-HDR (high data rate) system. In the scheme, a utility function was defined as a ratio of the supported data rate and the average data rate, where the supported data rate was determined by channel condition and the average data rate was the window average of the transmitted throughput. Unfortunately,this algorithm may lead to large transmission delay for some terminals. Alternatively, Shakkottai and Stolyar proposed an *exponential rule* criterion [56] for the utility function of the scheme to make a good balance between the system throughput and the transmission delay. However, applying the exponential rule to the uplink transmission should have taken the location factor into consideration such that the adjacent cell interference could be maintained to a sustained level. Therefore, in Chapter 4, a novel situation-aware data access manager is proposed by using fuzzy Q-learning technique (FQ-SDAM) for the multi-cell WCDMA systems. The FQ-SDAM contains a fuzzy Q-learning-based residual capacity estimator (FQ-RCE) and a data rate scheduler(DRS): the FQ-RCE can accurately estimate the situation-dependent residual system capacity and the DRS can effectively allocate the resource for non-real-time terminals by adopting a modified exponential rule.

In the past decade, intelligent techniques, such as fuzzy logic control systems and neural networks, have replaced conventional technologies in many scientific applications and engineering systems including the network control systems. They can provide decision-support and expert systems with powerful reasoning capabilities bound by a minimum of rules. The major feature of the fuzzy logic is its ability to express the amount of ambiguity in human thinking and subjectivity in a comparatively undistorted manner. On the other hand, neural networks are a new generation of information processing systems that are constructed to

utilize some of the organizational principles which characterize the human brain. They are able to learn arbitrary nonlinear input/output mapping directly from training data, sensibly interpolate input patterns that are new to the network, and automatically adjust their connection weights to optimize system behaviors [16]. Both fuzzy systems and neural networks are numerical model-free estimators and dynamical systems; they are the intelligent techniques that can improve systems working in uncertain and nonstationary environments. Among many intelligent techniques, the ANFIS, Q-leaning and fuzzy Q-learning are adopted in the works.

1.3 Dissertation Organization

In this dissertation, the radio resource allocation schemes for mobile communication networks by neural/fuzzy techniques are studied. The mobile communication networks which employ TDMA and CDMA in the common air interface are considered. Also, the RRA schemes for long-term and short-term time scales are both studied.

In Chapter 2, the basic concepts of fuzzy systems, neural networks, and integrated neural fuzzy systems are briefly reviewed. The various inference models of fuzzy systems, the learning rules of neural networks, and the benefits of integrated neural fuzzy systems are discussed. Also, their application to the mobile communication network are given.

In Chapter 3, the *Sugeno fuzzy model* is applied to design fuzzy resource allocation controller (FRAC) for wireless communication systems. Among many fuzzy logic system models, the *Sugeno fuzzy model* is the most widely applied one for its high interpretability [17], [20], which provides a systematic approach to generating fuzzy rule from a given input-output data set. The FRAC is designed in a two-layer architecture and properly selects the capacity requirement of new call request, the capacity reservation for future handoffs, and the air interface performance as input linguistic variables.

In Chapter 4, a multi-rate transmission control scheme by Q-learning technique (Q-MRTC) for the multimedia WCDMA systems is proposed to maximize the system utilization and fulfill the users' satisfaction, subject to QoS requirements of packet error probability and packet transmission delay. An evaluation function is defined to appraise the cumulative cost of the consecutive decisions for the Q-MRTC. Without knowing the state transition behavior, the evaluation function is calculated by a real-time RL technique, Q-learning [40]. Also, for the Q-function approximation, a feature extraction method and a RBFN neural network are employed in the Q-MRTC. The feature extraction method maps the state space of the Q-function into a more compact set; the RBFN neural network performs the function approximation for the Q function.

In Chapter 5, a novel situation-aware data access manager using fuzzy Q-learning technique (FQ-SDAM) is proposed for multi-cell WCDMA systems. The FQ-SDAM contains a fuzzy Q-learning-based residual capacity estimator (FQ-RCE) and a data rate scheduler (DRS). The fuzzy Q-learning (FQL) [60] is a reinforcement learning technique applying to FIS. The FQL technique combines the benefits of FIS and reinforcement learning. By applying the FQL technique, the radio resource, therefore, can be managed under partial, uncertain information, and the optimal resource management can be reached in an incremental way. In the FQ-SDAM, the FQ-RCE can accurately estimate the situation-dependent residual system capacity and the DRS can effectively allocate the resource for non-real-time terminals by adopting a modified exponential rule.

Finally, concluding remarks and future research topics are addressed in Chapter 6.

Chapter 2

An Overview of Neural/Fuzzy Techniques

In this chapter, the basic concepts of fuzzy systems, neural networks, and integrated neural fuzzy systems are briefly reviewed. Fuzzy systems and neural networks are both numerical model-free estimators and dynamical systems, which have the capability of modelling complex nonlinear processes to arbitrary degrees of accuracy. Also, the integrated neural fuzzy systems are combining fuzzy systems and neural networks into a functional system to overcome their individual weaknesses; that is, neural networks provide fuzzy systems with learning abilities and fuzzy systems provide neural networks with structural reasoning.

2.1 Introduction

In light of the recent developments of mobile communication networks, future telecommunication networks will consists of heterogeneous access networks and comprise of content-rich services with heterogeneous service characteristics and QoS requirements. Thus, the future mobile communication networks will be highly dynamic communication environments, which require comprehensive and real-time RRM techniques. Traditional modelling and computation techniques are not well-suited to fulfill the requirements of future mobile communication networks. On the other hand, intelligent techniques, such as fuzzy logic systems and neural networks, have attracted the numerous interests in various scientific and engineering areas. These intelligent techniques have the capabilities of soft-computing and adaptation, which are more flexible for network designers to cope with the network control problems. In this chapter, the concept of fuzzy, neural network and integrated neural fuzzy techniques will be briefly introduced.

Both fuzzy and neural network are mimicked the behaviors of human brain: fuzzy logic operates on the way the brain deals with vague information and neural networks are modelled according to the physical architecture of the brain [16]. There are a number of parallels that point out their similarities. Fuzzy systems and neural networks are both numerical model-free estimators and dynamical systems. Also, they have been shown to have the capability of modelling complex nonlinear processes to arbitrary degrees of accuracy. Although the two intelligent techniques are somewhat similar, some significant differences do exist. Fuzzy systems employ fuzzy *if-then* rules as a kind of expert knowledge to formalize insights about the structure of categories founding the real world. Fuzzy systems combine fuzzy sets with fuzzy rules to produce overall complex nonlinear behavior. On the other hand, neural networks are dynamical systems and are adaptively fitting the behavior of the real-world through various their connectionist structures and learning techniques. Neural networks have a large

number of highly interconnected processing elements (nodes) which demonstrate the ability to learn and generalize from training patterns or data; these simple processing elements also collectively produce complex nonlinear behavior.

Alternatively, a recent surge of interests of intelligent techniques is to merge or combine fuzzy systems and neural networks into a functional system to overcome their individual weaknesses. This innovative concept of integration reaps the benefits of both fuzzy systems and neural networks. That is, neural networks provide fuzzy systems with learning abilities, and fuzzy systems provide neural networks with a structural framework with high-level fuzzy *if-then* rule thinking and reasoning. Consequently, the two technologies can complement each other.

The rest of this chapter is organized as follows. The concept of fuzzy inference system (FIS) and three popular architectures of FIS are stated in section 2.2. The learning mechanisms of neural networks are presented in section 2.3. In section 2.4, the concept of integrated neural fuzzy system is described. Finally, the concluding remarks are given in section 2.5.

2.2 Fuzzy Inference System (FIS)

The *fuzzy inference system* (FIS) is a popular computing framework based on the concept of fuzzy set theory, fuzzy *if-then* rules, and fuzzy reasoning. As shown in Fig. 2.1, a fuzzy inference system consists of four fundamental blocks: *fuzzifier*, *fuzzy rule base*, *inference engine*, and *defuzzifier*. The fuzzifier performs a mapping function from observed input x_i to a fuzzy set $T(x_i)$ with degree $M(x_i)$, $i = 1, \ldots, m$. The fuzzy rule base is a knowledge base characterized by a set of linguistic statements in a form of *"if-then"* rules that describe a fuzzy logic relationship between the m-dim input $\{x_i\}$ and the n-dim output $\{y_j\}$. The inference engine performs an implication function according to the pre-condition of the fuzzy rule with the input linguistic terms. It is a decision-making logic that acquires the input

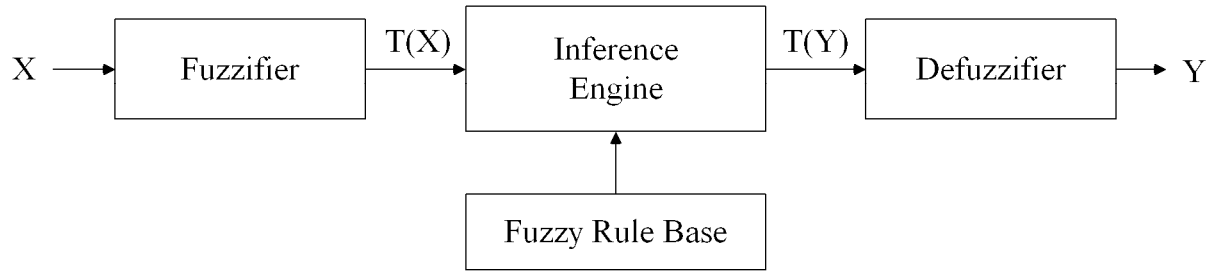

Figure 2.1: The basic structure of fuzzy inference system

linguistic terms of $T(x_i)$ from the fuzzifier and uses an inference method to obtain the output linguistic terms of $T(y_j)$. The defuzzifier adopts a defuzzification function to convert $T(y_j)$ into a non-fuzzy (crisp) value that represents the decision y_j. Among literatures, there are three popular fuzzy models: *Mamdani fuzzy model*, *Tsukamoto fuzzy model*, and *Sugeno fuzzy model* [20]. The brief descriptions of the three fuzzy models are given in the following subsections.

2.2.1 *Mamdani fuzzy model*

Mamdani fuzzy model was proposed as the first attempt to control a system by a set of linguistic control rules obtained from experienced human knowledge. Fig. 2.2 shows an example of Mamdani fuzzy model, where the overall output Z is derived from two linguistic variables X and Y. Here, the fuzzy rule is expressed by

if X is A_i and **Y** is B_i, **then** output Z is C_i with $\mu(C_i)$. i=1 and 2

In the Mamdani model, each input linguistic variable is firstly fuzzified by the membership function $\mu(\cdot)$. Then, the inferred value of the output of each fuzzy rule is determined by a pre-defined inference method. In this example, the min-max method is applied. That is, the inferred value of each fuzzy rule is obtained by *min* operator and the inferred value of the same fuzzy term is obtained by *max* operator. Finally, the overall crisp output is derived by a pre-defined defuzzification method. There are five defuzzification methods: centroid of area (COA), bisector of area (BOA), mean of maximum (MOM), smallest of maximum

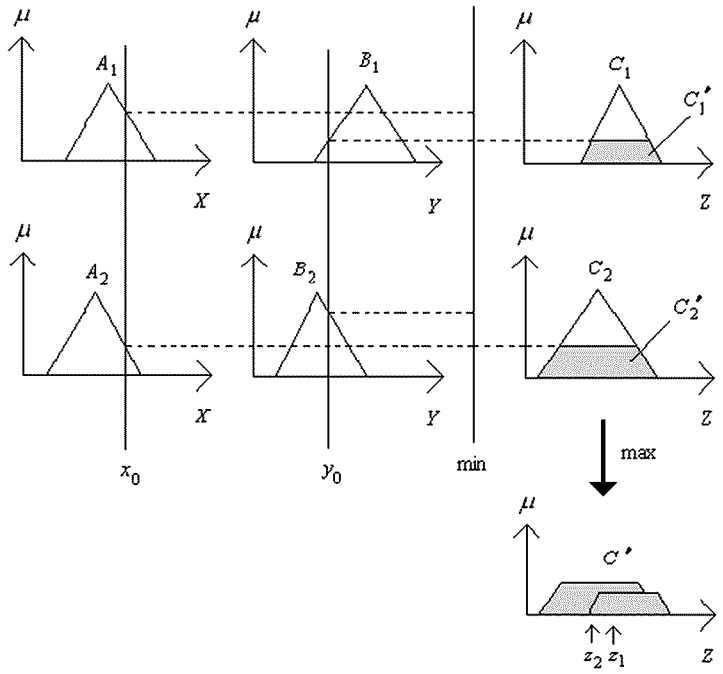

Figure 2.2: An example of Mamdani fuzzy model

(SOM), and largest of maximum (LOM), among which COA is the most popular one.

2.2.2 *Tsukamoto fuzzy model*

Tsukamoto fuzzy model is a special case of Mamdani model. In the Tsukamoto fuzzy model, the consequence part of the *if-then* fuzzy rule is represented by a fuzzy set with *monotonic* membership function, as shown in Fig. 2.3. Therefore, the inferred output of each fuzzy rule is defined as a crisp value obtained by the rule's firing strength. The overall output is calculated by *weighting average* method. It can be seen from Fig. 2.3, the final value of output Z is the weighting average of two fuzzy terms Z_1 and Z_2. The most obvious benefit of Tsukamoto fuzzy model is its simplicity of defuzzification. Since the output of each fuzzy rule is a crisp value, the time-consuming defuzzification process can be avoided. However, the Tsukamoto model lacks the transparency of the rule interpretation. The Tsukamoto fuzzy model is a good candidate of FIS only when the monotonic membership function is

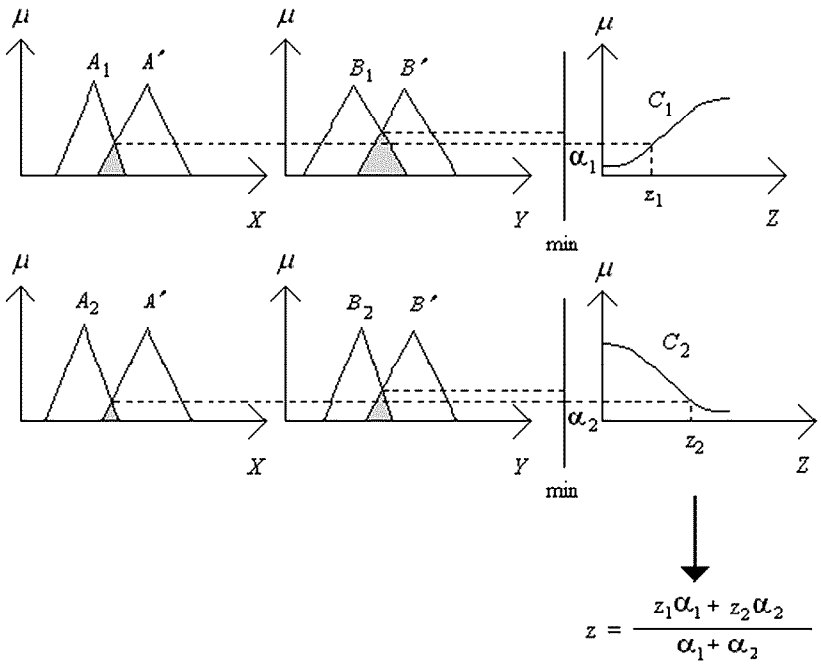

Figure 2.3: An example of Tsukamoto fuzzy model

applicable.

2.2.3 *Sugeno fuzzy model*

Sugeno fuzzy model was proposed by Takagi, Sugeno,and Kang [17]. The main idea of Sugeno fuzzy model is to provide a transparent interpretation of the fuzzy rule and a systematic approach to build up the fuzzy rule base. A typical fuzzy rule in Sugeno model is expressed by

if V_x is A_i and V_y is B_i, **then** output $Z = f(V_x, V_y)$,

where V_x and V_y are input linguistic variables, A and B are fuzzy terms, and the consequent part Z is a function of V_x and V_y. Obviously, the output Z is a crisp function. Also, the function $f(V_x, V_y)$ is usually in a polynomial form. However, the function can be any function as long as it can exactly represent the fuzzy relationship. The two most commonly used Sugeno model are *zero-order Sugeno fuzzy model* and *first-order Sugeno fuzzy model.*

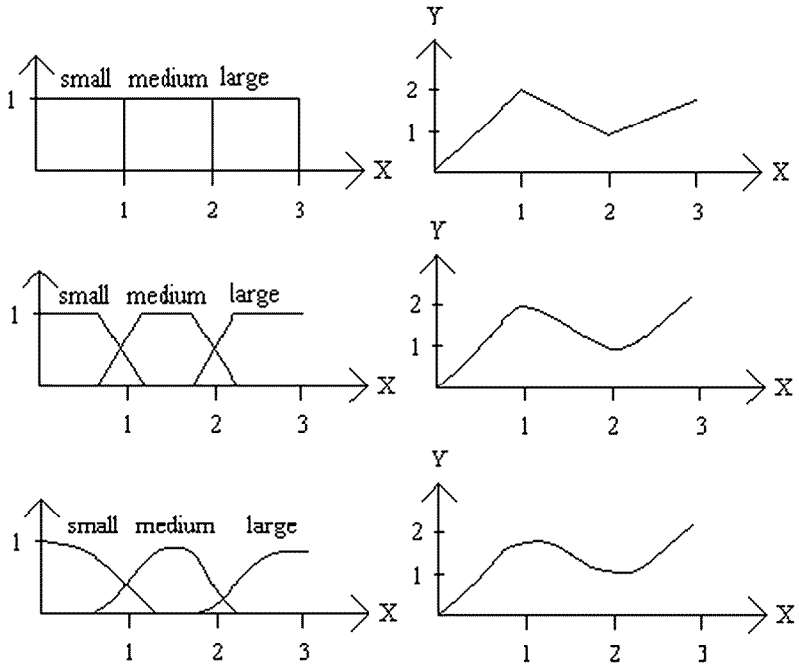

Figure 2.4: The basic concept of Sugeno fuzzy model

For the zero-order Sugeno fuzzy model, the consequent part Z is a fuzzy singleton, which can be viewed as a special case of Mamdani fuzzy model or Tsukamoto fuzzy model. For the first-order Sugeno fuzzy model, the consequent part Z is a linear combination of input linguistic variables. Fig. 2.4 shows an example of Sugeno fuzzy model with single input linguistic variable X. From the figure, it can be seen that the output Y is a linear function of X. The defuzzification method of Sugeno fuzzy model is *weighting sum* method.

Among the three fuzzy models, the Sugeno fuzzy model is the most widely applied one due to its transparency and high-interpretation. Therefore, in this dissertation, the Sugeno fuzzy model is applied in the design of RRA schemes for the mobile communication networks.

2.3 Neural Network

The building blocks of neural network consists of *connectionist structures* and *learning rules* [16]. The connectionist structures are applied to mimic how the human brain works

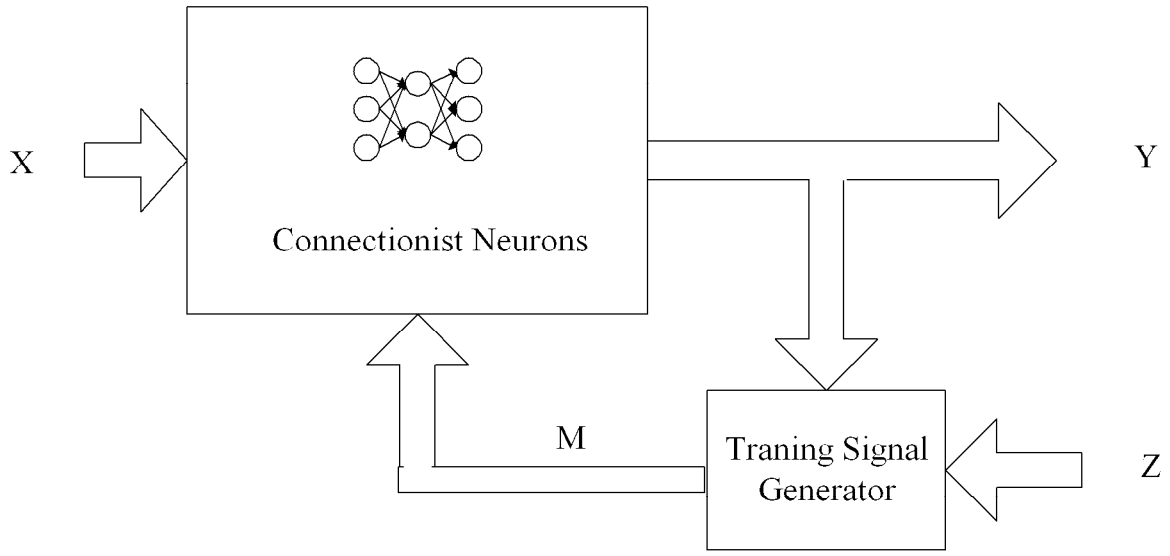

Figure 2.5: The basic structure of neural network

while the learning rules are applied to adaptively modify the behavior of the neural networks through past experience. Fig. 2.5 shows the basic concept of neural network. In the figure, X is the input signal, Y is the actual output, Z is the reference signal, and M is the training signal. The *connectionist neurons* block computes the output signal Y for input signal X and then the *training signal generator* block will generate a training signal according to a specified learning rules. The training signal is used to update the weighting of the nodes in the neural networks.

Generally speaking, the learning rules can be classified into three kinds of categories: *supervised learning*, *reinforcement learning*, and *unsupervised learning*. For different learning rules, there are different sets of Z and M. In the following, the main concepts of three learning rules are briefly described.

2.3.1 *Supervised Learning*

In supervised learning, each input signal X has its own *desired* output D. Here, the reference signal Z is equal to desired output D. When the actual output Y is different from reference signal Z, an error occurs. Then, the training signal will be generated to adjust the weighting

of the nodes in the neural network such that the actual output will approach the reference signal. Therefore, the supervised learning can be considered as a input/output mapping machine or a function approximation tool.

2.3.2 *Reinforcement Learning*

In the reinforcement learning, there is *no desired* output, only a reinforcement signal R. The reinforcement signal is an evaluation value of the actual output Y. For example, in the control problems, the reinforcement signal may be *"good"* or *"bad"*. Here, the reference signal Z is equal to reinforcement signal R. Using the reinforcement signal R, a training signal is generated to update the weighting such that the actual output will achieve a better evaluation value in the future. Therefore, the reinforcement learning is *learning with a teacher*. Using the reinforcement learning, the neural network acts as a controller to make the system work better according to a pre-defined evaluation function.

2.3.3 *Unsupervised Learning*

Unlike the previous two learning rules, there is no feedback information from the environment in the unsupervised learning. Neither the desired output or reinforcement signal are available. Instead, the training signal is generated from actual output Y and the internal weighting of the neural network. The training signal here is used to increase the weighings of the nodes that connect to the actual output. That is, the correlation between the chosen input nodes and output data will be enhanced. In the unsupervised learning, the neural network discovers its patterns and the correlation through experiments, which is called *self-organizing*. Therefore, the unsupervised learning are usually applied to deal with the classification or clustering problems.

2.4 Integrated Neural Fuzzy Technique

In the field of intelligent techniques, the fuzzy system and neural network are complementary techniques. Fuzzy systems provide a high-interpretable reasoning for the collected data, but the design of the fuzzy rules and the membership functions are not easy tasks which require much domain knowledge. Neural networks, on the other hand, are effective and efficient computing architectures or algorithms with self-learning capability, but the connectivity of hidden nodes of the neural network are somewhat like grey boxes. Thus, it is a promising approach to merge and integrate them into a single system. The integration of the two techniques can be classified into two categories: *neuro-fuzzy system* and fuzzy neural system.

The basic concept of a neuro-fuzzy system is to *use the neural network as tool in a fuzzy model.* The neuro-fuzzy systems can provide the self-learning (automatic tuning) capability for the fuzzy systems. In this approach, the system is firstly designed as a fuzzy inference system based on designers' domain knowledge. Then, via numerous experiments, the fuzzy rules and membership functions are tuned by the neural network. The whole design process would be simplified and the development time would be reduced consequently.

In Chapter 3, a kind of neuro-fuzzy technique, called *adaptive-network-based fuzzy inference system* (ANFIS) [18], is applied to deal with the radio resource allocation (RRA) problem in TDMA systems. Since the TDMA systems are the mainstreams of current mobile communication networks, much domain knowledge and experience are available to build up the basic structure of ANFIS-based controller. The values of the membership functions are then adaptively tuned while the ANIFS-based controller is applied to the dynamic TDMA environment. As to the detail of the ANFIS and its application, please refer Chapter 3.

The basic concept of a fuzzy neural system is to *fuzzify the conventional neural network models.* In the fuzzy neural system, the basic properties and node connectivity of neural

network are retained, but the operations and activation functions of the nodes are fuzzified. In this approach, a network's domain knowledge becomes formalized in terms of fuzzy sets, later being applied to enhance the learning of the network in such a way that it learns the mapping between input-output fuzzy sets. Generally speaking, the benefits of the fuzzy neural systems are three-folded: firstly, the input nodes are continuous-valued by fuzzification; secondly, the domain knowledge is applied; and thirdly, some degree of uncertainty of the collected data is allowed.

In Chapter 5, a kind of fuzzy neural technique, *fuzzy Q-learning* (FQL) [60] is applied to deal with the RRA problems in multi-cell WCDMA systems. Since some of the input data are obtained by observation in the multi-cell WCDMA environments, these collected data are vague and partial. By applied the FQL technique, the input data are fuzzified into fuzzy terms and then choose corresponding operation according to domain knowledge. Also, with the capability of learning, the FQL-based RRA scheme can approach an optimal decision policy through experiments. As to the detail of the FQL and its application, please refer to Chapter 5.

2.5 Concluding Remarks

This chapter provides a fundamental overview of the neural/fuzzy techniques, including fuzzy systems, neural networks, and integrated neural fuzzy systems. Both the fuzzy systems and neural networks are mimicked the behaviors of human brains, where the neural network processes the low-level data clustering, classification, and mapping and the fuzzy system processes the high-level reasoning of the input data. The fuzzy systems and neural networks are complementary techniques. It would be beneficial to integrate the two techniques, which contributes to the rising of the integrated neural fuzzy systems.

In the mobile communication networks, the network operations and performance statistics

are chronically collected and stored. These data provide insight and meaningful information for the RRA schemes. However, with the emerging of future content-rich services, the operation of the mobile communication networks tend to be more dynamic and some service scenario may be far beyond imagination. It is almost impossible to design a comprehensive RRA schemes in advance. Therefore, the integrated neural fuzzy systems are promising approaches for the radio resource allocation schemes because, by the integrated neural fuzzy systems, the fuzzy system extracts the basic operation rules from the past records and the neural network adaptively modifies the operation rules of RRA schemes according to the network dynamics. In the following three chapters, the integrated neural fuzzy systems, such as ANFIS and FQL, are applied to design sophisticated RRA schemes for TDMA and WCDMA systems, respectively.

Chapter 3

A Radio Resource Allocation Scheme Using Adaptive-Network-Based Fuzzy Control Technique for Mobile Multimedia Networks

Sophisticated and robust resource management is an essential issue for future mobile multimedia networks. In this chapter, an adaptive-network-based fuzzy inference system (ANFIS) is applied to control the radio resource allocation for mobile multimedia networks. ANFIS, possessing the advantages of fuzzy logic system and neural networks, can provide a systematic approach to find appropriate parameters for the Sugeno fuzzy model. The fuzzy resource allocation controller (FRAC) is designed in a two-layer architecture and properly selects the capacity requirement of new call request, the capacity reservation for future handoffs, and the air interface performance as input linguistic variables. Therefore, the statistical multiplexing gain of mobile multimedia networks can be maximized in FRAC. Simulation results indicate that FRAC can keep the handoff call blocking rate low without jeopardizing the new call blocking rate. Also, compared to the guard channel scheme and ExpectedMax strategy [7], FRAC can indeed guarantee QoS contracts and achieve higher system performance.

3.1 Introduction

Future mobile multimedia networks have to support integrated services, which are with diverse traffic characteristics, in the common air interface. Since the wireless bandwidth is scarce, the design goal of a radio resource allocation (RRA) scheme is to achieve high spectrum efficiency. Therefore, future mobile multimedia networks will employ microcells to support a higher capacity, which will increase the frequency of call handoff and dramatize the effects of nonstationary traffic conditions due to fluctuations in new call arrivals and mobility pattern. The achieved handoff call blocking probability may be far away from the targeted objective [5]. Usually, the handoff blocking rate should be kept at an acceptable level in the mobile networks. Therefore, the RRA scheme must be sophisticated enough to take the QoS (Quality of Service) requirements of service, such as handoff blocking rate, into consideration, while keeping the new call blocking rate low.

In general, the RRA schemes can be categorized into two kinds: fixed guard channel scheme and dynamic resource allocation scheme. In the fixed guard channel schemes [1], [2], [3], some channels are reserved for handoff call requests, while remaining channels are shared by the new and handoff calls. Whenever the channel occupancy exceeds the guard channel threshold, new call requests will be rejected. This scheme is simple, and the simulation result shows that, with an appropriate threshold, it can indeed reduce the handoff blocking probability without jeopardizing the new call blocking probability. Unfortunately, the adequate guard channel threshold is hard to decide. The guard channel schemes were developed traditionally under the assumption of stationary loading condition, and it might not be able to adapt to nonstationary loading condition which is a more realistic environment for integrated services.

Instead of the fixed-threshold guard channel schemes, many dynamic resource allocation methods were proposed to reserve adequate number of channels for handoff call requests

[4]-[7]. That is, the resource allocation partition for the new call and handoff call requests is adaptively assigned. Naghshineh and Schwartz [4] developed a call admission control that took into account the projected future handoff call blocking probabilities in the originating and neighboring cells. The handoff call blocking probabilities were kept at a target objective by blocking the new call requests even if the capacity was currently available to serve these new call requests. Theoretical analysis was carried out for a simple three-cell configuration under stationary loading. In [5], Yu and Leung developed another call admission control scheme for a more realistic network model. They estimated the instantaneous handoff call arrival rate and made the guard channel number adaptation for handoff call requests. To calculate the future handoff blocking probability in a cell, the exponential channel holding time was assumed. Note that the channel holding time depends on the unencumbered cell residence time and the remaining connection duration. Since the unencumbered cell residence time may not be exponentially distributed [8], Yu and Leung's scheme may not be theoretically valid. In [6], Kim *et al.* proposed another dynamic scheme called "dynamic channel reservation scheme"(DCRS). Channels are divided into normal channels and guard channels in the DCRS scheme. Unlike other dynamic schemes, the new call requests are allowed to access the guard channels with a "request probability", which is a heuristic function of channels, reservation threshold, and user mobility. The higher the user mobility is, the smaller the request probability will be. That is, the guard channels are less likely to allocate to new calls with high mobility. All these dynamic schemes have similar results; however, only single traffic type is considered.

To deal with heterogeneous traffic types with diverse resource requirements, Ramanathan *et al.* proposed a dynamic scheme called *ExpectedMax* strategy [7]. In this scheme, when a new call request occurred at time t_0, the expected cell residence time of the new call, τ, and the expected maximum additional resources reserved for all possible handoff calls during the

time interval $[t_0, t_0+\tau)$ are estimated firstly. If the estimated maximum additional resources plus the new call requested resource are less than the available resources, the new call will be accepted. The simulation result showed that *ExpectedMax* strategy can achieve lower handoff blocking probability than the fixed guard channel scheme and the scheme proposed in [5]. To calculate the resource requirement of a call request, the *ExpectedMax* strategy employed the "effective bandwidth" method which had been widely applied to the radio resource allocation and call admission control in the ATM network [9], [10]. However, under dynamic non-stationary loading conditions, the effective bandwidth is difficult to exactly capture the complete statistics of the multimedia traffic [10], [14]. The spectrum efficiency would be low in turn.

Also as noted, in the future mobile multimedia network supporting packet-switching services, a good resource allocation scheme should consider not only the resource requirement of a call request and the resource reserved for handoff calls, but also the air interface performance parameter which can reflect the gain of the statistical multiplexing.

On the other hand, intelligent techniques, such as neural networks and fuzzy logic systems, have been applied to deal with such resource allocation related problems [11]-[14]. Therefore, in this chapter, a fuzzy control scheme is proposed for radio resource allocation in mobile multimedia networks. The fuzzy resource allocation scheme considers the capacity required by the call request, the capacity reservation for handoff requests from neighboring cells, and the performance in the air interface as input variables. Accordingly, a fuzzy resource allocation controller (FRAC) is designed, which is in a two-layer architecture. There are a *fuzzy capacity request estimator*, a *fuzzy capacity reservation estimator*, and a *fuzzy air interface performance estimator* in the first layer. Outputs from these three fuzzy estimators are fed into a *fuzzy call processor* in the second layer to determine whether to accept the call request or not. The fuzzy call processor consists of two sets of fuzzy rule base for new

call and handoff call requests. The FRAC adopts an adaptive-network-based fuzzy inference system (ANFIS) to construct the fuzzy estimators and call processor. ANFIS can provide a systematic way to find appropriate parameters for the wildly-applied *Sugeno fuzzy model*. Since the architecture and the input linguistic variables of FRAC are properly designed, simulation results show that, compared with the guard channel and *ExpectedMax* schemes, the FRAC indeed can guarantee heterogeneous QoS contracts and achieve higher system performance. Also, for a heuristic cost function which is a linear function of new call and handoff call blocking rate, the FRAC has the smallest cost value. Henceforth, the FRAC can make the best balance for resource allocation between new call and handoff call.

The rest of the chapter is organized as follows. The system model is presented in section 2.2. In section 2.3, the concept of FIS and ANFIS are briefly described. The design of the fuzzy resource allocation controller is presented in section 2.4. In section 2.5, the performance comparison under homogeneous and non-homogeneous cases are simulated and discussed. Finally, the concluding remarks are given in section 2.6.

3.2 System Model

3.2.1 *Mobile Multimedia Network Using PRMA*

A mobile multimedia network consists of a cellular network and many nomadic mobile terminals. In each cell, a base station takes responsibility for communicating with the mobile terminals. It keeps the continuity of the call connection when the mobile terminal moves from cell to cell. It will also share its loading information with other neighboring cells for capacity reservation estimation. In the mobile multimedia network, there are N classes of service. Each class of call service has its own traffic parameters and QoS service requirements.

For high spectrum utilization, many future mobile multimedia networks will operate in the packet-switching mode, such as: GPRS. Here, it is assumed that the contention-based

access protocol, such as: packet reservation multiple access (PRMA) protocol, is employed to support multimedia services with heterogeneous traffic characteristics. When a mobile terminal wants to make a call connection, it must gain an access acknowledge through the access contention procedure. Also, it will commit its traffic characteristics and desired QoS requirements (delay bound, delay jitter, loss bound and etc.) during the connection establishment phase.

3.2.2 *Fuzzy Resource Allocation Controller*

The proposed fuzzy resource allocation controller (FRAC) adopts a two-layer architecture. As shown in Fig. 3.1, the first layer contains a *fuzzy capacity requirement estimator*, a *fuzzy air interface performance estimator*, and a *fuzzy capacity reservation estimator*; the second layer contains a *fuzzy call processor*.

The *fuzzy capacity requirement estimator* predicts the equivalent capacity C_e of a connection request from its traffic parameters, peak rate R_p, mean rate R_m, and peak rate duration T_p. A set of fuzzy rules, resulting from knowledge about the equivalent capacity for a connection request in [9], is constructed here to give an appropriate estimation of the required capacity C_e. The *fuzzy capacity reservation estimator* adaptively predicts the capacity reservation C_R for future handoffs so as to keep the handoff blocking rate guaranteed. Choosing the number of possible handoff mobile terminals for i-th service type, $1 \leq i \leq N$, in the home cell, $\hat{SO}_i$, and the number of possible handoff mobile terminals from the neighboring cells, $\hat{SI}_i$, as input linguistic variables, this fuzzy estimator generates an overall capacity reservation index C_R from a set of fuzzy inference rules. The larger the C_R is, the more the capacity reservation is allocated for the future handoff requests will be. The *fuzzy air interface performance estimator*, which adopts a fuzzy logic to reflect the status of the air interface, generates a performance criterion P_c from real-time packet dropping ratio, P_{drop}, and non-real-time packet delay time, D_{delay}. The more positive the P_c is, the less congested

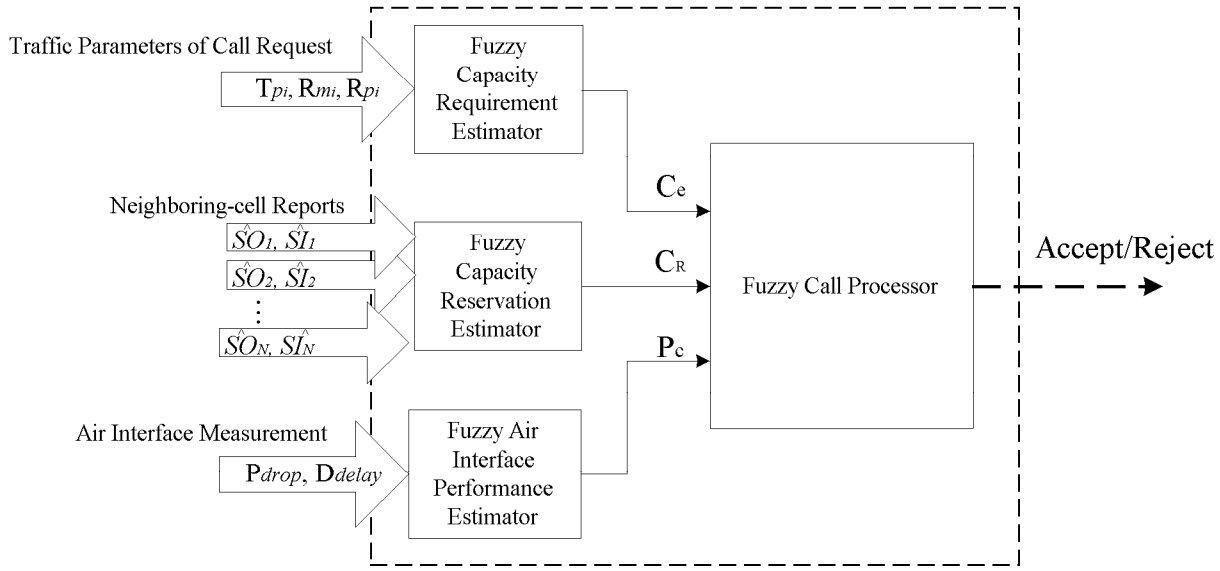

Figure 3.1: The fuzzy resource allocation controller

the air interface will be.

The *fuzzy call processor* has two sets of fuzzy rule base for new call and handoff call requests separately. For a new-call request, the three estimated parameters (C_e, C_R, and P_c) are chosen as the input linguistic variables and a fuzzy new-call rule base is employed. Clearly, the larger C_e, the larger C_R, and the smaller P_c are, the less possible the new call request would be accepted. On the other hand, for the handoff-call request, the two estimated parameters (C_e and P_c) are chosen as input linguistic variables and a fuzzy handoff-call rule base is employed. The smaller C_e and the larger P_c are, the more possible the handoff call would be accepted.

3.3 Fuzzy Inference System and ANFIS

3.3.1 *Fuzzy Inference System*

The fuzzy inference system (FIS) is a popular computing framework based on the concept of fuzzy set theory, fuzzy if-then rules and fuzzy reasoning. Among many fuzzy inference

system models, the *Sugeno fuzzy model* is the most widely applied one for its high interpretability [17], [20]. The *Sugeno fuzzy model* provides a systematic approach to generate fuzzy rule from a given input-output data set. The *first-order Sugeno fuzzy model* is applied to design the proposed fuzzy estimators in which the crisp output is a polynomial of the input linguistic variables. In the *first-order Sugeno fuzzy model*, the fuzzy rule may be stated as

$$\text{if } X \text{ is } A \text{ and } Y \text{ is } B, \text{ then } z = f(X,Y) = p \times X + q \times Y + r, \tag{3.1}$$

where A and B are terms of the fuzzy sets in the antecedent, $z = f(X, Y)$ is a crisp output in the consequent, and p, q, r are the parameters of the polynomial. Since each rule has a crisp output, in the defuzzification process, the overall output is simply obtained by a weighted average as

$$z = \frac{\sum_i w_i \times z_i}{\sum_i w_i}, \tag{3.2}$$

where w_i and z_i represent the weight and output of the i-th fuzzy rule, respectively. In the application of *Sugeno fuzzy model*, the main task is to appropriately select the membership functions and parameters of the polynomial functions.

3.3.2 *ANFIS: Adaptive-Network-based Fuzzy Inference System*

The adaptive network based FIS (ANFIS) system employs the adaptive network architecture to represent the fuzzy inference system. Combined with the hybrid learning scheme, ANFIS can provide a systematic way to find appropriate membership functions and polynomial parameters for the *Sugeno fuzzy model* [18]. ANFIS can be applied to a wide range of areas, such as nonlinear function modelling, time series prediction, and fuzzy controller design [19], [20]. To describe the structure and node functions of the ANFIS, take the following case as an example.

Consider a fuzzy system with 2 linguistic variables (X and Y) and each variable is divided

into two fuzzy terms. Fig. 3.2 illustrates how the ANFIS represents the *first-order Sugeno fuzzy model*. The node function of each layer is described as below:

Layer 1: Every node i in this layer is a square node and its node function, denoted by $Q_{1,i}$, is given by

$$Q_{1,i} = \begin{cases} \mu_{A_i}(X), & \text{for } i\text{=}1,\ 2 \\ \mu_{B_{i-2}}(Y), & \text{for } i\text{=}3,\ 4, \end{cases} \tag{3.3}$$

where X (or Y) is the input to the node i, A_i (or B_{i-2}) is a linguistic term associated with the node, and μ_{A_i} ($\mu_{B_{i-2}}$) is the membership function for the term A_i (B_{i-2}). In other words, each node function specifies the degree to which the given input X (or B) satisfies the qualifier A_i (or B_{i-2}).

Layer 2: Every node i in this layer is a circle node labelled Π, which represents the firing strength of i-th rule and performs the fuzzy AND operation, $1 \leq i \leq 4$. The output of node i, denoted by $Q_{2,i}$, is the product of all the incoming signals for the i-th rule is given by

$$Q_{2,i} = w_i = \begin{cases} \mu_{A_1}(X) \times \mu_{B_i}(Y), & \text{for } i\text{=}1,\ 2 \\ \mu_{A_2}(X) \times \mu_{B_{i-2}}(Y), & \text{for } i\text{=}3,\ 4. \end{cases} \tag{3.4}$$

Layer 3: Every node i in this layer is a circle node labelled N. The ith node calculates the ratio of the i-th rule's firing strength to the sum of all rules' firing strength. That is, the output of node i, denoted by $Q_{3,i}$ is the *normalized firing strength* and calculated as

$$Q_{3,i} = \bar{w_i} = \frac{w_i}{\sum_j w_j}, 1 \leq i \leq 4. \tag{3.5}$$

Layer 4: Every node i in this layer is a square node with a node function

$$Q_{4,i} = \bar{w_i} \times f_i = \bar{w_i} \times (p_i \times X + q_i \times Y + r_i), 1 \leq i \leq 4, \tag{3.6}$$

where $Q_{4,i}$ is the output and p_i, q_i, r_i are the consequent parameter sets of node i.

Later 5: The single node in this layer is a circle node labelled Σ that computes the overall output Q_5 as the summation of all incoming signals.

$$Q_5 = \sum_i Q_{4,i} = \sum_i \bar{w_i} \times f_i = \frac{\sum_i w_i \times f_i}{\sum_j w_j} \tag{3.7}$$

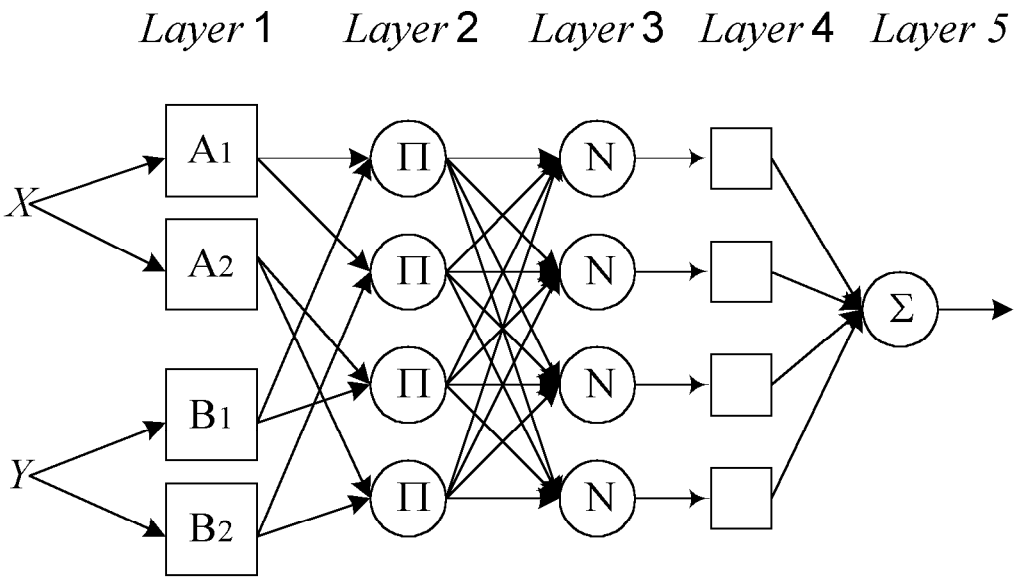

Figure 3.2: The example of ANFIS system

3.3.3 *Hybrid Learning Rule for ANFIS*

For short training epochs, ANFIS adopts a hybrid learning rule, combining the "gradient decent method" and the "least square estimate" (LSE) method, as the learning rule for ANFIS. In the hybrid learning rule, each training epoch is composed of a *forward pass* and a *backward pass*. In the *forward pass*, after the input data is presented, the node output $Q_{4,i}$ can be calculated with current node parameters. The node output is compared with the desired output, and the measure error is derived. Then, the LSE method is employed to adjust the parameter sets (p_i, q_i, and r_i). On the other hand, in the *backward pass*, the error signals, the derivative of the measured error with respect to each node output, propagate from the output end to the input end. Henceforth, the gradient decent method is employed to adjust the parameters of the membership functions. Since the training errors are de-coupled and separately treated, the hybrid learning rule can dramatically reduce the required training epochs. The details of the hybrid learning rule can be found in [20].

3.4 Fuzzy Resource Allocation Controller

3.4.1 *Fuzzy Capacity Request Estimator*

The fuzzy capacity request estimator is a fuzzy implementation of the effective bandwidth method proposed in [9]. It has three input linguistic variables R_p, R_m, T_p and a crisp output C_e. In order to accommodate a wide variety of different traffic sources, a logarithmic function is employed for input linguistic variables R_p and T_p based on the analytic results of the equivalent capacity method. The membership functions for the variable R_m are divided by R_p so as to use as an indicator of burstiness. Via extensive experiments, it is good enough to fuzzify the linguistic variables into three terms for R_p and two terms for both R_m and T_p. Hence, the fuzzy term sets are $T(R_p)$={Small, Medium, Large}={*Sm, Me, La*}, $T(R_m)$={Low, High}={*Lo,Hi*}, and $T(T_p)$={Short, Long}={*Sh, Lg*}. The membership functions for $T(R_p)$, $T(R_m)$, and $T(T_p)$ are defined as $M(R_p) = \{\mu_{Sm}, \mu_{Me}, \mu_{La}\}$, $M(R_m) = \{\mu_{Lo}, \mu_{Hi}\}$, and $M(T_p) = \{\mu_{Sh}, \mu_{Lg}\}$. For being differentiable in the training phase, the bell-shape function is adopted as the membership function, which are given by

$$b(x; m, \sigma) = e^{-\frac{(x-m)^2}{\sigma^2}}, \tag{3.8}$$

Therefore, the membership functions are expressed as

$$\mu_{Sm}(R_p) = b(log(R_p); m^{Sm}, \sigma^{Sm}), \tag{3.9}$$

$$\mu_{Me}(R_p) = b(log(R_p); m^{Me}, \sigma^{Me}), \tag{3.10}$$

$$\mu_{Lg}(R_p) = b(log(R_p); m^{Lg}, \sigma^{Lg}), \tag{3.11}$$

$$\mu_{Lo}(R_m) = b(\frac{R_m}{R_p}; m^{Lo}, \sigma^{Lo}), \tag{3.12}$$

$$\mu_{Hi}(R_m) = b(\frac{R_m}{R_p}; m^{Hi}, \sigma^{Hi}), \tag{3.13}$$

$$\mu_{Sh}(T_p) = b(log(T_p); m^{Sh}, \sigma^{Sh}), \tag{3.14}$$

$$\mu_{Lg}(T_p) = b(log(T_p); m^{Lg}, \sigma^{Lg}). \tag{3.15}$$

The crisp output C_e is expressed in the first-order polynomial form as Eq. (3.1). The implementation of the estimator utilizes the MATLAB fuzzy tool box and the procedure is described in Fig. 3.3. In the beginning, the numerical data are divided into two data sets: In_data for training the fuzzy estimator and $Test\_data$ for verifying the function parameters. Two fuzzy commands, *genfis1* and *anfis*, are applied to construct the ANFIS model: the *genfis1* command constructs the initial parameters (membership functions and the output crisp function) for fuzzy inference system, and the *anfis* command adopts the hybrid learning rule to find the appropriate parameters. After the system is fine-tuned, a consequent verification is done by feeding the testing data into the estimator. If the verifying performance is not good, the estimator would enlarge the training epochs to minimize the error.

After training phase, the membership functions of the input linguistic variables and the polynomial parameters of the output crisp are derived. Note that, the following fuzzy estimators still take the same MATLAB design procedure to obtain the settings of membership functions and polynomial parameters in the ANFIS.

3.4.2 *Fuzzy Capacity Reservation Estimator*

The *fuzzy capacity reservation estimator* adaptively predicts the capacity reservation for the possible handoff calls from neighboring cells during the time interval $[t_0, t_0+\tau)$. Dealing with heterogeneous traffic characteristics, the estimator takes a two-step approach for the capacity reservation. In the first step, the estimator calculates the possible net terminal change for i-th service type, HC_i, by fuzzy operation. In the second step, based on the equivalent capacity C_e from the *fuzzy capacity requirement estimator*, the estimator computes the overall capacity reservation index, C_R.

In the *ExpectedMax* strategy, the estimated maximum additional resource is an expectation value of the change of possible incoming and outgoing calls at the target cell, not just the difference between these calls. Here, the *fuzzy capacity reservation estimator* takes advantage

```
% training data
In_data = [...]
Test_data = [...]

% calculate the data size
Data_size = length( In_data(:,1));
trn_data = In_data(1:1:Data_size,:);
trn_data = In_data(2:2:Data_size,:);

% number of fuzzy term sets
NumMfs = 3;

% Membership function
MfType = 'gbellmf';

% training epoch
NumEpochs = 100; StepSize = 0.1;

% generate the Sugeno FIS
InputFismat = genfis1(In_data, NumMfs, MfType);

% Utilize the ANFIS
OutputFismat = anfis(In_data, InputFismat, [NumEpochs NaN StepSize]);

% Test result
   Result = evalfis(Test_data, OutputFismat);
```

Figure 3.3: The procedure of *fuzzy capacity requirement estimator*

of soft computing capability of fuzzy system to reduce the time-consuming computation in *ExpectedMax* strategy. In accordance with knowledge of calculating the possible terminal change from the *ExpectedMax* strategy [7], for the estimator, $\hat{SO}_i$ in the home cell and $\hat{SI}_i$ in the neighboring cells are chosen as the 2 input linguistic variables, while HC_i is the crisp output. $\hat{SO}_i$ is the number of terminals of i-th service type that residue in the target cell at time t_0 and will handoff to neighboring cells during the time interval [t_0, $t_0+\tau$); $\hat{SI}_i$ is the average number of terminals of i-th service type that residue in neighboring cells at time t_0 and will handoff to the target cell during the time interval [t_0, $t_0+\tau$). For explanation, it is assumed that a new call request in cell 0 at time t_0 and the surrounding cells, cell 1 $\sim$ cell

6, are considered. The $\hat{SO}_i$ and $\hat{SI}_i$ can be generally obtained by

$$\hat{SO}_i = N_{0,i} \times p_{h,i} \tag{3.16}$$

and

$$\hat{SI}_i = \frac{1}{6} \sum_{j}^{6} N_{j,i} \times p_{h,i}, \tag{3.17}$$

where $N_{0,i}$ is the number of terminals of i-th service type in the target cell, $N_{j,i}$ is the current number of terminals of i-th service type in the neighboring cell j, and $p_{h,i}$ is the probability that a terminal of i-th service type will handoff to the adjacent cells during the time interval $[t_0, t_0+\tau)$. Here it is assumed that the terminal moves to each of the neighboring cells with equal probability.

To extract the exact knowledge of the *ExpectedMax* strategy, large numerical data were acquired by extensively calculating the capacity reservation in [7] for the various combination of system parameters. From conclusion of the numerical results, each of the input linguistic variable is divided into 3 fuzzy terms. Accordingly, the estimator has 9 fuzzy rules. The term sets of the variables are T($\hat{SO}_i$) = {Small, Medium, Large} ={Sm_o, Me_o, Lg_o}, and T($\hat{SI}_i$) = {Small, Medium, Large} ={Sm_i, Me_i, Lg_i}. The corresponding membership functions are defined as M($\hat{SO}_i$) = {μ_{Sm_o}, μ_{Me_o}, μ_{Lg_o}} and M($\hat{SI}_i$) = {μ_{Sm_i}, μ_{Me_i}, μ_{Lg_i}}. Therefore, the membership functions for the input linguistic variables are expressed as:

$$\mu_{Sm_o}(\hat{SO}_i) = b(\hat{SO}_i; m^{Sm_o}, \sigma^{Sm_o}), \tag{3.18}$$

$$\mu_{Me_o}(\hat{SO}_i) = b(\hat{SO}_i; m^{Me_o}, \sigma^{Me_o}), \tag{3.19}$$

$$\mu_{Lg_o}(\hat{SO}_i) = b(\hat{SO}_i; m^{Lg_o}, \sigma^{Lg_o}), \tag{3.20}$$

$$\mu_{Sm_i}(\hat{SI}_i) = b(\hat{SI}_i; m^{Sm_i}, \sigma^{Sm_i}), \tag{3.21}$$

$$\mu_{Me_i}(\hat{SI}_i) = b(\hat{SI}_i; m^{Me_i}, \sigma^{Me_i}), \tag{3.22}$$

$$\mu_{Lg_i}(\hat{SI}_i) = b(\hat{SI}_i; m^{Lg_i}, \sigma^{Lg_i}). \tag{3.23}$$

By the fuzzy operation, the possible net terminals change for each service type HC_i, is calculated individually in the estimator. Then, the overall capacity reservation index C_R is calculated by summing the capacity reservation for each service type; that is,

$$C_R = \sum_{i=1}^{N} HC_i \times C_{e_i}, \tag{3.24}$$

where C_{e_i} is the capacity request for i-th service type and is calculated at the *fuzzy capacity requirement estimator*.

3.4.3 *Fuzzy Air Interface Performance Estimator*

In the mobile multimedia networks, the resource usage of a call request is affected by not only the source traffic parameters but also the noisy transmission channel conditions and access procedure. The *fuzzy air interface performance estimator* is designed to reflect the real resource usage in the air interface.

In order to reflect the status of the air interface and keep the QoS contract, a performance criterion P_c is heuristically defined, which is a function of the real-time packet dropping ratio, P_{drop}, and the non-real-time packet delay time, D_{delay}, in the air interface, as

$$P_c = r \ln \frac{P^*_{drop}}{P_{drop}} + (1 - r) \ln \frac{{D_{delay}}^*}{D_{delay}}, \tag{3.25}$$

where P^*_{drop} and D^*_{delay} are the QoS requirements of P_{drop} and D_{delay} for the real-time and non-real-time services in the air interface, respectively, and r is a weighting parameter, $0 \leq r \leq 1$ [21]. In this chapter, the value of r is chosen to be 0.7. Here it is assumed that the lost non-real-time packets will be re-transmitted while the lost real-time ones will not. Therefore, P_{drop} for real-time services and D_{delay} for non-real-time services are the two performance measurements in the air interface.

The *fuzzy air interface performance estimator* is a fuzzy computation of the performance criterion P_c, which takes P_{drop} and D_{delay} as two input linguistic variables. After many simulation experiments, the term set of P_{drop} is defined as $T(P_{drop})$={Low, Medium, High}=

$\{Lo,\ Me,\ Hi\}$ and the term set of D_d as $T(D_{delay})$={Short, Long}=$\{Sh,\ Lg\}$. The membership functions for $T(P_{drop})$ and $T(D_{delay})$ are defined as $M(P_{drop}) = \{\mu_{Lo}, \mu_{Me}, \mu_{Hi}\}$ and $M(D_{delay}) = \{\mu_{Sh}, \mu_{Lg}\}$, where

$$\mu_{Lo}(P_{drop}) = b(P_{drop}; m^{Lo}, \sigma^{Lo}), \tag{3.26}$$

$$\mu_{Me}(P_{drop}) = b(P_{drop}; m^{Me}, \sigma^{Me}), \tag{3.27}$$

$$\mu_{Hi}(P_{drop}) = b(P_{drop}; m^{Hi}, \sigma^{Hi}), \tag{3.28}$$

$$\mu_{Sh}(D_{delay}) = b(D_{delay}; m^{Sh}, \sigma^{Sh}), \tag{3.29}$$

$$\mu_{Lg}(D_{delay}) = b(D_{delay}; m^{Lg}, \sigma^{Lg}). \tag{3.30}$$

3.4.4 *Fuzzy Call Processor*

The *fuzzy call processor* is responsible for deciding the acceptance of the call request. For a new call request, the call processor takes the C_e, C_R, and P_c as three input linguistic variables, which reflect capacity requirement of the call request, capacity reservation for future handoffs, and the degree of congestioness in the air interface. The synergy of C_e and P_c can reflect the shaping effect of the contention procedure and in turn takes the advantage of the multiplexing gain of serving different QoS requirement services. For a handoff call request, the call processor just takes C_e and P_c as two input linguistic variables. It is not necessary to take the C_R as the input variable since the handoff call is a priority call that must be served first. Accordingly, two sets of rule base are designed for the two different call requests.

The term set of C_e is defined as $T(C_e)$={Small, Medium, Large}=$\{Sm,\ Md,\ Lg\}$, C_R as $T(C_R)$={ Low, Medium, High}=$\{Lo,\ Me,\ Hi\}$, and P_c as $T(P_c)$={Good, Common, Bad}=$\{Gd,\ Cm,\ Bd\}$. The membership functions for $T(C_e)$, $T(C_R)$,and $T(P_c)$ are defined as $M(C_e) = \{\mu_{Sm}, \mu_{Md}, \mu_{Lg}\}$, $M(C_R) = \{\mu_{Lo}, \mu_{Me}, \mu_{Hi}\}$, and $M(P_c) = \{\mu_{Gd}, \mu_{Cm}\, \mu_{Gd}\}$, where

$$\mu_{Sm}(C_e) = b(C_e; m^{Sm}, \sigma^{Sm}), \tag{3.31}$$

$$\mu_{Md}(C_e) = b(C_e; m^{Md}, \sigma^{Md}), \tag{3.32}$$

$$\mu_{Lg}(C_e) = b(C_e; m^{Lg}, \sigma^{Lg}), \tag{3.33}$$

$$\mu_{Lo}(C_R) = b(C_R; m^{Lo}, \sigma^{Lo}), \tag{3.34}$$

$$\mu_{Me}(C_R) = b(C_R; m^{Me}, \sigma^{Me}), \tag{3.35}$$

$$\mu_{Hi}(C_R) = b(C_R; m^{Hi}, \sigma^{Hi}), \tag{3.36}$$

$$\mu_{Gd}(P_c) = b(P_c; m^{Gd}, \sigma^{Gd}), \tag{3.37}$$

$$\mu_{Cm}(P_c) = b(P_c; m^{Cm}, \sigma^{Cm}), \tag{3.38}$$

$$\mu_{Bd}(P_c) = b(P_c; m^{Bd}, \sigma^{Bd}). \tag{3.39}$$

3.5 Simulation Results and Discussion

The performance of the FRAC is compared with those of *ExpectedMax* [7] and guard channel schemes under stationary and non-stationary traffic loading environments. The simulated mobile network contains 49 concatenated cells, and all the cells are wrapped around at the edges so as to avoid the edge effects. The mobile multimedia network provides voice and data services. The air interface adopts the PRMA protocol for media access control. The frame structure is the same as the one used in [22], where each frame time T_f is $16msec.$, the number of time slots per frame is 20, and each time slot has 576 bits, including 64 bits header and 512 bits information. For the PRMA access protocol, the permission probability of voice (p_v) and data (p_d) are set to be 0.65 and 0.03, respectively, to give the voice service with priority much higher than the data service.

The voice service is modelled as an ON-OFF traffic source, and the mean talkspurt time ($1/\alpha$) is 1 sec. and the mean silence time ($1/\beta$) is 1.35 sec. On the other hand, the data service is modelled as a batch Poisson traffic source, and the interarrival time of two successive data messages is exponentially distributed with mean message arrival rate $1/\lambda_d = 0.4$. The

length of data message is assumed to be a geometric distribution function with mean length $L_m = 3$ and maximum length $L_x = 10$. The QoS requirement of voice-packet dropping rate P^*_{drop} is set to 1×10^{-2} and the QoS requirement of the data transmission delay D^*_{delay} is $1sec.$ The input linguistic variables, P_{drop} and D_{delay}, are measured per 1250 frames and the estimation period τ is $10sec.$

Conventionally, the guard channel scheme is considered in the circuit-switching network. To apply this scheme in the QoS-guaranteed, packet-switching mobile network, the activity factor (expected busy period) for voice (L_v) and data (L_d) services are defined as:

$$L_v = \frac{\frac{1}{\alpha}}{\frac{1}{\alpha} + \frac{1}{\beta}} \tag{3.40}$$

$$L_d = \lambda_d \times T_f \times L_m. \tag{3.41}$$

The activity factor represents the channel capacity that the specified service may occupy. The activity factor is 0.43 for voice service and 0.12 for data service. In the simulations, the guard channel schemes G_1, G_2, and G_3 with 1, 2, and 3 reserved channels are considered. Also, for fair comparison, the *fuzzy capacity requirement estimator* is adopted as the effective bandwidth calculation block for the *ExpectedMax* strategy.

3.5.1 *Stationary Load Case*

This case is meant to capture the behavior of a uniform network where all cells are identical in terms of new call arrival rate and cell dwell time. The probabilities of moving to neighboring cells are also uniform. Here, it is assumed that the service time and cell dwell are both 100 sec., and four different new call arrival rates: 1/4.0, 1/3.75, 1/3.5, and 1/3.25 are simulated. The simulation results are shown in Fig. 3.4 - Fig. 3.6.

Fig. 3.4(a) and Fig. 3.4(b) show the new call blocking rate and handoff call blocking rate of the voice service ($B_{n,v}$, $B_{h,v}$) and data service ($B_{n,d}$, $B_{h,d}$), respectively. In Fig. 3.4(a), for

voice service, the new call blocking rate of FRAC is the smallest, and the handoff blocking rate of FRAC is almost the same as that of G_2 scheme except when the new call arrival rate is 1/3.25. The new and handoff call blocking rates of the *ExpectedMax* strategy are between those of G_1 and G_2 schemes, but larger than those of the FRAC. The FRAC outperforms the *ExpectedMax* strategy. It is because FRAC takes not only the capacity requirements (C_e and C_R) as the factors for the radio resource allocation but also the air interface performance criterion P_c. FRAC can still accept a voice handoff call request when C_R and C_e are large but P_c is still good or common. That is, FRAC can take advantage of the multiplexing gain of packet-switching from the input linguistic variable P_c. In Fig. 3.4(b), for data service, the new call blocking rate and the handoff blocking rate of FRAC are the smallest among all the compared schemes. This is because the data service is non-real-time and can be buffered when the resource is temporarily unavailable. Therefore, the multiplexing gain of data service would turn out to be larger than that of voice service.

To make an overall performance evaluation, the cost functions are heuristically defined by

$$\begin{aligned} CF_v &= \zeta \times B_{n,v} + (1-\zeta) \times B_{h,v}, \text{ for voice service,} \\ CF_d &= \zeta \times B_{n,d} + (1-\zeta) \times B_{h,d}, \text{ for data service,} \end{aligned} \tag{3.42}$$

where ζ is a weighting parameter and $\zeta = 0.25$. Fig. 3.5 shows the cost function versus the new call arrival rate. The cost values of the FRAC are the smallest under all load conditions. It is because the proposed FRAC adaptively utilizes the gain of the statistical multiplexing in the mobile multimedia networks and makes the proper capacity reservation for future handoffs according to the network loading, while keeping QoS contracts.

Fig. 3.6 shows the voice packet dropping rate and data packet delay versus the new call arrival rate. All the schemes can meet the QoS requirements, but the FRAC has higher packet dropping rate and larger data delay than the other schemes. It is because the FRAC

takes the advantage of the multiplexing gain and accommodates more terminals consequently.

3.5.2 *Non-stationary Load Case*

This case is meant to capture the behavior of a non-stationary loading network where each cell has its unique new call arrival rate and each service type has its cell dwell time. The network simulates the work-hour traffic pattern which is similar to the one described in [7]. For each cell, the new call arrival rate increases in the first half of the simulation and then decreases in the second half. In the first half, the new call arrival rate starts at 0.15 and increase every 30 minutes. The increase ratio is uniformly distributed between 1.0 and 1.3, and differs from cell to cell. Similarly, in the second half, the call arrival rate decreases every 30 minutes and the decrease ratio is also uniformly distributed between 1.3 and 1.0. It is assumed that the service time of voice terminal is 200 seconds and that of data terminal is 150 seconds. The cell dwell time of voice terminal is 125 seconds and that of data terminal is 100 seconds. The QoS requirement of handoff blocking rate of voice ($B^*_{h,v}$) and data ($B^*_{h,d}$) both are 0.02. The simulation results are measured every 20 minutes, and shown in Fig. 3.7 - Fig. 3.10.

Fig. 3.7 and Fig. 3.8 show the new call blocking rate and the handoff call blocking rate of the voice service ($B_{n,v}$, $B_{h,v}$) and data service ($B_{n,d}$, $B_{h,d}$), respectively. Evidently, the blocking rate increases in the first half as the new call arrival rate increases, and it decreases in the second half as the new call arrival rate decreases. The FRAC has the smallest new call blocking rates of voice and data services while keeping the handoff blocking rate lower than QoS thresholds ($B^*_{h,v}$ and $B^*_{h,d}$). For the *ExpectedMax* strategy, the handoff blocking rate of voice and data service are lower than QoS threshold in the non-congested period, but are higher than the QoS threshold at higher traffic loading. As to the fixed guard channel schemes, the G_2 and G_3 schemes can keep the handoff blocking rate lower than the QoS thresholds but G_1 scheme can't. Fig. 3.9 shows the overall utilization versus simulation

time. The system utilization is defined as the percentage of the number of slots that are occupied by active terminals. The system utilization of FRAC is the highest and that of the guard channels schemes (G_2 and G_3) are the lowest. At the beginning period (simulation time 1), the system utilization of FRAC, *ExpectedMax*, G_1, G_2 and G_3 are 0.72, 0.69, 0.7, 0.66, 0.62, respectively. At the most congested period (simulation time 6), the system utilization of FRAC, *ExpectedMax*, G_1, G_2 and G_3 are 0.83, 0.77, 0.78, 0.74, 0.7, respectively. Therefore, the system utilization of FRAC is the highest and that of the guard channels schemes (G_2 and G_3) are the lowest.

During the entire simulation, only the G_2, G_3 and FRAC can exactly meet the QoS requirement of the handoff blocking rate. FRAC has the highest system utilization; however, the G_2 and G_3 schemes have lower and guaranteed handoff blocking rate at the expense of the low system utilization. Since the new call arrival rate is different in every cell, the number of handoff call request is also different in every cell. While the fixed guard channel schemes are applied in the non-stationary network, the system performance may be suffered from the network dynamics. In the non-stationary load case, the handoff blocking rate in the hot-spot cell may be higher than the QoS threshold, but that in the neighboring cells may be much lower than the QoS threshold. The fixed resource allocation schemes would be inadequate as a consequence. However, FRAC and *ExpectedMax* strategy can make capacity reservation according to the network dynamics. Also, FRAC measures the air interface performance to get real traffic usage of heterogeneous traffic services. Therefore, in the heavier loading condition, FRAC can still meet the QoS requirement while *ExpectedMax* scheme violates.

Fig. 3.10 shows the voice packet dropping rate and data packet delay time versus simulation time. It can be found that all the schemes can meet the QoS requirement of voice and data service.

3.6 Concluding Remarks

In this chapter, a *fuzzy resource allocation controller* (FRAC) is proposed. The FRAC adopts an active-network-based fuzzy inference system, which takes the advantage of expert knowledge of fuzzy logic system and learning capability of neural network. And the FRAC considers the gain of statistical multiplexing via choosing the air-interface performance as input linguistic variables, together with the capacity requirement of a call request and the capacity reservation for future handoff calls. The air-interface performance criterion, which is a fuzzy logic function of voice-packet dropping rate and data packet delay, can reflect the effect of multiplexing gain. That is, it makes the FRAC act as a closed-loop system, which would result in a stable operation. Simulation results show that FRAC performs the best, compared with the *ExpectedMax* strategy and guard schemes. Also, it has the lowest new call blocking rate and handoff blocking rate while keeping the QoS contracts of different services according to the network dynamics. Moreover, data services can achieve more multiplexing gain than voice services because data services are non-realtime and data packets can be buffered. No matter in the stationary loading or non-stationary loading case, FRAC is sophisticated and robust.

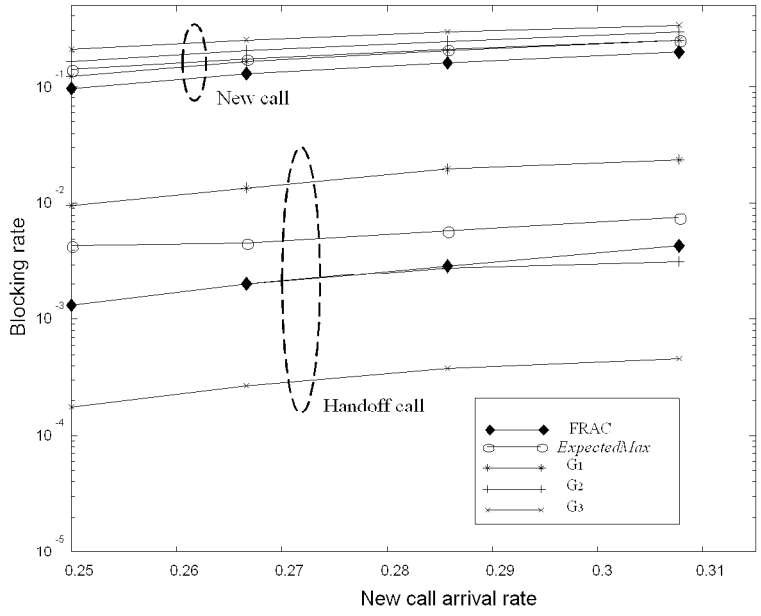

(a)

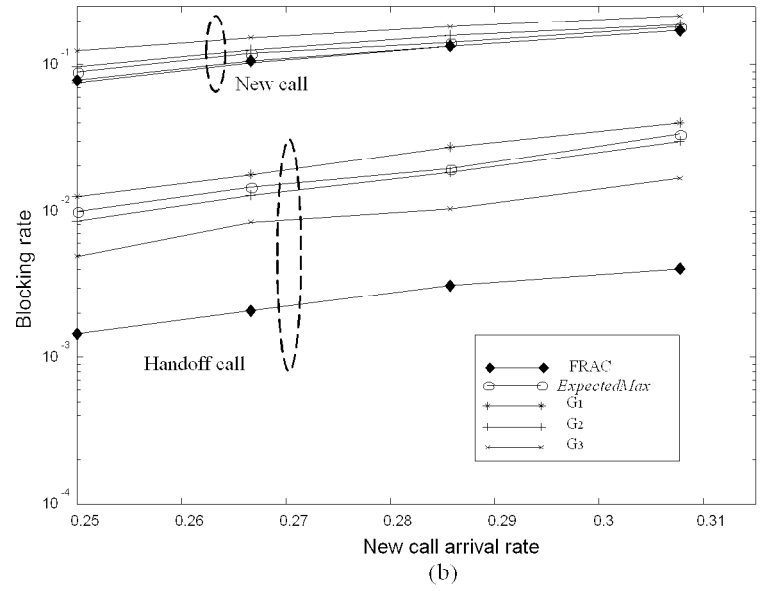

(b)

Figure 3.4: The new call and handoff call blocking rates (a) voice service (b) data service

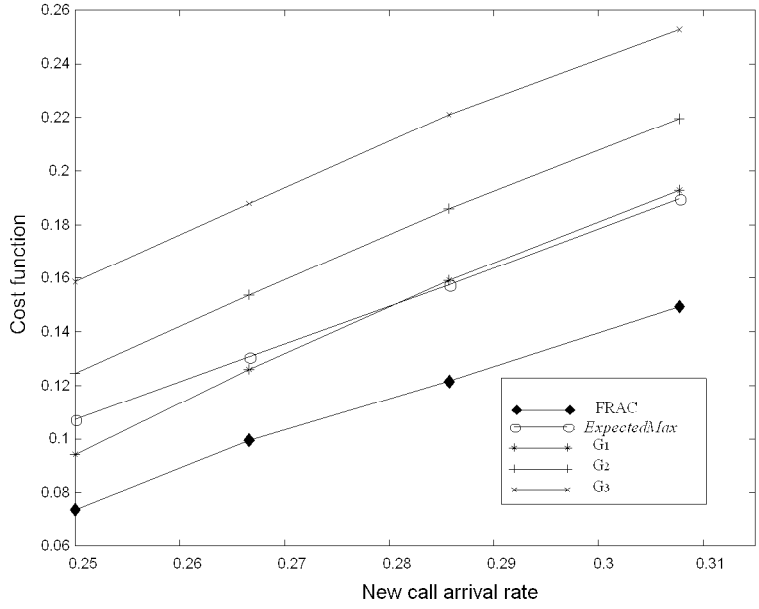

(a)

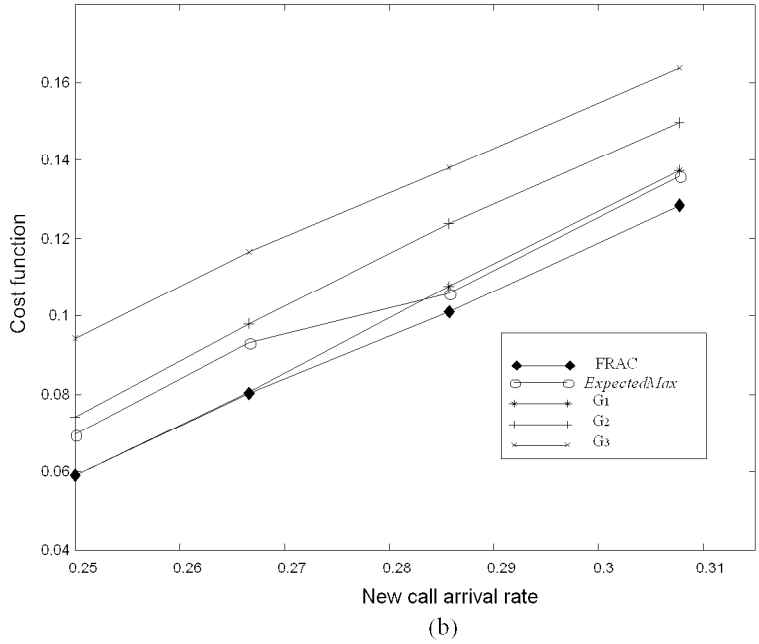

(b)

Figure 3.5: The cost functions (a) voice service (b) data service

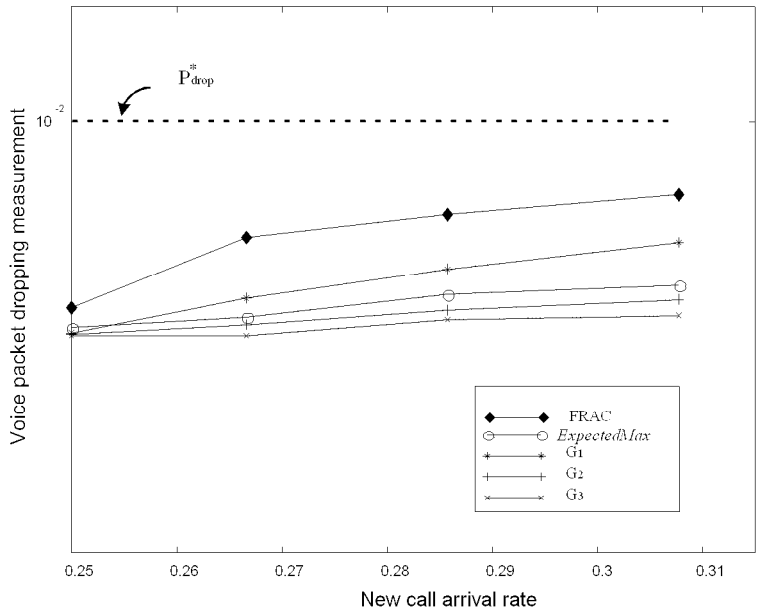

(a)

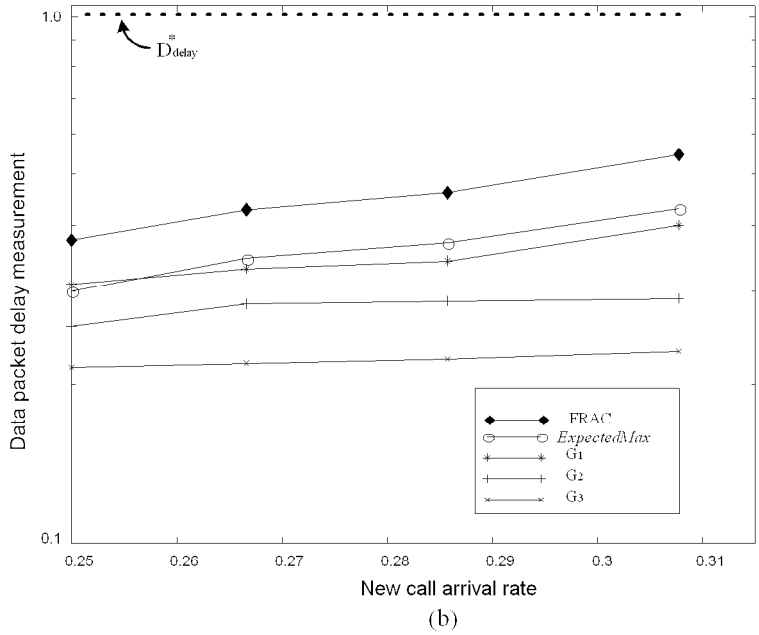

(b)

Figure 3.6: The QoS measurement (a) voice packet dropping rate (b) data packet delay

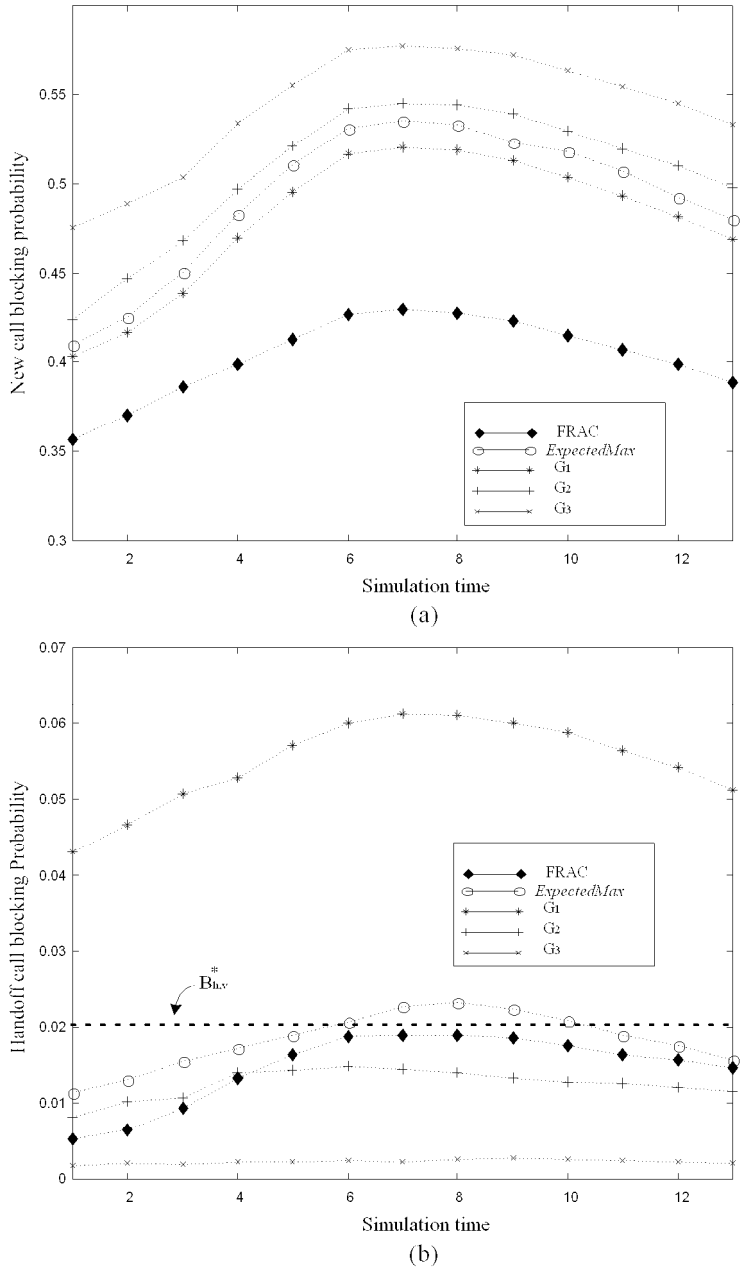

Figure 3.7: (a) new call blocking rate (b) handoff call blocking rate, of voice service

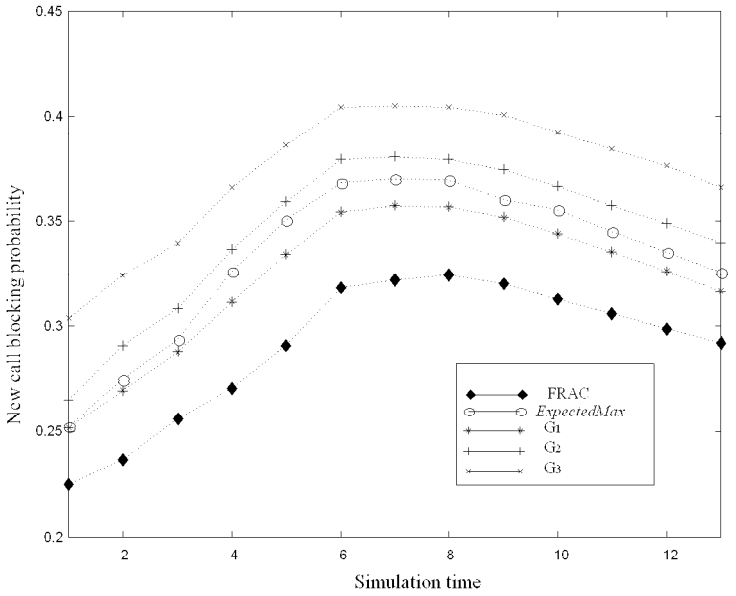

(a)

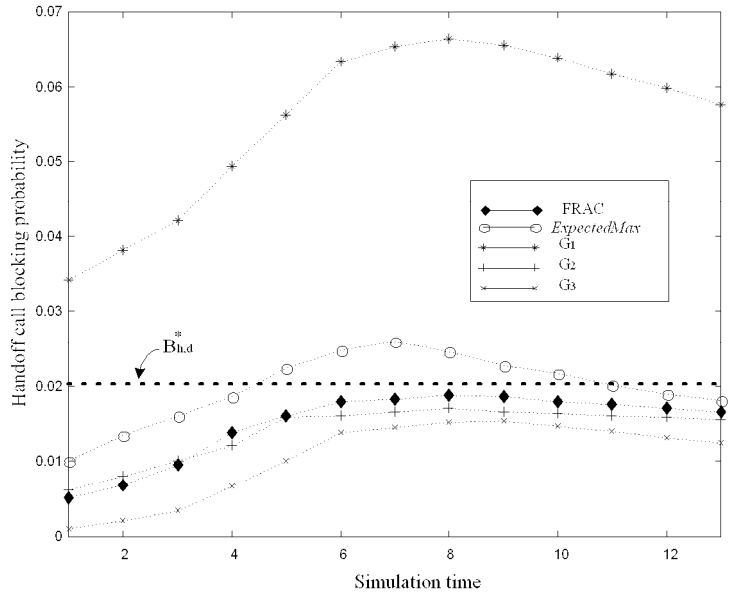

(b)

Figure 3.8: (a) new call blocking rate (b) handoff call blocking rate, of data service

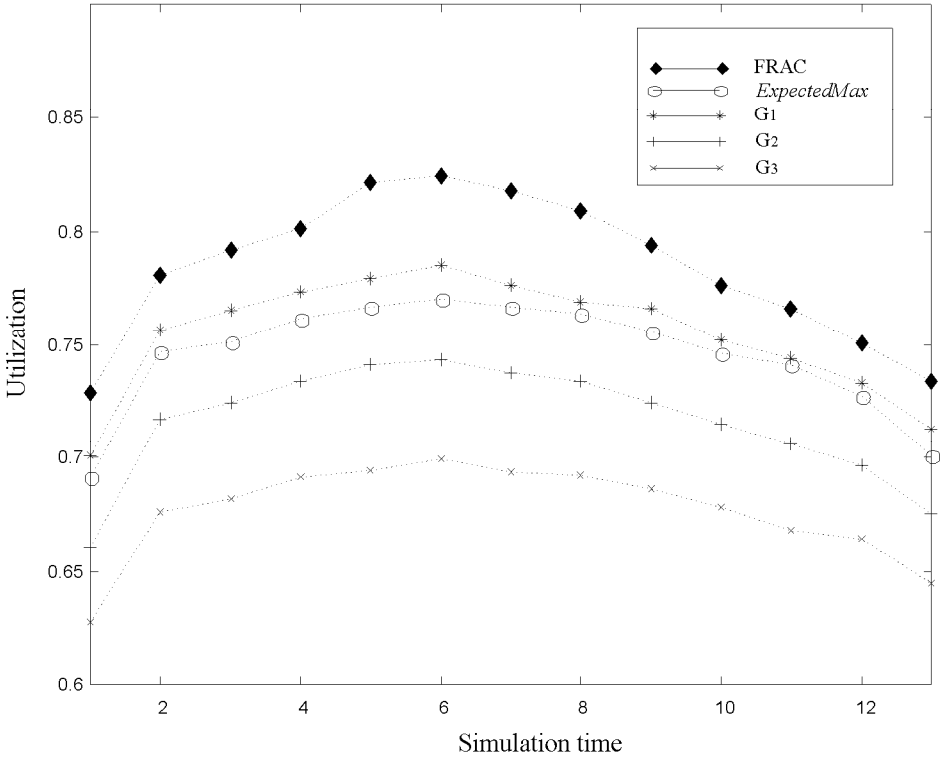

Figure 3.9: The system utilization

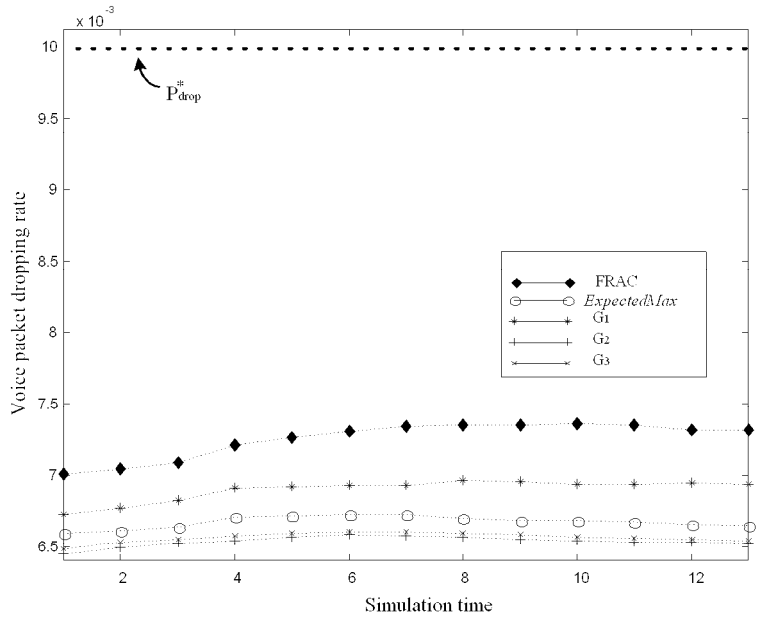

(a)

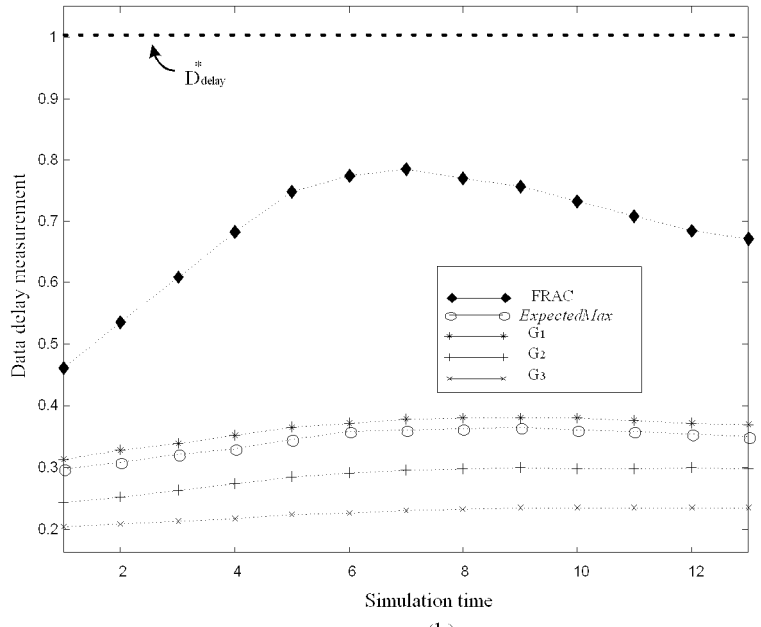

(b)

Figure 3.10: The QoS measurement (a) voice packet dropping rate (b) data packet delay

Chapter 4

A Multi-Rate Transmission Control Scheme Using Q-learning Technique for RRM in Multimedia WCDMA Systems

In this chapter, a Q-learning-based multi-rate transmission control (Q-MRTC) scheme for RRM in multimedia WCDMA communication systems is proposed. The multi-rate transmission control problem is modelled as a Markov decision process, where the transmission cost is defined in terms of the QoS parameters for enhancing spectrum utilization subject to QoS constraint. The Q-learning reinforcement algorithm is adopted to accurately estimate the transmission cost. In the meanwhile, the feature extraction method and RBFN network are successfully employed for the Q-function approximation. The state space and memory storage requirement are then reduced, and the convergence property of Q-learning algorithm is improved. Simulation results show that, for a multimedia WCDMA system, the Q-MRTC can achieve higher system throughput by an amount of 80% and better users' satisfaction than the interference-based multi-rate transmission control scheme, while the QoS requirements are guaranteed. Also, compared to the table lookup method, the storage requirement is reduced by an amount of 41%.

4.1 Introduction

Wideband CDMA (WCDMA) is one of the promising radio access technologies for IMT-2000. The objective of a multimedia WCDMA system is to provide users a radio link access to services comparable to those currently offered by fixed networks, resulting in a seamless convergence of both fixed and mobile services. Different types of services, such as voice, data, image, and compressed video, are integrated in the multimedia WCDMA system. Therefore, an adequate radio resource management (RRM), such as: admission control, is required to enhance the spectrum utilization while meeting the QoS requirements of heterogeneous services. In this chapter, the multi-rate transmission control scheme for RRM in the WCDMA systems is studied.

The multi-rate transmission control in the multimedia WCDMA system is to assign *power* and *processing gain* to service requests for maximizing the spectrum utilization and fulfilling QoS requirements and users' satisfaction. In [26], Choi and Shin proposed an uplink CDMA system architecture to provide diverse QoS guarantees for heterogeneous traffic: real-time traffic and non-real-time traffic. They theoretically derived the admission region of real-time connections, transmission power allocation, and the optimum target signal-to-interference ratio of non-real-time traffic so as to maximize the system throughput and satisfy the predefined QoS of heterogeneous traffic.

There is no absolute number of maximum available channels in the WCDMA system because WCDMA system is interference-limited. Its capacity is affected by multiple access interference (MAI), which is a function of the number of active users, users' location, channel impairments, and heterogeneous QoS requirements. Many researches for CDMA capacity estimation are based on MAI and other considerations [27]-[30]. In [27], a single-service CDMA network with respect to MAI caused by users in the same and adjacent cells was studied. In [28], Huang and Bhargava investigated the uplink performance of a slotted

direct sequence-CDMA (DS-CDMA) system providing voice and data services. A lognormal-distributed MAI model was proposed to estimate the remaining capacity in the CDMA system, where its mean and variance were given by a function of the number of users, and the mean and variance of each service type. However, in multimedia WCDMA systems, the measured MAI value may not be stationary, and it may also be affected by user locations and service profiles. Hämäläinen and Valkealahti [29] proposed an MAI estimation method to facilitate load control, admission control, and packet scheduling. Kim and Honig [30] studied the resource allocation for multiple classes of traffic in a single cell DS-CDMA system. A joint optimization was investigated over the power and the processing gain of the multiple classes to determine flexible resource allocation for each user subject to QoS constraints.

Shin, Cho, and Sung proposed an interference-based channel assignment scheme for DS-CDMA cellular systems [31]. A channel is assigned if the interference is less than an allowed level which is determined by the network, subject to the QoS constraints. Instead of a fixed system capacity, this interference-based scheme can adaptively assign a channel according to the actual system capacity dependent of interference such that the system utilization and the grade of service can be improved. The interference-based scheme was further extended to call admission control in multimedia CDMA cellular systems [32], [33]. Dimitriou and Tafazolli [32] developed a mathematical model to determine the outage limits of a multiple-service CDMA system and to achieve the maximum aggregated capacity for different system parameters. Phan-Van and Luong [33] proposed a soft-decision call admission control scheme (SCAC), where the upper bound and the lower bound of the interference-limited WCDMA system capacity are derived. In the SCAC, the new call request obtains an admission grant according to a predefined probability function when the system operates between the upper bound and the lower bound of the system capacity.

Maximizing spectrum utilization (revenue) while meeting QoS constraints suggests a

constrained Markov decision process (MDP) [38] or semi-Markov decision process (SMDP) [34], [35]. These methodologies have been successfully applied to solve many network control problems; however, they require extremely large state space to model these problems exactly. Consequently, the numerical computation is intractable due to the curse of dimensionality. Also, *a priori* knowledge of state transition probabilities is required. Alternatively, many researchers turned to use the reinforcement learning (RL) algorithms to solve the large state space problems [36]-[39]. The most obvious advantage of RL algorithm is that it could approach an optimal solution from the on-line operation if the RL algorithm is converged.

In this chapter, a Q-learning-based multi-rate transmission control (Q-MRTC) scheme for RRM in the multimedia WCDMA systems is proposed to maximize the system utilization and fulfill the users' satisfaction, subject to QoS requirements of packet error probability and packet transmission delay. For the interference-limited system, system interference profile is chosen as system state, and the multi-rate transmission control is modelled as a total expected discounted problem. Also, an evaluation function is defined to appraise the cumulative cost of the consecutive decisions for the Q-MRTC. Without knowing the state transition behavior, the evaluation function is calculated by a real-time RL technique known as Q-learning [40]. After a decision is made, the consequent cost is used as an error signal feedback to the Q-MRTC to adjust the state-action pairs. Thus the learning procedure is performed in a closed-loop iteration manner which will help the value of evaluation function converge to optimal radio resource control point.

Noticeably, the Q-function approximation is the key design issue in the implementation of Q-learning algorithm [41], [42]. Here, a *feature extraction* method and a *radial basis function network* (RBFN) are employed in the Q-MRTC. With the feature extraction method, the state space of the Q-function is mapped into a more compact set which represents *resultant interference profile*. The *resultant interference profile* aggregates the states and improves the

convergence property consequently. With the RBFN neural network, the storage requirement of the Q-function can be significantly reduced. Simulation results show that, while keeping the QoS constraints of the packet error probability and packet transmission delay guaranteed, the Q-MRTC scheme can have higher system throughput by an amount of 80% and better users' satisfaction than the interference-based scheme [32] . Also, compared to the table lookup method, the storage requirement is reduced by the amount of 41%.

The rest of the chapter is organized as follows. The system architecture and RRM are described in section 3.2. The design of Q-MRTC is proposed in section 3.3. The simulation results are presented in Section 3.4 and the performance comparison between the Q-MRTC scheme and the interference-based scheme is also made. Finally, concluding remarks are given in Section 3.5.

4.2 System Model

The physical layer and the MAC specifications for WCDMA are defined by 3GPP [43]-[44]. The WCDMA has two types of uplink dedicated physical channels (DPCHs): the uplink dedicated physical data channel (DPDCH) and the uplink dedicated physical control channel (DPCCH). A DPDCH is used to carry data generated by layer 2 and above, and a DPCCH is used to carry layer 1 control information. Each connection is allocated a DPCH including one DPCCH and zero or several DPDCHs. The channel is defined in a frame-based structure, where the frame length $T_f = 10$ ms is divided into 15 slots with length $T_{\text{slot}} = 2560$ chips, each slot corresponding to one power control period. Hence, the power control frequency is 1500 Hz. The spreading factor (SF) for DPDCH can vary between $4 \sim 256$ by $\text{SF} = 256/2^k, k = 0, 1, \cdots, 6$, carrying 10×2^k bits per slot, and the SF for DPCCH is fixed at 256, carrying 10 bits per slot. In addition, a common physical channel, named physical random access channel (PRACH), is defined to carry uplink random access

burst(s).

Two types of services are considered in this chapter: real-time service as type-1 and non-real-time service as type-2. The system provides connection-oriented transmission for real-time traffic and best-effort transmission rate allocation for non-real-time traffic. To guarantee the timely constraint of real-time service, a UE always holds a DPCH while it transmits real-time packets regardless the variation of the required transmission rate. The real-time UE may generate variable rate information whose characteristics are indicated in its request profile. On the other hand, a UE should contend for the reservation of a DPCH to transmit a burst of non-real-time packets and will release the DPCH immediately while the burst of data is completely transmitted. The non-real-time data are transmitted burst by burst.

When a UE has traffic to transmit, it first sends its service request embedded in a random access burst via PRACH. The UE may generate a call-level request or a burst-level request. The service request is a call-level request if real-time continuous transmission is required; the service request is a burst-level request if non-real-time data transmission is required. A new call-level request will be initiated only after the UE terminates its current real-time call connection. However, a new burst-level request will be initiated at any time instant according to the data source model. For the service request profile, a real-time request provides the mean rate and rate variance to indicate its transmission rate requirement, while a non-real-time request provides the maximum and minimum rate requirements. As the base station receives the new request, the admissible transmission rate will be evaluated. Due to the service requirements, RRM performs two different kinds of decision. For a real-time request, the request will be accepted or rejected. On the other hand, for a non-real-time request, an appropriate transmission rate will be allocated. A non-real-time request specifies the range of the required transmission rates for itself, and would be blocked if the WCDMA

system cannot provide a suitable transmission rate to satisfy its required transmission rate. In this chapter, it is assumed that all packets have the same length. Also, a data packet is assumed to be transmitted in a DPDCH frame by a basic rate channel, and therefore a multi-rate channel can transmit multiple data packets in a DPDCH frame.

The transmission power of a physical channel should be adjusted dependent of its spreading factor, coding scheme, rate matching attributes, and BER requirement. Here, it is assumed that all physical channels adopt the same coding scheme and have the same rate matching attributes and BER requirement. Therefore, the power allocation for a physical channel is simply dependent of its spreading factor, and it is in inverse proportion [45]. Since each UE determines its up-link transmission power in a distributed manner, the total received interference power at base station is time-varying. For operational stability, the transmission power is determined under the consideration of maximal allowed interference power. In this way, for WCDMA systems, the SIR-based power control scheme which is specified by 3GPP is equivalent to the strength-based power control scheme. Consequently, the complexity of the multi-rate transmission control is reduced and the operation can disregard the variation of the received interference.

To maximize the spectrum utilization, the radio resource management is designed to accommodate the access requests as many as possible and to allocate the transmission rate of each request as large as possible, while the QoS requirements are fulfilled. An erroneous real-time packet will be dropped since there is no re-transmission for real-time packets, while the erroneous non-real-time packets will be recovered via ARQ (automatic repeat request) scheme. The packet error probability, denoted by P_e, and packet transmission delay, denoted by D_d, are considered as the system performance measures. Also, the maximum tolerable packet error probability, denoted by P_e^*, and maximum tolerable packet transmission delay time, denoted by D_d^*, are defined as the system QoS requirements.

4.3 The Design of Q-MRTC

4.3.1 State, Action, and Transmission Cost Function

The radio resource management of a multimedia WCDMA system is regarded as a discrete-time MDP problem, where major events are arrivals of service requests in a cell. The service request arrivals would trigger the transition of the system state such that the radio resource control is executed. For the arrival of the k-th request, the *system state* is assumed at x_k, defined as

$$x_k = (I_m, I_v, i, \mathbf{R}_i), \tag{4.1}$$

where I_m and I_v denote the mean and the variance of the interference from existing connections, i indicates that x_k is an arrival of type-i, and $\mathbf{R}_i$ is transmission rate requirement of the type-i request, $i = 1, 2$. The $(I_m,\ I_v)$ is the interference profile. Since the capacity of the WCDMA system is interference-limited, the interference profile is employed to indicate the system load [28]. The $\mathbf{R}_1 = (r_m, r_v)$, where r_m and r_v denote the mean rate and the rate variance of a real-time request, respectively; the $\mathbf{R}_2 = (r_{\max}, r_{\min})$, where $r_{\max}$ and $r_{\min}$ denote the maximum rate and the minimum rate requirements of a non-real-time request, respectively.

Based on the system state x_k, the multi-rate transmission controller will determine an *action*, denoted by A_k, for the k-th request arrival. The action A_k is defined as:

- Real-time request:

$$A_k = \begin{cases} 1 & \text{if accepted,} \\ 0 & \text{if rejected,} \end{cases} \tag{4.2}$$

- Non-real-time request:

$$A_k = \begin{cases} r,\ r_{\min} \le r \le r_{\max} & \text{if accepted,} \\ 0 & \text{if rejected.} \end{cases} \tag{4.3}$$

If the state-action pair $(x_k,\ A_k)$ has been determined, an immediate transmission cost is defined as

$$(x_k,A_k) = \alpha[\frac{P_e(x_k,A_k) - P_e^*}{P_e^*}]^2 + (1-\alpha)[\frac{D_d(x_k,A_k) - D_d^*}{D_d^*}]^2, \tag{4.4}$$

where $P_e(x_k,A_k)$ is the packet error probability, $D_d(x_k,A_k)$ is the packet transmission delay, and α is the weighting factor. The $c(x_k,A_k)$ is a random variable because channel fading and imperfect power control are not included in the state-action pair yet. An evaluation function, denoted by $Q(x,A)$, is further defined as the expected total discounted cost counting from the initial state-action pair (x,A) over an infinite time. It is given by

$$Q(x,A) = E\left\{\sum_{k=0}^{\infty}\nu^k c(x_k,A_k)|x_0 = x, A_0 = A\right\}, \tag{4.5}$$

where $0 \leq \nu < 1$ is a discounted factor. The multi-rate transmission control is to determine an optimal action, denoted by A^*, which minimizes the Q-function with respective to the current state. The minimization of Q-function represents the maximization of the system capacity and the fulfillment of QoS requirements.

Let $P_{xy}(A)$ be the transition probability from state x with action A to the next state y. Then $Q(x,A)$ can be expressed as

$$\begin{aligned} Q(x,A) &= E\{c(x_0,A_0)|x_0 = x, A_0 = A\} + \\ &\quad E\left\{\sum_{k=1}^{\infty}\nu^k c(x_k,A_k)|x_0 = x, A_0 = A\right\} \\ &= E\{c(x,A)\} + \nu\sum_y P_{xy}(A) \times \\ &\quad E\left\{\sum_{k=1}^{\infty}\nu^{k-1} c(x_k,A_k)|x_1 = y, A_1 = B\right\} \\ &= C(x,A) + \nu\sum_y P_{xy}(A)Q(y,B), \end{aligned} \tag{4.6}$$

where $C(x,A) = E\{c(x,A)\}$. Eq. (4.6) indicates that the Q function of the current state-action pair can be represented in terms of the expected immediate cost of the current state-action pair and the Q function of the next state-action pairs.

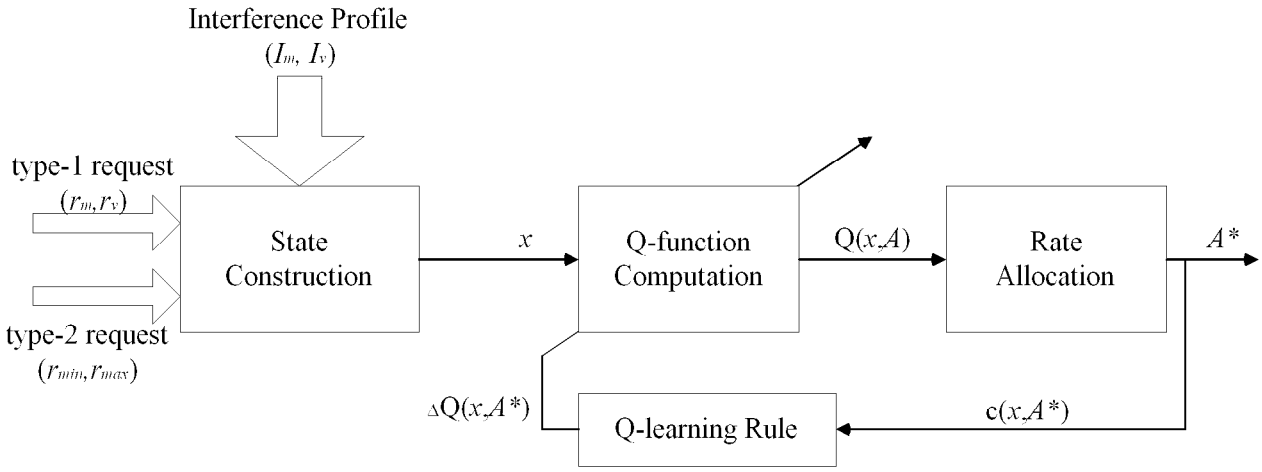

Figure 4.1: Structure of the Q-learning-based multi-rate transmission control (Q-MRTC) scheme

Based on the principle of Bellman's optimality [46], the optimal action A^* can be obtained by a two-step optimality operation. The first step is to find an intermediate minimal of $Q(x, A)$, denoted by $Q^*(x, A)$, where the intermediate evaluation function for every possible next state-action pair (y, B) is minimized and the optimal action is performed with respective to each next state y. $Q^*(x, A)$ is given by

$$Q^*(x, A) = C(x, A) + \nu \sum_y P_{xy}(A) \left\{ \min_B \left[Q^*(y, B) \right] \right\}$$

$$\text{for all } (x, A). \tag{4.7}$$

Then the optimal action A^* can be determined with respective to the current state x such that $Q^*(x, A)$ is minimal, which can be expressed as

$$Q^*(x, A^*) = \min_A \left[Q^*(x, A) \right]. \tag{4.8}$$

However, it is difficult to find the $C(x, A)$ and $P_{xy}(A)$ to solve Eq. (4.7). In this chapter, a real-time reinforcement learning algorithm, named Q-learning algorithm [40], [41], is adopted

to find the optimal resource allocation without *a priori* knowledge of $C(x, A)$ and $P_{xy}(A)$. To find the optimal $Q^*(x, A)$, the Q-learning algorithm computes the Q value in a recursive method using available information (x, A, y, $c(x, A)$), where x and y are the current and the next states, respectively; and A and $c(x, A)$ are the action for current state and its immediate cost of the state action pair, respectively.

4.3.2 Q-MRTC

Fig. 4.1 shows the structure of Q-learning-based multi-rate transmission control (Q-MRTC) scheme. When a service request arrives at system state x, the *Q-function computation* block computes the value of $Q(x, A)$ for every possible action A. The *rate allocation* block then determines the optimal rate allocation A^* or call rejection with respect to all the current Q values of all possible actions. In the *Q-learning rule* block, the immediate cost $c(x, A^*)$ can be observed and the Q-learning rule is used to adjust the value of $Q(x, A)$. The Q-learning rule is formulated by

$$Q(x, A) = \begin{cases} Q(x, A) + \eta \Delta Q(x, A), & \text{if } A{=}A^* \\ Q(x, A) & \text{otherwise.} \end{cases} \tag{4.9}$$

where η is the learning rate, $0 \leq \eta \leq 1$, and

$$\Delta Q(x, A^*) = \left\{ c(x, A^*) + \nu \min_B [Q(y, B)] \right\} - Q(x, A^*). \tag{4.10}$$

Since only one action-pair is chosen for evaluation in each learning epoch, for the Q-learning rule, only the Q value of the chosen action-pair is updated while others are kept unchanged. Also, in Eq. (4.10), the operation of $\min_B [Q(y, B)]$ is executed by comparing the Q values of all the possible action candidates for state y and then choosing the desired action B with minimal Q value.

In [40], Watkins and Dayan had proved the convergence theorem of Q-learning. Here, the theorem is re-stated as following: *if the value of each admissible pair is visited infinitely*

often and the learning rate is decreased to zero in a suitable way, then the value of $Q(x, A)$ *in (4.9) will converge to* $Q^*(x, A)$ *with probability 1.*

Usually, if the state space is too large, it would require a huge amount of memory to store the values of Q-function and take a long time for the Q-learning algorithm to converge. To tackle the above problems, in the Q-function computation block, the *feature extraction* method and *radial basis function network* (RBFN) are employed for the Q-function approximation in the proposed Q-MRTC. Here, the state-action pair is firstly transformed into a dimension-reduced feature vector, and then the feature vector is used as input parameters to compute the corresponding Q value that is stored in the RBFN network.

Feature extraction method maps the original state-action pair into a feature vector, which must be properly chosen to reflect the important behavior characteristics of the state-action pair [42]. In the WCDMA system, after the state-action is performed, the change of interference is the most significant corresponding response. Therefore, the feature vector of (x, A) is selected to be the *resultant interference profile*, denoted by $(I_m + \Delta I_m, I_v + \Delta I_v)$, where $(\Delta I_m, \Delta I_v)$ indicates the change of interference profile (I_m, I_v) due to action A at state x. In other words, the state-action pair (x, A) can be converted to resultant interference profile $(I_m + \Delta I_m, I_v + \Delta I_v)$. It is noted that the dimension of the resultant interference profile is smaller than that of the original state-action pairs. While a strength-based closed-loop power control is assumed, the received power for a unit of transmission rate is set to 1. Consequently, $(\Delta I_m, \Delta I_v)$ is obtained by

$$(\Delta I_m, \Delta I_v) = \begin{cases} (r_m, r_v) & \text{if accepts a real-time request,} \\ (r, 0) & \text{if accepts a non-real-time request with rate } r, \\ (0, 0) & \text{if rejects a request.} \end{cases} \tag{4.11}$$

Radial basis function network (RBFN) is a three-layer, self-growing neural network, including an input layer, an output layer, and a hidden layer [41]. The hidden layer consists of a sequence of nodes whose activation functions are normalized Gaussian. The RBFN

neural network performs a function approximation for the Q function. When the RBFN is well-trained, the Q values of all the state-action pairs are stored in the RBFN. With the input parameters of the resultant interference profile, the RBFN calculate the corresponding Q value.

The key concept of RBFN is *local-tuning* and *separated storage*. Each node in the hidden layer represents a part of the characteristics of the input vectors and stores these characteristics locally. Thus, it breaks a large-dimensional mapping function into multiple small-dimensional functions. Due to the separated storage property, only some hidden nodes in the RBFN would be adjusted with respect to the new input error signal, which can reduce the training epoch significantly. Fig. 4.2 shows the Q-function computation performed by the RBFN. The state-action pair (x, A) is mapped into its corresponding resultant interference profile $(I_m + \Delta I_m, I_v + \Delta I_v)$, and the RBFN neural network then calculates $Q(x, A)$ as a function of $(I_m + \Delta I_m, I_v + \Delta I_v)$. The well-known back-propagation learning rule is applied in the training process.

The Q value for state-action pair (x, A) is updated by Eq. (4.9) when the next request arrives and $\eta \Delta Q(x, A)$ is served as an error signal which is backpropagated in the neural network. With the feature extraction method and RBFN neural network, the Q-MRTC can obtain $Q(x, A)$ efficiently through the online operation. As noted, $Q(x, A)$ will approach to $Q^*(x, A)$ through the training procedure while the convergence theorem of Q-learning holds.

4.3.3 Parameter Initialization

Before the Q-MRTC is performed for the online operation, it is necessary to assign a proper set of initial values. An appropriate initialization can provide a good relationship of the input parameters and the decision output for an event at the beginning of system operation such that the transient period of Q-learning procedure would be short. To obtain the initial Q values, the composite interference received at base station is assumed to be log-normally

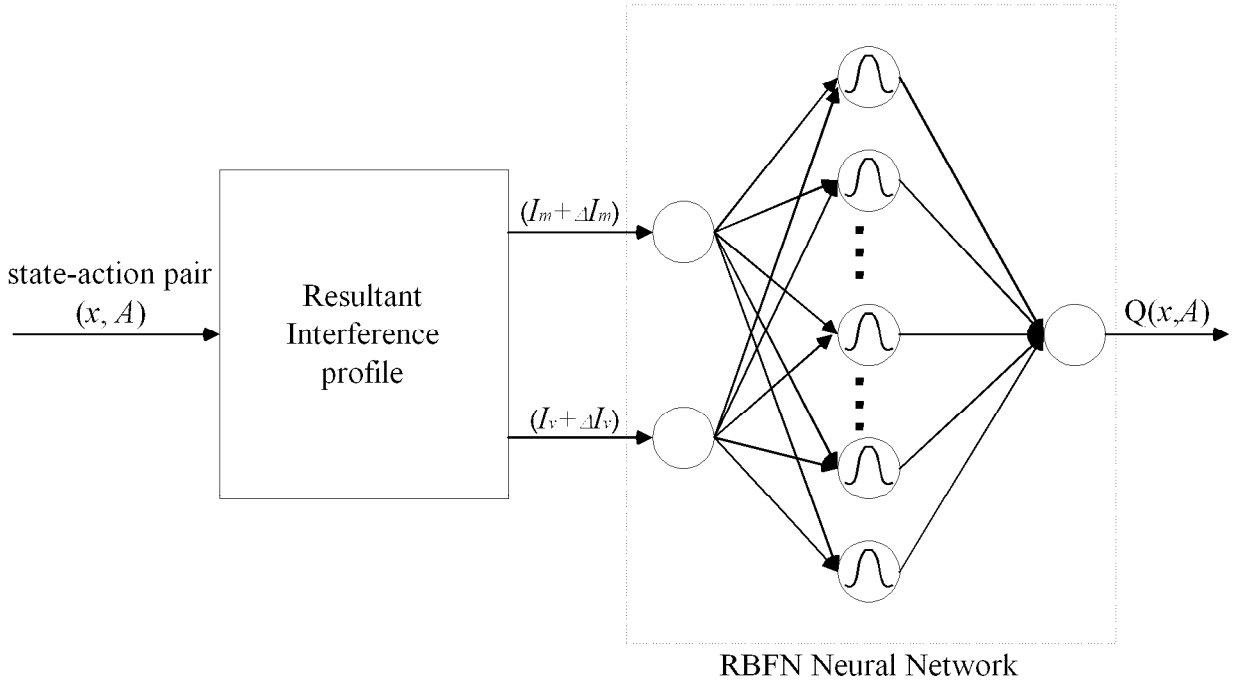

Figure 4.2: The Q-function computation by RBFN neural network

distributed. Although the assumption of log-normal distribution may not hold in some cases, it indeed provides a meaningful initial guess rather than a random initialization.

For a given state-action pair (x, A), the initial value of $Q(x, A)$ is set according to QoS measurements. Since the packet transmission delay cannot be calculated in advance, the normalized expected packet error probability is preferred as the initial value of $Q(x, A)$ and is expressed as $(\frac{\overline{P}_e(x,A)-P_e^*)^2}{P_e^*})$, where $\overline{P}_e(x, A)$ is the expected packet error probability if the state-action pair (x, A) is performed. The $\overline{P}_e(x, A)$ is given by

$$\overline{P}_e(x, A) = 1 - \left(1 - \int P_b(I)\mathcal{L}(I)dI\right)^L, \tag{4.12}$$

where L is the packet length, $P_b(I)$ is the bit error probability at the interference level I, and $\mathcal{L}(I)$ is the log-normal function for interference level I with mean $(I_m + \Delta I_m)$ and variance $(I_v + \Delta I_v)$. The $P_b(I)$ is given by [30]

$$P_b(I) = \kappa \exp -\beta * G/I \tag{4.13}$$

with parameters of κ and β which are adjustable for matching with a particular coding scheme, and G is the spreading factor of a basic rate channel.

In summary, the procedure of Q-MRTC is described in the following.

- **Step 1:** [*State-Action Construction*]

  Construct the current state $x = (I_m, I_v, i, \mathbf{R}_i)$ and find a set of all possible actions for state x, denoted by $\mathbf{A}(x)$, when a new request arrives.

- **Step 2:** [*Q-Value Computation*]

  For the set of state-action pairs $\{(x,\ A) \mid A \in \mathbf{A}(x)\}$, compute the respective $Q(x, A)$ values by the RBFN neural network.

- **Step 3:** [*Rate Allocation*]

  Determine the optimal action A^* such that the value of $Q(x, A^*)$ is minimum, i.e., $Q(x, A^*) = \underset{A \in \mathbf{A}(x)}{\text{Min}} \left[Q(x, A)\right]$.

- **Step 4:** [*Q-Value Update*]

  Update the Q values by Eq. (4.9) as the next event arrives with state y and the online cost $c(x, A^*)$ is obtained. Since the Q value is stored in a neural network, $\eta \Delta Q(x, A^*)$ is used as an error signal backpropagated into the neural network, instead of the error between the desired and the actual outputs. Goto **Step 1**.

4.4 Simulation Results and Discussion

In this simulation, two kinds of traffic are transmitted via the real-time service: one is 2-level transmission rate traffic and the other is M-level transmission rate traffic. They are modelled by 2-level and M-level MMDP (Markov modulated deterministic process), respectively. The 2-level MMDP is generally used to formulate ON-OFF voice traffic stream, and the M-level MMDP is to formulate the advanced speech or other real-time traffic streams, e.g., video.

Table 4.1: Traffic Parameters in The Multimedia WCDMA System

Traffic Type	Traffic Parameters
2-level real-time	Call holding time: 30 seconds Mean talkspurt duration: 1.00 seconds Mean silence duration: 1.35 seconds
M-level real-time	Call holding time: 30 seconds Peak rate (M): 4-fold of basic rate Mean rate: 2-fold of basic rate
Non-real-time	Mean data burst size: 200 packets $r_{\min}$: 1-fold of basic rate $r_{\max}$: 8-fold of basic rate

On the other hand, the non-real-time service is considered to transmit variable-length data bursts. The arrival process of the data burst is Poisson and the data length is assumed to be with a geometric distribution. A data burst can carry any type of wireless data, e.g., e-mail, WML (wireless markup language) pages, and etc. The detailed traffic parameters are listed in Table. 4.1. A basic rate in the WCDMA system is assumed to be a physical channel with SF=256. For each connection, DPCCH is always active to maintain the connection reliability. To reduce the overhead cost of interference produced by DPCCHs, the transmitting power of a DPCCH is smaller than its respective DPDCH by an amount of 3 dB. The other simulation parameters are given as $P_e^* = 0.01$, $D_d^* = 0.5s$, and $\alpha = 0.3$.

A conventional interference-based scheme proposed in [32] is used as a benchmark for comparison with Q-MRTC. The interference-based scheme would admit the connection for a real-time request or allocate a transmission rate for a non-real-time request if the expected packet error probability in terms of the resultant SIR is smaller than the QoS requirement.

Fig. 4.3 illustrates the throughput of the Q-MRTC and the interference-based scheme versus the request arrival rate. The Q-MRTC has throughput higher than the interference-based scheme, and the throughput improvement becomes greater as the request arrival rate becomes larger. Generally speaking, Q-MRTC can improve the maximum throughput by an

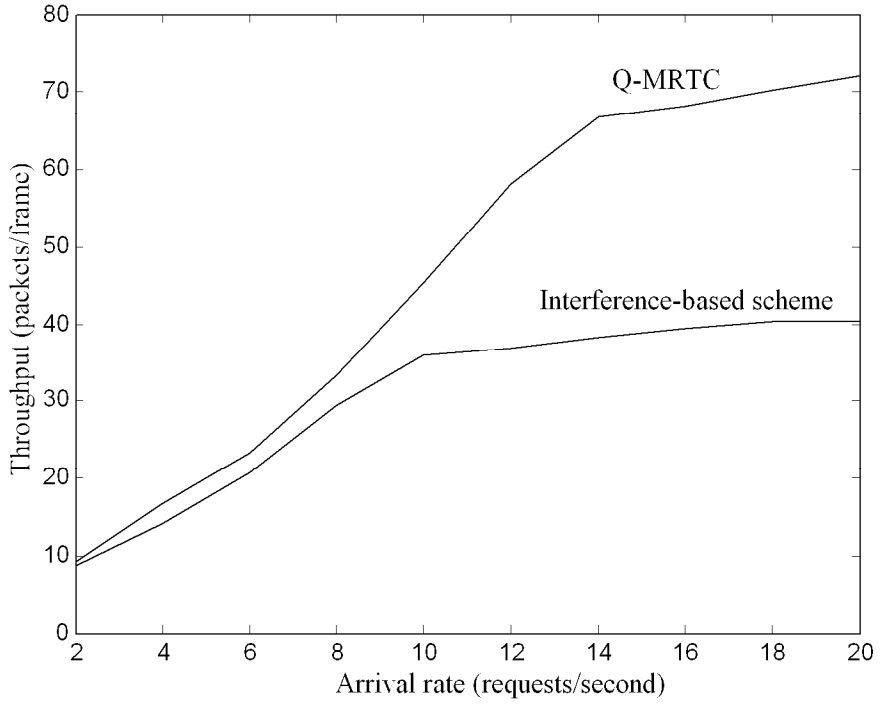

Figure 4.3: Throughput versus the request arrival rate

amount of 80% over the interference-based scheme. The reason is that, in the Q-MRTC, the transmission cost comprises the cost of immediate and consecutive decision, and the behavior of interference variation is taken into the consideration for multi-rate transmission control. Also, the Q-MRTC performs an on-line reinforcement learning algorithm to estimate the transmission cost. The estimation error is backpropagated to the Q-MRTC and reduced through the closed-loop learning procedure. Therefore, the Q-MRTC could provide more accurate estimation for multi-rate transmission cost and greater throughput improvement when traffic load becomes large. On the other hand, the interference-based scheme generally estimates the multi-rate transmission cost of packet error probability at the instant of a request arrival. Actually, some existing connections may terminate (or handoff) between two consecutive arrivals and the received interference level decreases subsequently. Therefore, the interference-based scheme would over-estimate the multi-rate transmission cost.

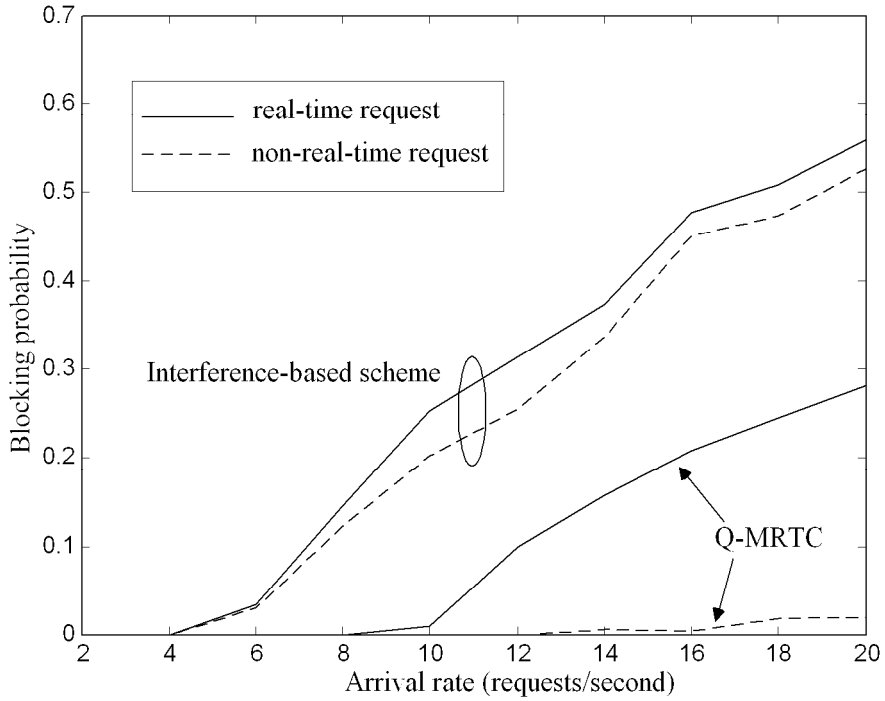

Figure 4.4: The blocking probability versus the request arrival rate.

Fig. 4.4 illustrates the blocking probability versus the request arrival rate. It can be found that the blocking probability of the Q-MRTC is much smaller than that of the interference-based scheme for real-time and non-real-time requests, and the blocking probabilities of the real-time requests are higher than those of the non-real-time requests. The reason is that the admitted transmission rate of the non-real-time requests are negotiable. It can also be seen that Q-MRTC has a larger difference between the real-time and non-real-time blocking probabilities than the interference-based scheme. It is because the interference-based scheme generally accommodates fewer connections and operates in a lower interference condition so that the interference variation due to the variable-rate transmission behavior of the real-time requests is smaller. By contrast, Q-MRTC accommodates more requests and operates in a higher interference situation so that the interference variation produced by the real-time requests becomes more critical. That is, the variable-rate transmission behavior

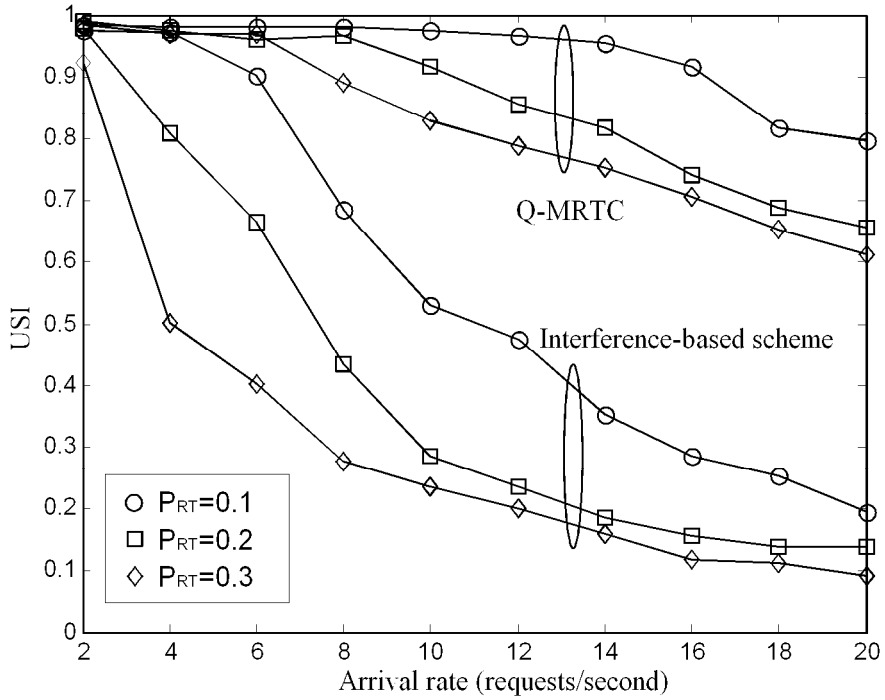

Figure 4.5: The users' satisfaction index versus the request arrival rate

contributes a higher admission cost for the Q-MRTC.

An overall users' satisfaction index (USI) is further defined, which is a linear combination of $\frac{A_{a1}}{A_{d1}}$ (type-1) and $\frac{A_{a2}}{A_{d2}}$ (type-2), where the A_{a1} (A_{a2}) is the admitted transmission rate for type-1 (type-2) and the A_{d1} (A_{d2}) is the desired transmission rate for type-1 (type-2); $A_{d1} = 1$ and $A_{d2} = r_{\max}$. That is, USI is expressed as

$$USI = \gamma \frac{A_{a1}}{A_{d1}} + (1-\gamma)\frac{A_{a2}}{A_{d2}}, \tag{4.14}$$

where γ is the weighting factor.

Fig. 4.5 depicts USI versus the request arrival rate for different traffic patterns, where P_{RT}, denoting the percentage of the real-time traffic arrival requests in the traffic load, varies from 0.1 to 0.3. It can be found that Q-MRTC has higher USI than the interference-based scheme, and the improvement is more significant as the traffic load becomes heavier. This is because Q-MRTC can accurately estimate the multi-rate transmission cost. Also, USI

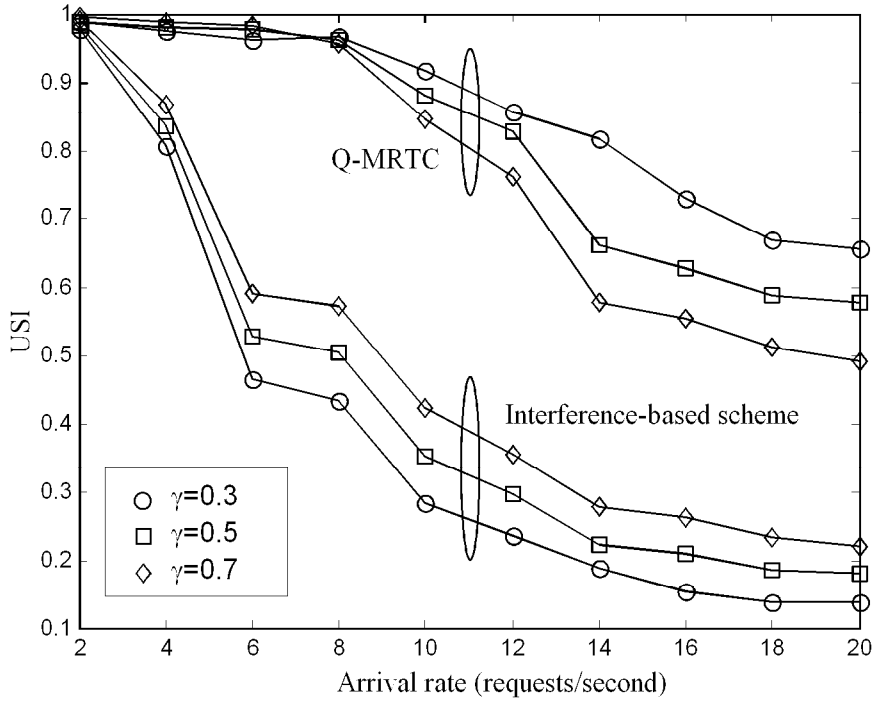

Figure 4.6: The users' satisfaction index versus the request arrival rate

decreases as the request arrival rate increases. Since the high traffic load may decrease the admitted transmission rate for new requests, the USI value decreases consequently. Another observation is that under the fixed weighting factor ($\gamma = 0.3$), the USI decreases as P_{RT} increases. This is because that the real-time requests produce interference variation higher than non-real-time ones do, which leads to larger real-time blocking probability and less non-real-time admitted transmission rate.

Fig. 4.6 depicts USI versus the request arrival rate for different weighting factors $\gamma = 0.3$, 0.5, and 0.7. It can be found that the USI of Q-MRTC is lower when γ is larger (more weighting on type-1 service) because Q-MRTC accommodates more requests and operates under higher interference condition. Thus, the interference variation produced by real-time requests becomes critical. From Fig. 4.5 and Fig. 4.6, it can be concluded that the variable-rate transmission characteristic of real-time requests plays an important role for the

multi-rate transmission control in the multimedia WCDMA systems.

Fig. 4.7 shows the QoS measures: (a) the packet error probability and (b) the packet transmission delay versus the request arrival rate. It can be seen that Q-MRTC can always keep the QoS requirements of packet error probability and packet transmission delay. By contrast, only the QoS requirement of packet error probability is kept in the interference-based scheme. It is because Q-MRTC dynamically evaluates the transmission cost which is in terms of packet error probability and packet transmission delay. The Q-MRTC is more suitable for multimedia WCDMA systems than the interference-based scheme is. Also, it can be seen that the average packet error probability of the Q-MRTC is larger than that of the interference-based scheme; however, the Q-MRTC can still hold the packet error probability within the QoS constraint. This is because the interference-based scheme is too conservative in the multi-rate transmission control, and it admits less requests and allocates lower transmission rates. On the other hand, the Q-MRTC obtains the transmission cost from the on-line operation of the WCDMA system. Consequently, it can accommodate more requests and appropriately allocate transmission rates as much as possible, under the QoS constraints.

To evaluate the performance of storage requirement reduction, it is assumed that a table lookup method in which the continuous-valued parameters of the resultant interference profile are partitioned into several discrete levels. Generally, different number of discrete levels leads to different system throughput and different storage requirement. Take an example for comparison, the interference mean $(I_m + \Delta I_m)$ of the resultant interference profile are divided into 40 levels and the interference variance $(I_v + \Delta I_v)$ into 10 levels, which has similar system performance as RBFN neural network. Table 4.2 shows the number of required storage units. There are 400 storage units required in the table lookup method. On the contrary, only 118 hidden neuron nodes are required in the RBFN neural network. While there are 2 parameters

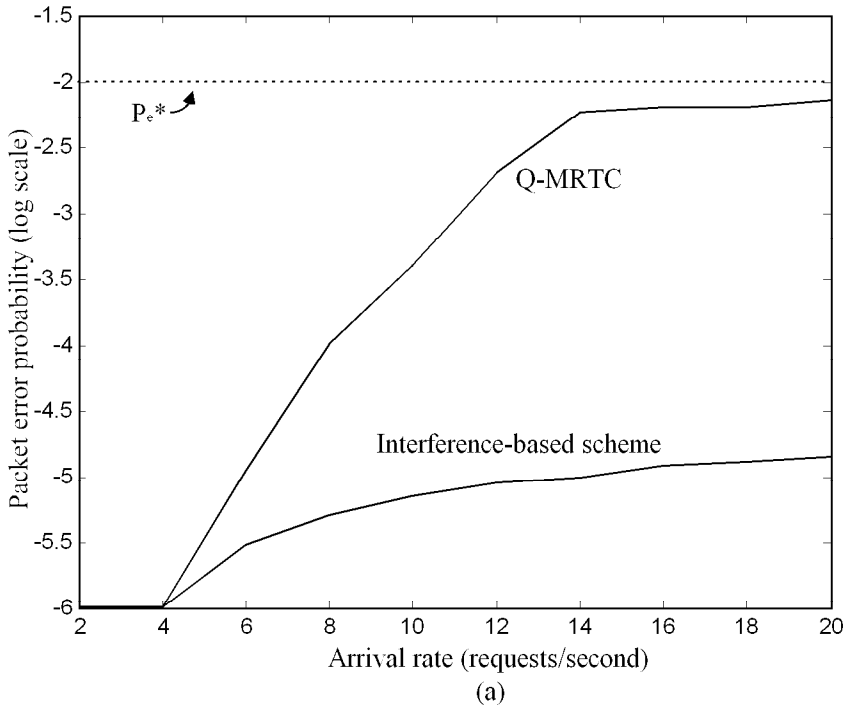

Figure 4.7: The QoS measures: (a) packet error probability and (b) transmission delay versus the request arrival rate

Table 4.2: The Number Of Required Storage Units: An Example

Method	Storage Units
Table lookup	400
RBFN	236 (118 hidden nodes)

in each hidden node, there are 236 storage units required for RBFN. Therefore, RBFN can achieve storage requirement reduction by the amount of 41%. Furthermore, the table lookup method is static-partioned and is hard to find a proper partition level especially for bursty traffic. However, in the RBFN neural network, the value of each meaningful state-action pair is stored and adjusted separately in a corresponding hidden node. That is, the storage space is non-linearly partitioned in the RBFN neural network. While the traffic load and pattern change with time, the hidden nodes of the RBFN neural network can self-organize dynamically and the storage space be re-partitioned accordingly.

4.5 Concluding Remarks

In this chapter, a Q-learning-based multi-rate transmission control scheme for radio resource management in multimedia WCDMA systems is proposed. The Q-learning algorithm is applied to accurately estimate the transmission cost for the multi-rate transmission control, and the feature extraction method and radial basis function network are employed for Q-function approximation that maps the original state-action pairs into the *resultant interference profile*.

Simulation results show that Q-MRTC can improve the throughput of multimedia WCDMA system by an amount of 80% over the conventional interference-based scheme proposed in [32], under the constraint of the QoS requirements of packet error probability and packet transmission delay. Also, the Q-MRTC provides better users' satisfaction. It is because the Q-learning algorithm performs closed-loop control by applying the system performance measures as a feedback to adjust the multi-rate transmission cost, and correspondingly the

Q-MRTC can have self-tuning capability to adaptively estimate the transmission cost. Moreover, the storage requirement of RBFN neural network is less than that of the conventional table-lookup method by the amount of 41%.

Chapter 5

A Situation-Aware Data Access Manager Using Fuzzy Q-learning Technique for Multi-cell WCDMA Systems

In this chapter, a novel situation-aware data access manager using fuzzy Q-learning technique (FQ-SDAM) is proposed for multi-cell WCDMA systems. The FQ-SDAM contains a fuzzy Q-learning-based residual capacity estimator (FQ-RCE) and a data rate scheduler (DRS). The FQ-RCE can accurately estimate the situation-dependent residual system capacity; it appropriately chooses the received interferences from home-cell and adjacent-cell as input linguistic variables and simplifies the multi-cell environment into a single-cell one by applying a perceptual coordination mechanism. Also, the DRS can effectively allocate the resource for non-real-time terminals by adopting a modified exponential rule which takes the interference influence on adjacent cells into consideration. Simulation results show that the FQ-SDAM can effectively reduce the packet error probability and improve aggregate throughput of the non-real-time services in both the homogeneous and non-homogeneous multi-cell WCDMA environment.

5.1 Introduction

The WCDMA cellular system will support integrated services with mixed QoS (quality of services) requirements: real-time services require continuous transmission and intolerance to time delay, while non-real-time services require bursty transmission and tolerate moderate time delay. For maximizing the system capacity and fulfilling the complementary QoS requirements, an adequate radio resource management (RRM) is required. The RRM adopts a call admission control scheme to ensure that the system will not be overloaded, based on the long-term availability of radio resources. On the other hand, it employs a *data access control scheme* to provide bursty transmission permission for non-real-time services, based on the short-term availability of radio resources.

The main purpose of the *data access control scheme* in WCDMA systems supporting integrated services is to maximize the throughput of non-real-time services while maintaining the transmission quality of real-time services [47]-[51]. To achieve this goal, dynamic access probability schemes [48]-[50] and a base station-controlled scheduling scheme [51] were proposed, where the residual system capacity for non-real-time services was firstly estimated and then shared to non-real-time terminals. A single-cell environment was considered in [48]-[50], while a multi-cell environment was studied in [51]. In the multi-cell scheme [51], the interference generated from other-cell terminals was treated as if from several home-cell ones, and consequently the multi-cell environment was regarded as a single-cell one. However, the mutual-affected behavior of radio resource allocation in the multi-cell environment was still not considered. Note that, in the multi-cell WCDMA system, the increment of data transmission power in one cell would cause the rising of interference level in the adjacent cells. If each cell allocates the whole possible residual capacity for bursty transmission without taking the interference influence from adjacent cells into account, the system would trap into an overloading condition.

The over-loading phenomenon could be alleviated by an appropriate coordination scheme among cells [52]. Knowing the information of radio resource of all cells, a centralized data access scheme for the multi-cell WCDMA system can maximize the system throughput by applying a global optimization method. Unfortunately, the coordination procedure takes long time to transact the resource information between cells so that it is infeasible for practical implementation. Usually, the data access control scheme operates in the short-term time scale, *e.g.* frame time, and thus distributed schemes are preferable. Kumar and Nanda [53] proposed a distributed scheme called load and interference-based demand assignment (LIDA). The LIDA is a kind of resource reservation-based scheme in which some portions of resource in each cell are reserved against the interference variation. Also, it employs the concept of burst admission threshold for high-rate transmission in a cell to avoid excess interference to adjacent cells . In this scheme, only when the strength difference between the received pilot signals from home cell and adjacent cell is larger than the threshold, the bursty transmission is permitted. The effectiveness of this scheme relies on the selection of the reservation threshold, which should be dynamically performed according to the system loading and the received interference power level.

Additionally, a rate scheduling scheme is also embedded in the data access control scheme to allocate the residual capacities for non-real-time terminals according to a service principle. Ramakrishna and Holtzman adopted a *maximization throughput* criterion for the scheduling scheme [54]. Indeed, this criterion can maximize the system throughput, but the low-class users may suffer from starvation. Alternatively, Jalali, Padovani, and Pankai proposed a *proportional fairness* criterion [55] for a down link scheduling scheme in a CDMA-HDR (high data rate) system. In the scheme, a utility function was defined as a ratio of the supported data rate and the average data rate. The supported data rate was determined by channel condition, while the average data rate was the window average of the transmitted throughput.

The terminal with the highest utility value would transmit in the next frame time. This algorithm may lead to large transmission delay for some terminals. Also, Shakkottai and Stolyar proposed an *exponential rule* criterion [56] for the utility function of the scheme to make a good balance between the system throughput and the transmission delay. However, applying the exponential rule to the uplink transmission should have taken the terminal's location factor into consideration such that the adjacent-cell interference could be maintained within a sustained level.

This chapter proposes a situation-aware data access manager using fuzzy Q-learning technique (FQ-SDAM) for multi-cell WCDMA systems. The FQ-SDAM scheme consists of two parts: *fuzzy Q-learning-based residual capacity estimator* (FQ-RCE) and *data rate scheduler* (DRS). The FQ-RCE, by fuzzy Q-learning technique, estimates the appropriate situation-dependent residual system capacity, in term of interference power, for non-real-time services; the DRS assigns transmission rates for non-real-time terminals by a modified exponential rule.

The fuzzy inference system (FIS) and the reinforcement learning technique have been separately applied to solve network resource management problems [57]-[59]. A fuzzy resource allocation controller was proposed in [58], where the FIS technique was adopted to estimate the resource availability. A reinforcement learning technique, Q-learning, was applied respectively to deal with the dynamic channel assignment in [36] and multi-rate transmission control problems in [59] for wireless communication systems. By means of learning from the system environment, the Q-learning technique can converge to a pre-defined optimal control target. In [60], Jouffle proposed a reinforcement learning technique for FIS, called fuzzy Q-learning (FQL). The FQL technique combines the benefits of FIS and reinforcement learning. The FIS provides a good function approximation for the FQL and *a priori* knowledge can be easily applied to the system design; also, the reinforcement learning provides a model-free

approach to obtain a control target. By applying the FQL technique, the radio resource can be managed under partial, uncertain information, and the optimal resource management can be reached in an incremental way.

The FQ-RCE chooses three essential measures of interferences: the received real-time interference from home cell, the received non-real-time interference from home cell, and the received interference from adjacent cells, as input linguistic variables to estimate the situation-dependent residual capacity in the multi-cell environment. Note that the received interference from adjacent cells is regarded as a different variable from the received interference from home cell in order to distinguish their according variations. Therefore, via the linguistic variable of the adjacent-cell interference, the FQ-RCE at home cell can *perceive* the situation of the radio resource allocation by those FQ-SDAMs in adjacent cells, or say, be aware of the loading situation of adjacent cells, and precisely estimate the residual resource in a distributed fashion; thus, an explicit action coordination scheme is negligible in the multi-cell WCDMA environment.

On the other hand, the DRS adopts a modified exponential rule to assign the transmission rates for non-real-time terminals, based on the residual capacity estimated by FQ-RCE. The modified exponential rule is a utility function-based scheduling algorithm which considers factors of transmission delay, average transmission rate, and link capacity. Its main difference from the original exponential rule [56] is on the definition of the link capacity. For the modified exponential rule, the link capacity is defined as the maximum available rate under the current link condition of that the interference influence on adjacent cells by the transmission power is below a threshold. With the feature of location awareness, the modified exponential rule is more suitable for applications in the uplink transmission of multi-cell WCDMA systems. Simulation results show that the proposed FQ-SDAM outperforms the LIDA scheme; it can effectively reduce the packet error probability and improve the aggregate

throughput in both homogeneous and non-homogeneous multi-cell WCDMA environments. Also, the modified exponential rule can achieve better system performance than the original exponential rule. In the homogeneous case, the FQ-SDAM achieves higher aggregate throughput by 75.3% (53.3%) than the LIDA scheme with β=10%, under high-bursty (low-bursty) real-time traffic. As to the nonhomogeneous case, the FQ-SDAM achieves greater aggregate throughput by 31.53%, 35.5%, and 34.2% for the cells in the central, first-tier, and second-tier, respectively, than the LIDA scheme with β=10%.

The rest of the chapter is organized as follows. The system model is described in Section 4.2. The concept of fuzzy Q-learning is briefly stated and the design of FQ-SDAM is proposed in Section 4.3. Simulation results are presented in Section 4.4, where the performance comparison between the FQ-SDAM and a conventional LIDA scheme is made. Finally, concluding remarks are given in Section 4.5.

5.2 System Model

A multi-cell WCDMA system containing N cells is considered, where each cell has a base station with an omni-directional antenna to take charge of communicating with real-time and non-real-time terminals within its coverage area. The reverse link that supports slotted transmission is adopted. Each terminal transmits at the same frequency band and is distinguished by its own spreading code. As to the detail description of the WCDMA system, please refer to section 4.2.

Two types of traffic are considered: real-time (type-1) traffic and non-real-time (type-2) traffic. The system provides continuous transmission for real-time traffic and bursty transmission for non-real-time traffic. The real-time terminals may transmit at any possible data rate while necessary; on the other hand, the transmission of non-real-time terminals is controlled by the data access manager at the base station. Considering terminal's link

gain and the received interference strength from both home and adjacent cells, the data access manager assigns an appropriate data rate for each non-real-time terminal. For the bursty transmission, the available data transmission rates are 1X, 2X, 4x, and 8X , and 1X transmission rate is called the basic rate. A strength-based power control scheme is assumed such that the required transmission power is directly proportional to the transmission rate. Also, the overall capacity is determined by the upper bound of the total received interference power, and the residual capacity is defined as the allowable received interference power from the non-real-time terminals.

The link gain between terminal i to base station j, denoted by h_{ij}, is usually determined by the long-term fading FL_{ij} and the short-term fading FS_{ij} [62], which is given by

$$h_{ij} = FL_{ij} \times FS_{ij}. \tag{5.1}$$

The long-term fading FL_{ij}, combining the path loss and shadowing, is modelled as

$$FL_{ij} = k \times r^{-\alpha} \times 10^{\eta/10}, \tag{5.2}$$

where k is constant, r is distance from mobile i to base station j, α is path loss exponent whose value usually lies between two and five for mobile environment ($\alpha = 4$ in this chapter), and η is normal-distributed random variable with zero mean and variance σ_L^2. The parameter σ_L is affected by the configuration of the terrain and ranges from 5 to 12 (σ_L^2=10 in this chapter). The short-term fading FS_{ij} is mainly caused by multi-path reflections, and it is modelled by Rayleigh distribution.

The real-time service is modelled as an ON-OFF Markov process with a transition rate μ from ON to OFF and λ from OFF to ON state. The non-real-time service is modelled as a batch Poisson process; that is, the arrival process of the data burst is in Poisson distribution and the data length is assumed to be with a geometric distribution. An erroneous real-time packet will be dropped since there is no re-transmission for real-time packets, while

the erroneous non-real-time packets will be recovered via automatic repeat request (ARQ) scheme. The measure of the packet error probability, denoted by P_e, and packet transmission delay, denoted by D_d, are regarded as the system performance indices. Also, the maximum tolerable packet error probability, denoted by P_e^*, is defined as the system QoS requirement.

5.3 Design of FQ-SDAM

The FQ-SDAM contains two functional blocks of a fuzzy Q-learning-based residual capacity estimator (FQ-RCE) and a data rate scheduler (DRS). The FQ-RCE estimates the residual interference power budget, and then the DRS allocates the resource for the non-real-time terminals. In the following, the fuzzy Q-learning and the detailed design of the two function blocks are described.

5.3.1 The Fuzzy Q-Learning (FQL)

Denote **S** the set of state vectors for the system, $\mathbf{S}=\{S_i,\ i=1,2,\cdots,M\}$; each state vector S_i is constituted by L fuzzy linguistic variables selected to describe the system. Denote **A** the set of actions that are possibly chosen by system states, $\mathbf{A}=\{A_j,\ j=1,2,\cdots,N\}$. For an input state vector $\mathbf{x}$ containing the L linguistic variables, the rule representation of FQL for state S_i is in the form by

if $\mathbf{x}$ is S_i, **then** A_j with $q[S_i, A_j]$, $1 \le i \le M$ and $1 \le j \le N$,

where A_j is the j-th action candidate that is possibly chosen by state S_i, and $q[S_i, A_j]$ is the Q-value for the state-action pair (S_i, A_j). The number of state-action pairs for each state S_i is equal to the number of the elements in the action set; *i.e.*, there are N possible consequence parts for the same antecedent. Every fuzzy rule has to choose an action A_i out of the action candidates set **A** by an action selection policy. In the FQL, the action selection policy for each fuzzy rule may be *select-max* or other exploration strategy. As to the defuzzification of the M fuzzy rules, the inferred action $a(\mathbf{x})$ for the input vector $\mathbf{x}$ is

expressed as

$$a(\mathbf{x}) = \frac{\sum_{i=1}^{M} \alpha_i \times A_i}{\sum_{i=1}^{M} \alpha_i}, \tag{5.3}$$

where α_i is the truth value of the rule representation of FQL for state S_i. Also, the Q-value for the state-action pair $(\mathbf{x}, a(\mathbf{x}))$ is

$$Q(\mathbf{x}, a(\mathbf{x})) = \frac{\sum_{i=1}^{M} \alpha_i \times q[S_i, A_i]}{\sum_{i=1}^{M} \alpha_i}. \tag{5.4}$$

For the current system state $\mathbf{x}$, after applying the chosen action $a(\mathbf{x})$, the next-stage system state is assumed at $\mathbf{y}$ and the system reinforcement signal is $c(\mathbf{x}, a(\mathbf{x}))$. To update the Q-value, the next-stage optimal Q-value, $Q^*(\mathbf{y}, a(\mathbf{y}))$, is defined as

$$Q^*(\mathbf{y}, a(\mathbf{y})) = \frac{\sum_{i=1}^{M} \alpha_i \times q[S_i, a_i^*]}{\sum_{i=1}^{M} \alpha_i}, \tag{5.5}$$

where $q[S_i, a_i^*]$ is the Q-value of state-action pair $(S_i,\ a_i^*)$ and $a_i^* = \underset{A_j}{\text{argmax}}\ \{\text{q}[S_i,\ A_j]\}$. According to the Q-learning rule [40], the Q-value update in the FQL can be expressed as

$$q[S_i, a_i] = q[S_i, a_i] + \eta \Delta q[S_i, a_i], \tag{5.6}$$

where η is the learning rate, $0 \leq \eta \leq 1$, and

$$\Delta q[S_i, a_i] = \{c(\mathbf{x}, a(\mathbf{x})) + \gamma Q^*(\mathbf{y}, a(\mathbf{y})) - Q(\mathbf{x}, a(\mathbf{x}))\} \times \frac{\alpha_i}{\sum_{k=1}^{M} \alpha_k}. \tag{5.7}$$

$c(\mathbf{x}, a(\mathbf{x}))$ in (5.7) is the reinforcement signal.

5.3.2 Fuzzy Q-learning-based Residual Capacity Estimator (FQ-RCE)

The FQ-RCE chooses three interference measures: the received real-time interference from home cell (I_{h1}), the received non-real-time interference from home cell (I_{h2}), and the received interference from adjacent cells (I_o), as input linguistic variables. Note that the received interference in the WCDMA system is a good indicator of system loading; also, the

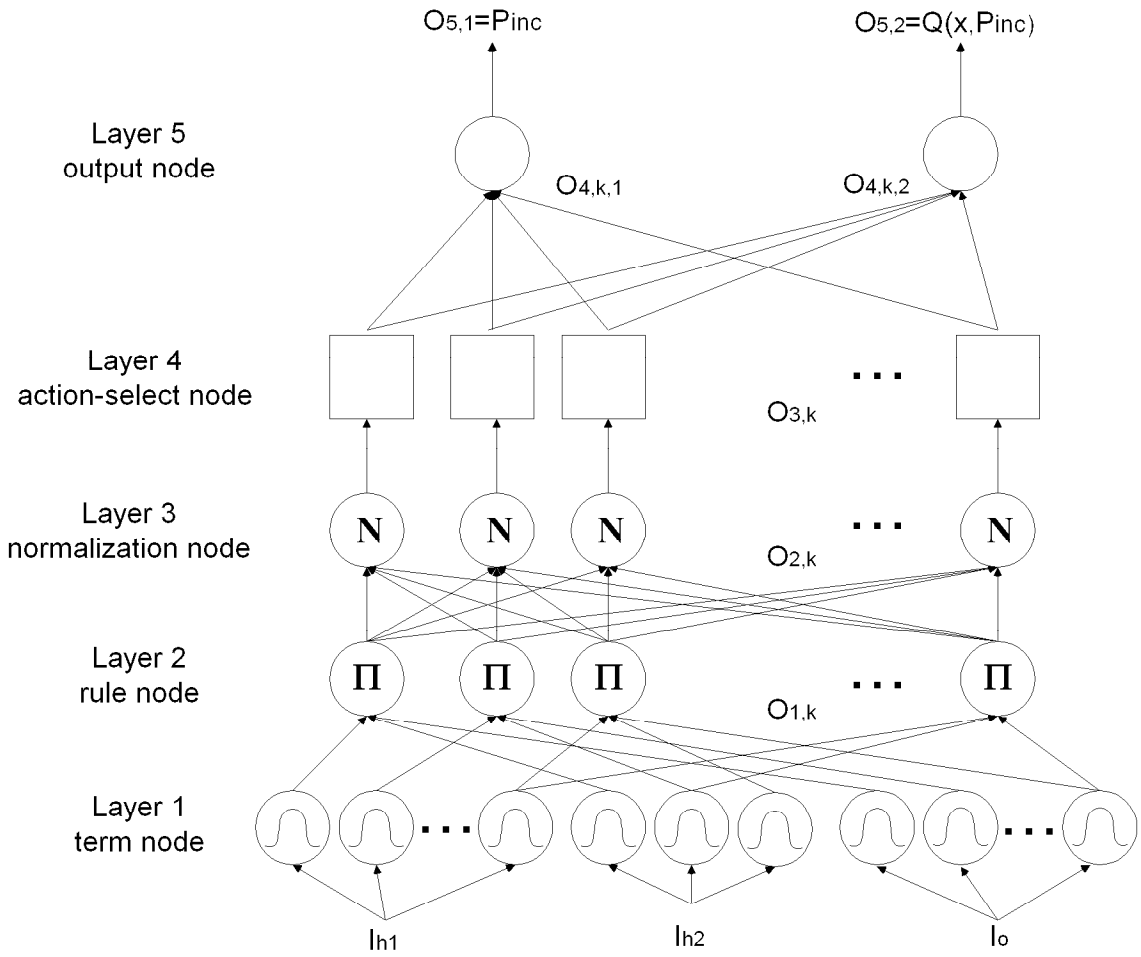

Figure 5.1: Structure of FQ-RCE

interference generated from home cell can be identified by PN codes and the interference from adjacent cells can be distinguished by long scrambling codes [63]. Accordingly, the system state vector $\mathbf{x}$ containing the three linguistic variables input to FQ-RCE is defined as

$$\mathbf{x} = (I_{h1}, I_{h2}, I_o). \tag{5.8}$$

After comprehensive simulation experiments, it is found that five terms for both I_{h1} and I_o, and three terms for I_{h2} are proper. Hence, their fuzzy term sets are T(I_{h1})={Largely High, HiGh, MeDium, LoW, Largely Low}={LH, HG, MD, LW, LL}, T(I_{h2})={HiGh, MeDium, LoW}={HG, MD, LW}, and T(I_o)={Largely High, HiGh, MeDium, LoW, Largely

Low}={LH, HG, MD, LW, LL}. From the fuzzy set theory, the fuzzy rule base forms with dimensions |T(I_{h1})|×|T(I_{h2})|×T|(I_o)|. Accordingly, M=75. On the other hand, the step-wise incremental/decremental action of the interference power budget for the non-real-time services, denoted by P_{inc}, is selected as the output linguistic variable. Here, seven levels of increment actions (N=7) are decided, and the corresponding fuzzy term set is T(P_{inc})={PI_1, PI_2, PI_3, PI_4, PI_5, PI_6, PI_7}. After the interference increment is estimated by the FQ-RCE, the residual system capacity (RC) being allocated for the non-real-time services is defined as

$$RC = I_{h2} + P_{inc}, \tag{5.9}$$

where I_{h2} is the capacity assigned to the non-real-time services last time. Also, the reinforcement learning signal $c(\mathbf{x}, a(\mathbf{x}))$ is defined as

$$c(\mathbf{x}, a(\mathbf{x})) = [\frac{P_e(\mathbf{x}, P_{inc}) - P_e^*}{P_e^*}]^2, \tag{5.10}$$

where $P_e(\mathbf{x}, P_{inc})$ is the packet error probability of real-time services for the state-action pair $(\mathbf{x}, P_{inc})$, which is a performance measure of the system, and P_e^* is the QoS requirement of real-time packet error probability.

Fig. 5.1 shows the structure of FQ-RCE; it is a five-layer adaptive-network-based implementation of fuzzy inference system. In the FQ-RCE, *layer 1* to *layer 3* are the antecedent part of the FIS while *layer 4* and *layer 5* represent the consequence part. The node function in each layer is described as follows.

Layer 1: Every node k, $1 \leq k \leq 13$, in this layer is a term node which represents a fuzzy term of an input linguistic variable, where k= 1, $\cdots$, 5 (6, 7, 8) (9, $\cdots$, 13) denotes node k being the k-th ($(k-5)$-th) ($(k-8)$-th) term in $T(I_{h1})$ ($T(I_{h2})$) ($T(I_o)$). The node function is defined to be the membership function with bell shape for the term. Thus, for an input

linguistic variable x, the output $O_{1,k}$ is given by

$$O_{1,k} = b(x; m^k, \sigma^k), \tag{5.11}$$

where $b(\cdot)$ is the bell-shaped function, and m^k and σ^k is the mean and the variance of the node k.

Layer 2: Every node k, $1 \leq k \leq 75$, in this layer is a rule node which represents the truth value of k-th fuzzy rule; it is a *fuzzy*-AND operator. Here, the product operation is employed as the node function. Since each fuzzy rule has three input linguistic variables, the node output $O_{2,k}$ is the product sum of three fuzzy membership values corresponding to the inputs. Therefore, $O_{2,k}$ is given by

$$O_{2,k} = \prod\{O_{1,l}\}, \forall l \in P_k, \tag{5.12}$$

where P_k=$\{l|$ all ls that are the pre-condition nodes of the k-th fuzzy rule$\}$.

Layer 3: Every node k, $1 \leq k \leq 75$, in this layer is a normalization node which performs a normalization operation; it makes the summation of the all truth values be unity. After the normalization, the output of this node $O_{3,k}$ is given by

$$O_{3,k} = \frac{O_{2,k}}{\sum_{l=1}^{75} O_{2,l}}. \tag{5.13}$$

Layer 4: Every node k, $1 \leq k \leq 75$, in this layer is an action-select node which represents the consequence part of k-th fuzzy rule. Based on the action selection policy and Q-values of the possible action candidates (PI_j, $j = 1, 2, \cdots 7$), the node is to choose an appropriate action. Since improper initial setting of fuzzy parameters would lead to a bad learning result, the Boltzmann-distributed exploration strategy in [41] is employed to explore the set of all the possible action candidates. In the Boltzmann-distributed exploration, the node chooses the state-action pair (S_k, a_k), $a_k \in T(P_{inc})$, for the k-th rule, with the probability $\xi(S_k, a_k)$ given by

$$\xi(S_k, a_k) = \frac{e^{q[S_k, a_k]/T}}{\sum_{j=1}^{7} e^{q[S_k, PI_j]/T}}, \tag{5.14}$$

where T is the *temperature* which reflects the randomness of action selection. After the action is chosen, the node sends two outputs $O_{4,k,1}$ and $O_{4,k,2}$ to the action node and Q-value node in layer 5, respectively. $O_{4,k,1}$ and $O_{4,k,2}$ are represented by

$$O_{4,k,1} = O_{3,k} \times a_k, \tag{5.15}$$

and

$$O_{4,k,2} = O_{3,k} \times q[S_k, a_k]. \tag{5.16}$$

Layer 5: There are two output nodes in this layer: action node $O_{5,1}$ and Q-value node $O_{5,2}$, which represent the fuzzy defuzzification of FQ-RCE. Here, the center of the area defuzzification method is applied. Since the truth value of the antecedent part of the i-th fuzzy rule is normalized in layer 3, the node functions in this layer are summation of the inputs from layer 4. Hence, $O_{5,1}$ and $O_{5,2}$ are given by

$$O_{5,1} = P_{inc} = \sum_{k=1}^{M=75} O_{4,k,1}, \tag{5.17}$$

and

$$O_{5,2} = Q(\mathbf{x}, P_{inc}) = \sum_{k=1}^{M=75} O_{4,k,2}. \tag{5.18}$$

After the action is performed, the FQ-RCE computes the reinforcement signal $c(\mathbf{x}, a(\mathbf{x}))$ by (5.10) and updates the Q-value of each state-action pair according to (5.6).

It is noted that the convergence property of Q-learning is held for the single-agent (learner) case and may not be held for multiple-agent cases; also, the convergence of Q-learning in multi-cell WCDMA systems would be a difficult task because decision policies of all cells concurrently change during the learning phase. To deal with this problem, the perceptual coordination mechanism [61] is applied in FQ-RCE by designing the input linguistic variables, which includes two parts: I_{h1} and I_{h2} represent the current state of the radio resource usage in home cell and I_o represents the radio resource allocations performed

in adjacent cells. Therefore, by measuring the adjacent-cell interference, the FQ-RCE at home cell can implicitly *perceive* the situation of radio resource allocation (action) in adjacent cells. The multi-cell learning environment can then be simplified as a single-cell one, and the convergence property for the FQ-RCE can be held henceforth.

5.3.3 The Data Rate Scheduler (DRS)

A modified exponential rule scheduling algorithm is proposed for DRS. The formula of the modified exponential rule is given by

$$j = \underset{i}{\text{argmax}} \{\frac{r_i}{\bar{r}_i} \times e^{\frac{W_i - \overline{\mathbf{W}}}{1+\sqrt{\overline{\mathbf{W}}}}}\}, \tag{5.19}$$

where r_i, $\bar{r}_i$, and W_i are the link capacity, the average transmission rate, and the waiting time, of the i-th data terminal, respectively, and $\overline{\mathbf{W}}$ is the average waiting time of all the data terminals. The main difference between the modified and the original exponential rules is the definition of the link capacity. The original exponential rule was proposed for downlink transmission in the CDMA HDR system [56], where the link capacity was defined as the maximum transmission rate under the current link condition. However, in the multi-cell WCDMA environment, the uplink transmission power would interfere adjacent cells. The closer the terminal near the cell boundary is, the larger the interference power will be. Therefore, the modified exponential rule algorithm sets a guard threshold of adjacent-cell interference for the uplink transmission power such that its incurred adjacent-cell interference is lower than a pre-defined level. Then, the location-dependent link capacity r_i is defined as the maximum available transmission rate that satisfies the following condition:

$$P(r_i) \times h_i^a \leq P_d, \tag{5.20}$$

where $P(r_i)$ is the transmission power of terminal i with rate r_i, h_i^a is the maximum link gain between the terminal i and adjacent cells, and P_d is the guard threshold of the adjacent-cell

interference. In the strength-based power control scheme, the transmission power $P(r_i)$ is given by

$$P(r_i) = \frac{r_i \times (E_b/N_0)^* \times I_{max}}{PG \times h_i}, \tag{5.21}$$

where $(E_b/N_0)^*$ is the signal-to-noise requirement, I_{max} is the maximum received interference power, PG is the processing gain, and h_i is the home-cell link gain of the terminal. Also, h_i and h_i^a can be measured by monitoring the received pilot strength from the home and adjacent cells. Hence, the modified exponential rule has the property that *the terminal with higher maximum available transmission rate, lower average transmitted rate, and longer delay will get higher transmission priority.* As the terminal moves toward the cell boundary, the emission power to the adjacent cells will go high, the transmission priority will be low, and the waiting time will accumulate. However, as the terminal's waiting time is long, the transmission priority will be high. Therefore, the modified exponential rule can make a balance among the link gain, the location, and the waiting time of terminals.

The DRS performs the rate allocation according to the terminal's priority. The terminal with the highest priority gets the rate allocation first, and other terminals get the allocation in order. The operation of the DRS will stop until all the data power budget is used out. Its procedure is described in the following:

[**The DRS Algorithm**]

Step 1 Obtain the residual system capacity (RC) for non-real-time services from FQ-RCE.

Step 2 Choose highest-priority terminal, j, out of data terminals that are not allocated yet, by (5.19).

Step 3 Compute the remaining RC by

$$RC = RC - P(r_j)/PG.$$

If the remaining RC is larger than 0, go back to **Step 2**. Otherwise, go to **Step 4**.

Table 5.1: Traffic Parameters in The multi-cell WCDMA System

Traffic Type	Traffic Parameters
2-level real-time voice	Mean talkspurt duration: 1.00 seconds Mean silence duration: 1.35 seconds
High-bursty real-time data traffic	Peak rate ($R_{p,h}$): 4-fold of basic rate Mean rate: 1-fold of basic rate ρ_h: 0.25
Low-bursty real-time data traffic	Peak rate ($R_{p,l}$): 2-fold of basic rate Mean rate: 1-fold of basic rate ρ_l: 0.5
Non-real-time data traffic	Mean data burst size: 200 packets $r_{\min}$: 1-fold of basic rate $r_{\max}$: 8-fold of basic rate

Step 4 Inform terminals the assigned data rate via signaling channel. **End**

5.4 Simulation Results and Discussion

In the simulations, a concatenated 19-cell (N=19) environment is configured as the multi-cell WCDMA system. The central cell is labelled as cell 1, the cells in the first tier are cell 2 $\sim$ cell 7, and the cells in the second tier are cell 8 $\sim$ cell 19. Three kinds of real-time traffic are considered: voice traffic, high-bursty real-time data traffic and low-bursty real-time data traffic. The voice traffic assumes 2-level transmission rate traffic which is modelled by a 2-level MMDP (Markov modulated deterministic process). The real-time data traffic is modelled by an ON/OFF traffic stream with specific burstiness $1/\rho_h$ ($1/\rho_l$) and peak rate $R_{p,h}$ ($R_{p,l}$) for high-bursty (low-bursty) real-time traffic. The two real-time data traffics have the same mean rate but different burstiness. On the other hand, the non-real-time data traffic is considered to have a Poisson arrival process with data burst length in geometric distribution. All the detailed traffic parameters are listed in Table 5.1. A basic rate in the WCDMA system is assumed to be a physical channel with SF=256. For each connection, DPCCH is always active to maintain the connection reliability. To reduce the overhead cost

of interference produced by DPCCHs, the transmitting power of a DPCCH is smaller than its respective DPDCH by an amount of 3 dB. The QoS requirement of the packet error parameter, P_e^*, is set to be 0.01.

The conventional resource reservation scheme proposed in [53], LIDA (load and interference demand assignment), is used as a benchmark for performance comparison. The basic concept of the LIDA scheme is two-folded: firstly, a portion of interference power budget, β, is reserved to avoid the over-loading situation; secondly, a burst-mode admission is applied for the high-rate traffic. Also, the allocation of the incremental of transmission power, P_{inc}, to the non-real-time data traffic in the LIDA scheme is given by

$$P_{inc} = (1 - \beta)I_{max} - I_{h1} - I_{h2} - I_o. \tag{5.22}$$

The performance of the LIDA scheme highly relies on the choice of reservation threshold, β. In the simulations, three different degrees of reservation threshold, $\beta = 0\%$, 5%, and 10%, are considered and the modified exponential rule with P_d=2dB is applied for the LIDA scheme . Moreover, a scheme which combines the FQ-RCE with the original exponential rule, called FQ-RCE/EXP, is considered to further evaluate the effectiveness of the modified exponential rule. Noted that all the considered schemes are applied to non-real-time terminals only, and all the real-time terminals initiate data transmission whenever they have packets in queues.

5.4.1 Homogeneous Case

In the homogeneous case, all cells are assumed to contain 22 voice terminals, 40 real-time data terminals and 20 non-real-time data terminals. The forty real-time data terminals consist of $N_{D,h}$ high-bursty and $N_{D,l}$ low-bursty data users; obviously, $N_{D,h}$+$N_{D,l}$=40.

Fig. 5.2 shows the packet error probabilities versus the number of high-bursty real-time data users. It can be found that the packet error probability of the LIDA scheme will violate the QoS requirement and the LIDA scheme without reservation (β=0%) has the largest packet error probability. The results justify the necessity of a precise residual capacity estimation to avoid the overloading condition in the multi-cell WCDMA environment. As to

the FQ-SDAM and FQ-RCE/EXP schemes, their packet error probabilities always satisfy the QoS requirement. The reason is as follows: the FQ-RCE adopts the FQL which inherently possesses the capability of reinforcement learning. Thus the FQ-RCE can precisely determine the residual system capacity by monitoring the loading status of the home cell and the interference variation of adjacent cells. Also, whatever the number of $N_{D,h}$ is, the FQ-SDAM scheme always achieves lower packet error probabilities than the FQ-RCE/EXP scheme does. This is because the up-link transmission powers emitted from terminals would interfere users at home cell and adjacent cells in the multi-cell environment. With the awareness of location of users, the modified exponential rule in FQ-SDAM will effectively curb the interference influence on adjacent cells within a sustainable level and consequently would reduce the packet error probabilities more.

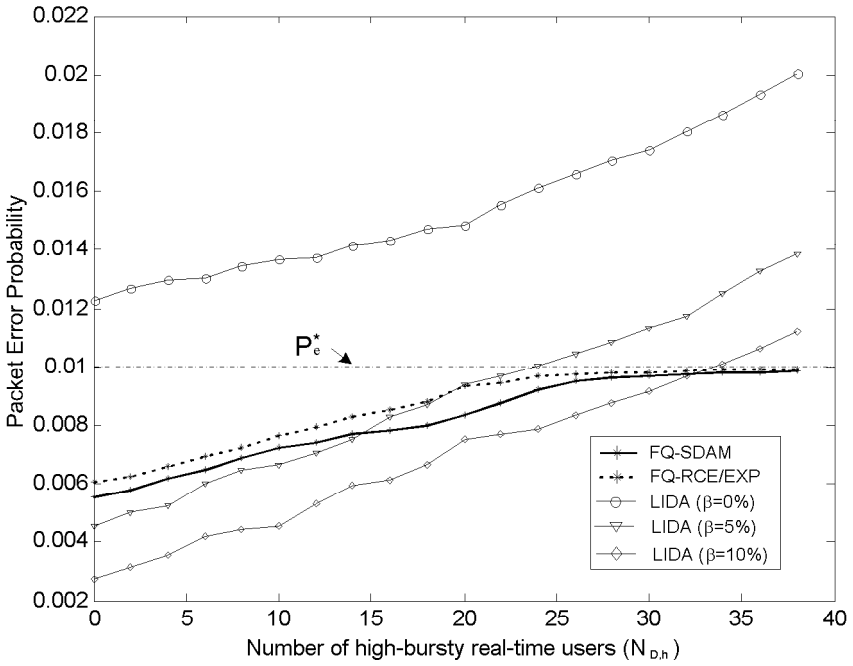

Figure 5.2: Packet error probabilities: homogeneous case

Fig. 5.3 shows the aggregate throughputs of non-real-time data traffic versus three numbers of high-bursty real-time users: $N_{D,h}$=10, 20 and 30. The three cases of different real-time data users are used to simulate the low-bursty, medium-bursty and high-bursty scenarios.

Here, the performance of the LIDA scheme with β=0% is not considered due to its QoS violation. It can be found that the FQ-SDAM achieves the highest data throughout for non-real-time services and the LIDA scheme with β=10% the lowest. Compared with the LIDA scheme with β=10%, the FQ-SDAM, FQ-RCE/EXP, and LIDA with β=5% schemes improve the throughput by an amount of 75.3%, 73.3% and 52.9% (53.3%, 51.1% and 49.2%), respectively, in the low-bursty (medium-bursty) case. In the high-bursty case, under QoS constraint, the FQ-SDAM and FQ-RCE/EXP schemes improve the throughput over the LIDA scheme with β=10% by an amount of 16.8% and 10.7%, respectively. The reason is that the FQ-SDAM scheme approaches the desired transmission target (P_e^*=0.01) by the fuzzy Q-learning. According to the definition of reinforcement signal $c(\mathbf{x}, a(\mathbf{x}))$, the FQ-SDAM would try to allocate the resource as much as possible under the QoS requirement. On the contrary, the LIDA scheme with β=10% is a conservative scheme, which has the lowest packet error probability at the expense of capacity waste. It can also be found that, for the three cases, the FQ-SDAM achieves aggregate throughput higher than the FQ-RCE/EXP by 1.4%, 1.43% and 5.5%, respectively. As the number of high-bursty real-time users goes up, the performance gain increases. This is because the modified exponential rule considers the terminal's location factor and reduces the packet error probability in the multi-cell WCDMA environment; with a reinforcement signal containing a lower packet error probability, the FQ-RCE will tend to allocate more capacity in the next-turn decision during the fuzzy Q-leaning period; as a result, the data throughput increases as more packets are successfully transmitted.

5.4.2 Non-homogeneous Case

In the non-homogeneous case, the real-time data terminals for the first-tier cells (cell 2 to cell 8) are: $N_{D,h} = 25 - 2 * (i-1)$ and $N_{D,l} = 40 - N_{D,h}$, i=2, $\cdots$, 8, while for the central and second-tier cells, the real-time data terminals are: $N_{D,h} = N_{D,l} = 20$.

Fig. 5.4 shows the packet error probabilities of the three tiers in the multi-cell WCDMA

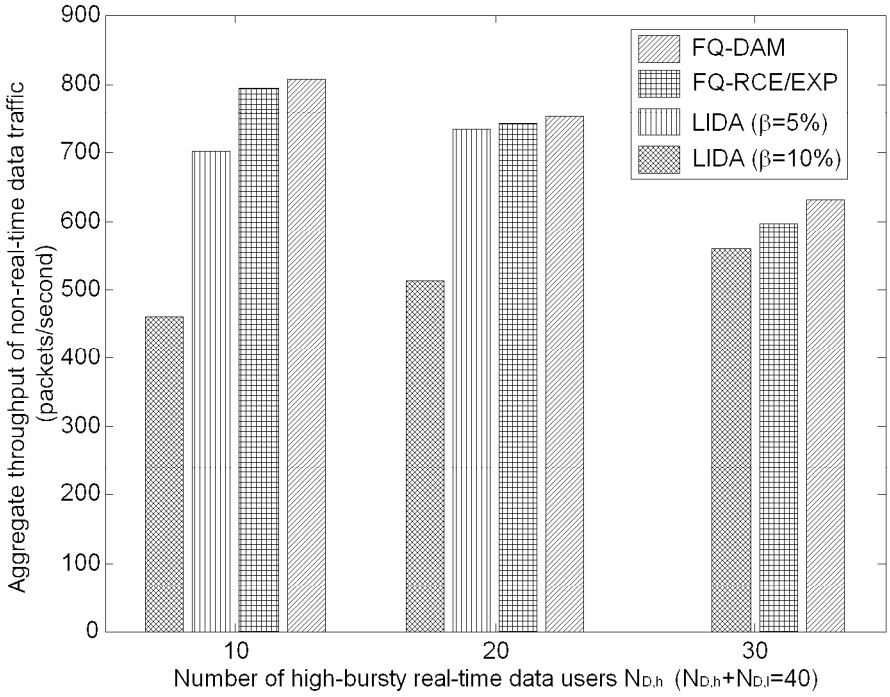

Figure 5.3: Aggregate throughput of non-real-time data traffic: homogeneous case

system. It can be seen that only FQ-SDAM, FQ-RCE/EXP, and LIDA with β=10% can meet the QoS requirement. It is because, in the FQ-SDAM and FQ-RCE/EXP schemes, the received adjacent-cell interference is considered as an input parameter for resource estimation. The resource allocation in the adjacent-cells is perceived by observing the fluctuation of interference. Consequently, the action of resource allocation between cells can be conceptually coordinated in the implicit way. Also, compared to Fig. 5.2 at $N_{D,h} = 20$, it can be found that the packet error probability in the non-homogeneous case is larger than that in the homogeneous case. The reason is that, in the non-homogeneous case, the fluctuation of received adjacent-cell interference differs from cell to cell when the cells compete for the residual capacity in the multi-cell environment. Without coordination, each cell allocates in the myopic fashion so that the system will tend to operate in the over-loading situation.

Fig. 5.5 shows the aggregate throughputs of non-real-time data traffic in the three tiers of the multi-cell WCDMA system. Here, the aggregate throughputs of the LIDA with β=0%

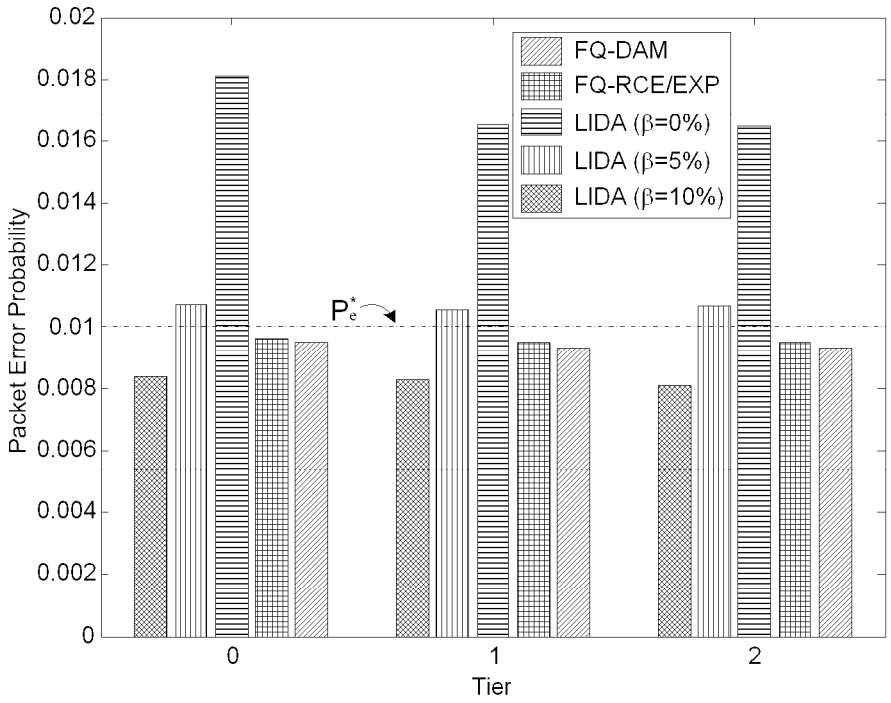

Figure 5.4: Packet error probabilities: non-homogeneous case

and β=5% are not considered due to their QoS violation. The aggregate throughput in the non-homogeneous case is smaller than that in the homogeneous case due to the higher interference fluctuation. Also, the FQ-SDAM and FQ-RCE/EXP schemes still achieves higher aggregate throughput by an amount of 31.53% and 28.346% (35.5% and 33.63%) (34.2% and 32%) for the cells in the central (first-tier) (second-tier) than the LIDA with $\beta = 10\%$ scheme does.

5.5 Concluding Remarks

A novel situation-aware data access manager using fuzzy Q-learning technique (FQ-SDAM) is proposed for multi-cell WCDMA systems. It is designed to contain a fuzzy Q-learning-based residual capacity estimator (FQ-RCE) and a data rate scheduler (DRS). By applying the perceptual coordination method, the FQ-RCE treats the received home-cell interference and adjacent-cell interference as two separate linguistic variables such that

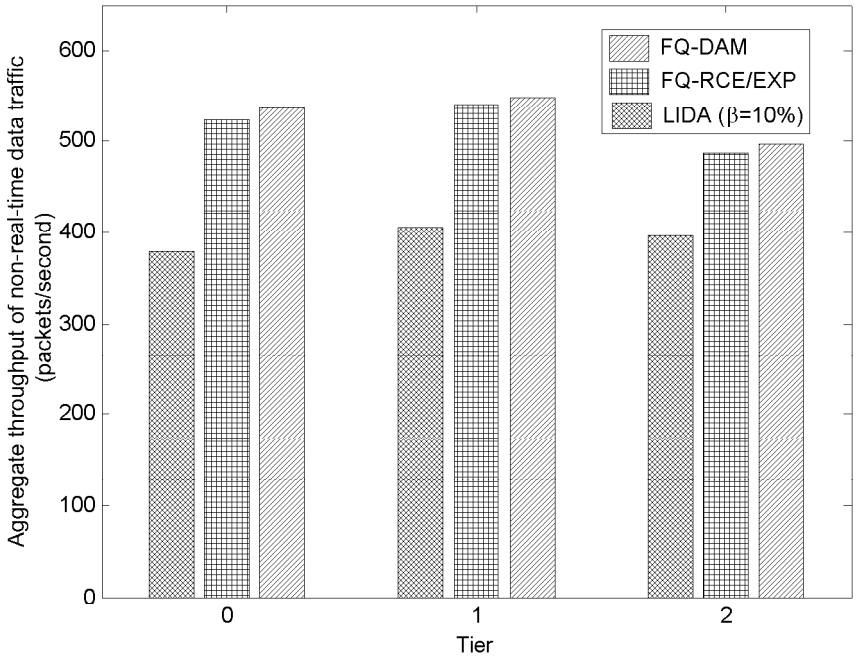

Figure 5.5: Aggregate throughput of non-real-time data traffic: non-homogeneous case

it can adaptively determine the residual capacity according to the current loadings in the home and adjacent cells. Simulation results show that, compared to the LIDA scheme [53], the proposed FQ-SDAM can effectively reduce the packet error probability and enhance the aggregate throughput of the non-real-time services in both the homogeneous and non-homogeneous multi-cell WCDMA environment. It is because, by applying the FQL technique, the FQ-RCE monitors the radio resource allocation in the adjacent cells, perceives the partial and uncertain information, and enhances the estimation of the residual system capacity in an incremental way. Also, the DRS effectively allocates the resource for the non-real-time terminals by adopting a modified exponential rule which takes the information of the location-dependent link capacity into consideration.

Chapter 6

Conclusions and Future Works

In this dissertation, the radio resource allocation schemes for mobile communication networks are studied by using neural/fuzzy techniques, including an adaptive-network-based fuzzy radio resource controller for TDMA systems, a Q-learning-based multi-rate transmission control scheme for WCDMA systems, and a fuzzy Q-learning-based data access manager for WCDMA systems.

In Chapter 3, the radio resource allocation problem in TDMA system is investigated and a fuzzy resource allocation controller (FRAC) is proposed. The FRAC adopts an active-network-based fuzzy inference system, which takes the advantage of expert knowledge of fuzzy logic system and learning capability of neural network. And the FRAC considers the gain of statistical multiplexing via choosing the air-interface performance as input linguistic variables, together with the capacity requirement of a call request and the capacity reservation for future handoff calls. The air-interface performance criterion, which is a fuzzy logic function of voice-packet dropping rate and data packet delay, can reflect the effect of multiplexing gain. That is, it makes the FRAC act as a closed-loop system, which would result in a stable operation. Simulation results show that FRAC performs the best, compared with the *ExpectedMax* strategy [7] and guard schemes. Also, it has the lowest new call blocking rate and handoff blocking rate while keeping the QoS contracts of different services according to the network dynamics. Moreover, data services can achieve more multiplexing gain than voice services because data services are non-real-time and data packets can be buffered. No

matter in the stationary loading or non-stationary loading case, FRAC is sophisticated and robust.

Many hardware implementations of fuzzy VLSI chip have been proposed recently [24], [25]. In [25], a VLSI fuzzy controller is designed for Sugeno fuzzy inference system. Also, the VLSI fuzzy controller takes the weighting sum method in the defuzzification procedure, which can avoid the limited accuracy and stability problems. Therefore, the hardware implementation of FRAC is feasible and the cost can be reduced. Moreover, the complexity and computation time of FRAC can be reduced by suitably delete or merge some fuzzy rules, which is an interesting topic deserved for further investigation.

In Chapter 4, the radio resource allocation problem in long-term time scale is investigated and a multi-rate transmission control scheme by using Q-learning technique (Q-MRTC) for WCDMA systems is proposed. The Q-learning algorithm is applied to accurately estimate the transmission cost for the multi-rate transmission control, and the feature extraction method and radial basis function network are employed for Q-function approximation that maps the original state-action pairs into the resultant interference profile. Simulation results show that Q-MRTC can improve the throughput of multimedia WCDMA system by an amount of 80% over the conventional interference-based scheme proposed in [32], under the constraint of the QoS requirements of packet error probability and packet transmission delay. Also, the Q-MRTC provides better users' satisfaction. It is because the Q-learning algorithm performs closed-loop control by applying the system performance measures as a feedback to adjust the multi-rate transmission cost, and correspondingly the Q-MRTC can have self-tuning capability to adaptively estimate the transmission cost. Moreover, the storage requirement of RBFN neural network is less than that of the conventional table-lookup method by the amount of 41%.

Actually, the Q-MRTC can be viewed as a "dynamic CAC" scheme while the interference-based scheme as a "static CAC" scheme. The Q-MRTC makes a decision according to current control policy and evaluates it by a delayed reward, which can take the behavior of network

dynamics into consideration. However, the interference-based scheme makes a decision only based on current information, which may suffer from temporary resource deficiency. That is why the Q-MRCT largely outperforms the interference-based scheme. It is noticeable that the control policy is determined by the evaluation function. It will be an interesting topic to further study the performance of Q-MRCT under different definition of evaluation functions. Another interesting topic is to investigate the convergency property of Q-MRCT. Since the traffic characteristics of future multimedia services vary vastly and dramatically, Q-MRTC scheme may require longer time to converge. It is possible to apply the *batch learning* technique for the Q-learning rule in Q-MRTC such that the learning time will be largely reduced and the system stability can be maintained regardless of short-term fluctuation.

In Chapter 5, the radio resource allocation problem in short-term time scale is investigated and a situation-aware data access manager using fuzzy Q-learning technique (FQ-SDAM) for multi-cell WCDMA systems is proposed. It is designed to contain a fuzzy Q-learning-based residual capacity estimator (FQ-RCE) and a data rate scheduler (DRS). By applying the perceptual coordination method, the FQ-RCE treats the received home-cell interference and adjacent-cell interference as two separate linguistic variables such that it can adaptively determine the residual capacity according to the current loadings in the home and adjacent cells. Simulation results show that, compared to the LIDA scheme [53], the proposed FQ-SDAM can effectively reduce the packet error probability and enhance the aggregate throughput of the non-real-time services in both the homogeneous and non-homogeneous multi-cell WCDMA environments. It is because, by applying the FQL technique, the FQ-RCE monitors the radio resource allocation in the adjacent cells, perceives the partial and uncertain information, and enhances the estimation of the residual system capacity in an incremental way. Also, the DRS effectively allocates the resource for the non-real-time terminals by adopting a modified exponential rule which takes the information of the interference influence on adjacent cells into consideration. Also, with the awareness of location of users, the modified exponential rule improves the system performance compared to the original

exponential rule. The perfect channel information and code orthogonality are assumed in Chapter 4. However, some measurement errors and imprecise clock synchronization occur in practical mobile communication environment. It requires further study to investigate the performance of FQ-SDAM operating under imperfect environment.

The high-speed data transmission in the uplink emerges as one the new issues in the WCDMA systems, and the work item on high speed uplink packet access (HSUPA) was created [64]-[66]. The goal of the HSUPA is to improve coverage and user throughput of the current 3GPP uplink dedicated transport channels in UTRA FDD Rel6. The HSUPA will include advanced features, such as: adaptive modulation and coding (AMC), hybrid ARQ (HARQ), shorter frame time, as well as Node-B controlled scheduling. For the packet scheduling in HSUPA, two fundamental methods exist: (1) *Node-B controlled rate scheduling*, where all uplink transmissions randomly occur with time overlap and with the selected rate restricted to keep the total noise rise at the Node-B at an acceptable level and (2) *Node-B controlled time and rate scheduling*, where only a subset of terminals that have traffic to send are selected to transmit over a given time interval also with selected rate restricted to meet noise rise requirement. During the preliminary study item phase, it has shown that these advanced techniques can enhance the uplink packet transfer performance significantly compared to Rel99/Rel4/Rel5 [65]. However, some open issues remain. It would be an interesting and essential research topic to study the scheduling algorithm and the cross-layer MAC design for the future HSUPA system.

Bibliography

[1] D. Hong and S. S. Rappaport, "Traffic Model and Performance Analysis for Cellular Mobile Radio Telephone Systems with Prioritized and Non-Prioritized Handoff Procedures," IEEE Trans. Veh. Technol, vol. VT-35, no. 3, pp. 77-92, Aug. 1986.

[2] —, "Priority oriented channel access for cellular systems serving vehicular and portable radio telephones," IEE Proceedings, vol. 136, pt. 1, no. 5, pp. 339-346, Oct. 1989.

[3] C. J. Chang, T. T. Su, and Y. Y. Chiang, "Analysis of a cutoff priority cellular radio system with finite queueing and Reneging/Dropping," IEEE/ACM Trans. Networking, vol. 2, no. 2, pp. 166-175, Apr. 1994.

[4] M. Naghshineh and M. Schwartz, "Distributed call admission control in mobile/wireless networks," IEEE J. Select. Areas Commun., vol. 14, no. 4, pp. 711-717, May 1996.

[5] O. T. W. Yu and V. C. M. Leung, "Adaptive resource allocation for prioritized call admission over an ATM-based wireless PCN," IEEE J. Select. Areas Commun., vol. 15, no. 7, pp. 1208-1225, Sep. 1997.

[6] Y. C. Kim, D. E. Lee, B. J. Lee, Y. S. Kim, and B. Mukherjee, "Dynamic Channel Reservation Based on Mobility in Wireless ATM Networks," IEEE Commun., pp. 47-51, Nov. 1999.

[7] P. Ramanathan, K. M. Sivalingam, P. Agrawal, and S. Kishore, "Dynamic Resource Allocation Schemes During Handoff for Mobile Multimedia Wireless Networks," IEEE J. Select.Areas Commun., vol. 17, no. 7, pp. 1270-1283, Jul. 1999.

[8] M. M. Zonoozi and P. Dassanyake, "User mobility modeling and characterization of mobility patterns," IEEE J. Select. Areas Commun., vol. 15, no. 7, pp. 1239-1252, Sep. 1997.

[9] R. Guèrin, H. Ahmadi, and M. Naghshineh, "Equivalent capacity and its application to bandwidth allocation in high-speed networks," IEEE J. Select. Areas Commun., vol.9, no. 7, pp. 968-981, Sep. 1991.

[10] G. Kesidis, J. Walrand, and C. S. Chang, "Effective bandwidth for multiclass Markov fluids and other ATM sources, " IEEE/ACM Trans. Networking, vol. 1, no. 4, pp. 424-428, Aug. 1993.

[11] T. D. Ndousse, "Fuzzy neural control of voice cells in ATM network," IEEE J. Select. Areas Commun., vol. 12, no. 9, pp. 1488-1494, Dec. 1994.

[12] R. G. Cheng and C. J. Chang, "Design of a fuzzy traffic controller for ATM network," IEEE/ACM Trans. Networking, vol. 4, no. 3, pp. 460-469, Jun. 1996.

[13] —, "Neural network connection admission control for ATM networks," IEE Proceedings, Communications, vol. 144, no. 2, pp.93-98, Apr. 1997.

[14] R. G. Cheng, C. J. Chang, and L. F. Lin "A QoS-Provisioning Neural Fuzzy Connection Admission Controller for Multimedia High-Speed Networks," IEEE/ACM Trans. Networking, vol. 7, no. 1, pp. 111-121, Feb. 1999.

[15] B. Kosko, Neural Networks and Fuzzy Systems, Prentice-Hall, 1992.

[16] C. T. Lin, C. S. G. Lee Neural Fuzzy Systems, Englewood Cliffs, NJ: Prentice-Hall, 1996.

[17] T. Takagi and M. Sugeno, "Fuzzy identification of systems and its applications to modeling and control," IEEE Trans. Syst., Man, and Cybern., vol.15, no.1, pp. 116-132, Jan./Feb. 1985.

[18] J.-S. R. Jang, "ANFIS: adaptive-network-based fuzzy inference system," IEEE Trans. Syst., Man, and Cybern., vol.23, no. 3, pp. 665-685, May 1993.

[19] J.-S. R. Jang and C.-T. Sun, "Neural-fuzzy modeling and control," IEEE Proceedings, vol.83, no.3 pp. 378-406, Mar. 1995.

[20] J.-S. R. Jang, C.-T. Sun and E. Mizutani, Neuro-fuzzy and soft computing, Prentice-Hall, 1997.

[21] C. J. Chang, and C. H. Wu, "Slot allocation for an integrated voice/data TDMA mobile radio system with a finite population of buffered users", IEEE Trans. Veh. Technol., vol. 43, no. 1, pp. 21-26, Feb. 1994.

[22] G. Wu, K. Mukumoto, and A. Fukuda, "Analysis of an integrated voice and data transmission system using packet reservation multiple access," IEEE Trans. Veh. Technol., vol. 43, no.2, pp. 289-297, May 1994.

[23] S. Nanda, "Stability evaluation and design of the PRMA joint voice data system," IEEE Trans. Comm., vol. 42, no. 5, pp.2092-2104, May 1994.

[24] J. L. Huertas, S. Sanchez-Solano, I. Baturone, I, and A. Barriga, "Integrated circuit implementation of fuzzy controllers," IEEE J. Solid-State Circuits, vol. 31, no. 7 , pp. 1051 -1058, Jul. 1996.

[25] B.M. Wilamowski, "Neuro-fuzzy systems and their applications," IECON '98, vol. 1 pp. T35- T49.

[26] S. Choi and K. G. Shin, "An uplink CDMA system architecture with diverse QoS guarantees for heterogeneous traffic," *IEEE/ACM Trans. Netorking*, vol. 7, no. 5, pp. 616-628, Oct. 1999.

[27] K. S. Gilhousen, I. M. Jacobs, R. Padovani, A. J. Viterbi, L. A. Weaver, and C. E. Wheatley, "On the capacity of a cellular CDMA system," *IEEE Trans. Veh. Technol.*, vol. 40, no. 2, pp. 303-312, May. 1991.

[28] W. Huang and V. K. Bhargava, "Performance evaluation of a DS-CDMA cellular system with voice and data services," *IEEE PIMRC'96*, pp. 588-592.

[29] A. Hämäläinen and K. Valkealahti, "Adaptive power increase estimation in WCDMA," *IEEE PIMRC'02*, vol. 3, pp. 1407-1411, Sep. 2002.

[30] J. B. Kim and M. L. Honig, "Resource allocation for multiple classes of DS-CDMA traffic," *IEEE Trans. Veh. Technol.*, vol. 49, no. 2, pp. 506-519, March 2000.

[31] S. M. Shin, C.-H. Cho, and D. K. Sung, "Interference-based channel assignment for DS-CDMA cellular systems," *IEEE Trans. Veh. Technol.*, vol. 48, no. 1, pp. 233-239, Jan. 1999.

[32] N. Dimitriou and R. Tafazolli, "Quality of service for multimedia CDMA," *IEEE Comm. Mag.*, vol. 38, no. 7, pp. 88-94, July 2000.

[33] V. Phan-Van and D. Luong, "Capacity enhancement with simple and robust soft-decision call admission control for WCDMA mobile cellular PCNs," *IEEE Vehicular Technology Conference (VTC2001)*, vol. 3, pp. 1349-1353, Oct. 2001.

[34] D. Mitra, M. I. Reiman, and J. Wang, "Robust dynamic admission control for unified cell and call QoS in statistical multiplexers," *IEEE J. Select. Areas. Commun.*, vol. 16, no. 5, pp. 692-707, 1998.

[35] K. W. Ross, Multiservice Loss Models for Broadband Communication Networks. Berlin, Germany: Springer-Verlag, 1995.

[36] J. Nie and S. Haykin, "A Q-learning-based dynamci channel assignment technique for mobile Communication systems," *IEEE Trans. Veh. Technol.*, vol. 48, no. 5, pp. 1676-1687, Sep. 1999.

[37] H. Tong and T. X. Brown, "Adaptive admission call admission control under quality of service constraints: a reinforcement learning solution," *IEEE J. Select. Areas. Commun.*, vol. 18, no. 2, pp. 209-221, Feb. 2000.

[38] B. Makarevitch, "Application of reinforcement learning to admission control in CDMA network," *IEEE PIMRC 2000*, pp. 1353 -1357.

[39] P. Marbach, O. Mihatsch, and J. N. Tsisiklis, "Call admission control and routing in integrated services networks using neuro-dynamic programming," *IEEE J. Select. Areas. Commun.*, vol. 18, no. 2, pp. 197-208, Feb. 2000.

[40] C. J. C. H. Watkins and P. Dayan, "Q-learning," *Machine Learning*, vol. 8, pp. 279-292, 1992.

[41] S. Haykin, Neural Networks 2nd. Prentice Hall, 1999.

[42] D. P. Bertsekas and J. N. Tsitsiklis, Neuro-Dynamic Programming. Athena Scientific, 1996.

[43] 3GPP TS25.211: "Physical Channels and Mapping of Transport Channels onto Physical Channels (FDD)," V3.1.1, Dec. 1999.

[44] 3GPP TS25.321: "MAC Protocol Specification," V3.2.0, Dec. 1999.

[45] 3GPP TS25.214: "Physical layer procedures (FDD)," v.4.0.0, Mar. 2001

[46] R. Bellman, *Dynamic Programming*, Princeton, NJ: Princeton Univ. Press, 1957.

[47] K. Das and S. D. Morgera, "Interference and SIR in integrated voice/data wireless DS-CDMA networks - a simulation study," *IEEE J. Select. Areas. Commun.*, vol. 15, no. 8, pp. 1527-1537, Oct., 1997.

[48] T. K. Liu and J. A. Silvester, "Joint admission/congestion control for wireless CDMA systems supporting integrated services," *IEEE J. Select. Areas. Commun.*, vol. 16, no. 6, pp. 845-857, Aug., 1998.

[49] C. Comaniciu and N. B. Mandayam, "Delta modulation based prediction for access control in integrated voice/data CDMA systems," *IEEE J. Select. Areas. Commun.*, vol. 18, no. 1, pp. 112-122, Jan., 2000.

[50] A. Sampath and J. M. Holtzman, "Access control of data in integrated voice/data CDMA systems: benifits and tradeoffs," *IEEE J. Select. Areas. Commun.*, vol. 15, no. 8, pp. 1511-1526, Oct., 1997.

[51] C. Comaniciu, N. B. Mandayam, D. Famolari, and P. Agrawal, "Wireless access to the world wide web in an integrated CDMA system," *IEEE J. Select. Areas. Commun.*, vol. 2, pp. 472-483, May, 2003

[52] L. Chen , H. Kayama, and N. Umeda, "Power resource cooperation control considering wireless QoS for CDMA packet mobile communication systems," *IEEE Int'l Symposium on Personal, Indoor and Mobile Radio Communications* (PIMRC 2002), vol. 3, pp. 1092 -1096.

[53] S. Kumar and S. Nanda, "High data-rate packet communication for cellular network using CDMA: algorithm and performance," *IEEE J. Select. Areas. Commun.*, vol. 17, no. 3, pp. 472-492, Mar., 1999.

[54] S. Ramakrishna and J. M. Holtzman, "A scheme for throughput maximization in a dual-class CDMA system, " *IEEE J. Select. Areas. Commun.*, vol. 16, no. 6, pp. 830-844, Aug., 1998.

[55] A. Jalali, R. Padovani and R. Pankaj, "Data throughput of CDMA-HDR a high efficiency-high data rate personal communication wireless system," *IEEE Vehicular Technology Conference* (VTC2000- Spring), Tokyo, May 2000, pp.1854-1858.

[56] S. Shakkottai and A. L. Stolyar, "Scheduling algorithms for a mixture of real-time and non-real-time data in HDR," *17th International Teletraffic Congress* (ITC-17), Sep., 2001.

[57] L. Wang(Ed), Soft Computing in Communications, Springer, 2003.

[58] Y. S. Chen and C. J. Chang, "A resource allocation scheme using adaptive-network based fuzzy control for mobile multimedia network," *IEICE Trans. Commun.*, vol. E85-B, no. 2, pp. 502-513, Feb. 2002.

[59] Y. S. Chen, C. J. Chang, and F. C. Ren, "A Q-learning-based multi-rate transmission control scheme for RRM in multimedia WCDMA systems," *IEEE Trans. Veh. Technol.*, vol. 53, no. 1, pp 38-48, Jan. 2004.

[60] L. Jouffle, "Fuzzy inference system learning by reinforcement methods," *IEEE Trans. Syst. Man. Cybern.*, vol. 8, no. 3, pp. 338-355, Aug. 1998.

[61] O. Abul, F. Polat, and R. Alhajj, "Multiagent reinforcement learning using function approximation," *IEEE Trans. Syst. Man. Cybern.*, vol. 30, no. 4, pp. 485-497, Nov. 2000.

[62] G. L. Stüber, Priniciple of Mobile Communication, Kluwer Academic Publishers, 1996.

[63] 3rd Generation Partnership Project. (Sep. 2002) Spreading and Modulation (FDD), 3GPP TS 25.213 [Online]http://www.3gpp.org

[64] R1-031422, "Feasibility study for enahnced uplink for UTRA FDD," 3GPP TR 25.896 v 1.1.1, Dec. 2003.

[65] R2-040973, 'HSUPA MAC architecture," 3GPP, May 2004.

[66] A. Ghosh, R. Love, N. Whinnett, R. Ratasuk, W. Xiao, and R. Kuchiahotla, "Overview of enhanced uplink for 3GPP W-CDMA," *IEEE Vehicular Technology Conference (VTC2004-Spring)*, May 2004.

Vita

Yih-Shen Chen was born in Miaoli, Taiwan. He received B.E. and M.E. degree in department of communication engineering from Nation Chiao-Tung University, Hsinchu, Taiwan, in 1995 and 1997, respectively. From 1997 to 1999, he worked at M Group, Computer and Communication Laboratory, Institute of Technology Research Industry, Taiwan. Currently, he is a candidate for the Ph. D. in the Institute of communication engineering in National Chiao Tung University, Taiwan. His research interests include performance analysis, protocol design, and mobile radio network.